QUASI-OPTIMUM RECEIVERS FOR ANALOG FM SIGNALS OVER RAYLEIGH FADING CHANNELS

A thesis submitted in fulfilment of the requirements for the degree of

DOCTOR OF PHILOSOPHY

in the

Department of Electrical Engineering, The University of Adelaide

by

NGUYEN HUU LE, B.E. (Hons.)

August 1977

To the memory

of my parents and my brothers.

TABLE OF CONTENTS

SUMMARY

The problem of demodulating an analog FM signal transmitted over a Rayleigh fading channel is considered in the framework of optimum design of communication receivers utilizing recent developments in nonlinear estimation theory.

An analog model is set up using state-variable formulation: The message, assumed to be sample function from a gaussian random process, is generated by a linear message model and is used to frequency-modulate a carrier signal before being transmitted over a Rayleigh fading channel. The fading is assumed to be slow and frequency nonselective (and thus can be considered as multiplicative noise). The fading signal is further contaminated by additive white gaussian noise and the received signal is sampled and processed by a discrete type of receiver. The output of the receiver is the desired estimate of the message and possibly the channel condition also.

To derive optimum demodulator structures, various discrete nonlinear estimation algorithms are considered. No prior knowledge of the demodulator structures is assumed. These algorithms are the results of recent developments in nonlinear estimation theory. The first one to be considered is the extended Kalman filter (EKF) algorithm. The second is the maximum *a posterior* probability (MAP) algorithm. Both algorithms are only approximate and their validity depends on two main factors:

(i) the "signal-to noise ratio" which is characterised by the ratio of the mean square values of the multiplicative and additive noise components, and

(ii) the error stability conditions which are inherent in all approximate algorithms and render the algorithms invalid

in the below threshold region of an angle-modulated system. With these limitations borne in mind, these algorithms can then be applied to the discrete equivalent of the analog communication model formulated above and result in a family of demodulators which all have a phase-locked type of structures.

The sampling is done by using by either uniform (or scalar) sampling or by quadrature sampling resulting in two class of receivers for each set of algorithms. Results obtained in the first stage of this work indicate best performance achieved by using the MAP algorithm with quadrature sampling and this will be used for the rest of the study.

Performance of receivers is investigated by extensive use of computers for simulation. Theoretical considerations and the actual procedure used are discussed fully in order to ascertain the validity of the simulation results.

The Rayleigh fading effecting the signal is normally assumed to be slow. The receiver will in fact cease to operate satisfactorily once this assumption is relaxed. On the other hand, if very slow fading occurs, a quasi-stationary analysis allows the receiver structure to be simplified into an adaptive version of the digital phase-locked loop.

The most severe problem in a fading environment is the problem of the signal going into a deep fade during which the receiver will be operating below threshold. The assumption of slow fading means a longer fraction of time spent once the received signal goes into a deep fade and limits the performance of receivers to the order of 5-7dB worse than those obtained with no fading.

To improve the overall performance of the receiver, fixed-lag smoothing techniques were used but the results show only better performance at high signal-to-noise ratios. To overcome

the deep fade problem, the use of diversity techniques recasted in the framework of estimation theory proves to be the only solution to the problem.

The main contributions of this thesis are related to the following areas:

(i) Derivation of the discrete receivers for demodulating an analog FM signal transmitted over Rayleigh fading channels using both scalar and quadrature sampling techniques and employing the EKF and MAP algorithms.

(ii) Simplification of the receiver into an adaptive phase-locked loop for very slow fading channels.

(iii) Illustration of the better performance of the MAP algorithm over the EKF algorithm for the communication problem considered in this thesis.

(iv) Showing that the use of fixed-lag smoothing does not improve the performance of the receivers to warrant the increased complexity.

(v) Derivation of optimum diversity receiver structure based on estimation theory and demonstrate its superiority.

STATEMENT

I declare that this thesis contains no material which has been accepted for the award of any other degree at this or any other University, and that to the best of my knowledge contains no material previously written or published by any other person, except where otherwise acknowledged in the text.

Nguyen Huu Le

ACKNOWLEDGEMENTS

It is a pleasure to express my sincere appreciation to my Supervisors Dr. B. R. Davis and Professor R. E. Bogner for their help and encouragement throughout this research. Dr. Davis has been very understanding when things do not seem to go well. Professor Bogner has been a constant source of professional inspiration and his advice on preparing the thesis is most appreciated.

I wish to acknowledge the many stimulating hours of discussion I had with my fellow colleagues Messrs. C. T. Beare and R. P. Coutts on various aspects of computer simulation.

I wish also to thank my wife for her quiet support during the last days of preparation.

Lastly, I wish to thank Jillian Sandison and Margaret Drake for typing this thesis. Jillian in particular has been most patient with my handwriting and my constant rearrangement.

LIST OF TABLES

1. INTRODUCTION

1.1. Motivation

The main motive behind the work to be presented in this thesis has been the tremendous success in applying modern estimation theory to the design of phase-locked loops for optimum demodulation of analog FM signals transmitted over additive noise channels. A brief review of these is presented in Section 1.2. When the analog FM signal is transmitted over multipath media, Rayleigh fading equivalent to multiplicative noise will be introduced. There have been a number of investigators studying the problem of demodulating an analog FM signal transmitted over Rayleigh fading channels using estimation theory as will be reviewed in Section 1.3. Most of these works, apart from those of Dharamsi and Gupta (1975a, 1975b) and Takhar and Gupta (1976), mainly dealt with theoretical novel demodulator structures and are presented without any simulation results. The aim of this thesis is to extend the works already in existence to provide a complete treatment of the problem of demodulating an analog FM signal transmitted over Rayleigh fading channels using discrete type of receivers. The rest of this chapter is to provide a review of the works relevant to this problem.

1.2 Phase-locked Loops for Optimal FM Demodulation

1.2.1. Analog Phase-locked Loops

Classical Approach:

The development of the analog phase-locked loop as an optimum FM demodulator has evolved through two distinct but related directions, the first via application of classical feedback theory and the second following an application of nonlinear estimation theory. No description of the works belonging to the first category is

given here but a good account can be found in Klapper and Frankle (1972). Lehan and Parks (1953) made the first attempt at applying estimation theory to the demodulation problem. Youla (1954) extended this work and introduced the maximum *a posterior* probability (MAP) estimate. Their receivers were interpreted as feedback structures very similar to the phase-locked loop. A good account of these works can be found in Van Trees (1971). Essentially, the MAP approach leads to an integral equation for the message estimate and the solution to this corresponds to a physically unrealisable demodulator (Figure 1.1). Van Trees suggests making an approximation to the unrealisable demodulator for the purpose of implementation. In consists of a cascade of a nonlinear realisable demodulator and a physically unrealisable linear filter (Figure 1.2). The whole system can then be approximated arbitrarily closely by allowing delay in the post-loop operations. For FM demodulation under low-noise case, the realisable portion of the receiver is recognised as a phase-locked loop (Figure 1.3).

State-Variable Techniques:

Another significant contribution was made by Snyder (1969) who first used the state-variable approach to the optimum demodulation problem based upon the theory of Markov processes (Kushner, 1967). The state-variable approach leads directly to a physically realisable demodulator which is equivalent to the realizable portion of the MAP demodulator discussed above. Snyder established quasi-optimum (optimum for large SNR) FM demodulators for a stationary Gaussian message corrupted by additive white gaussian noise and these reduce to the form of phase-locked loops for large SNR. The state-variable approach has several advantages, notably

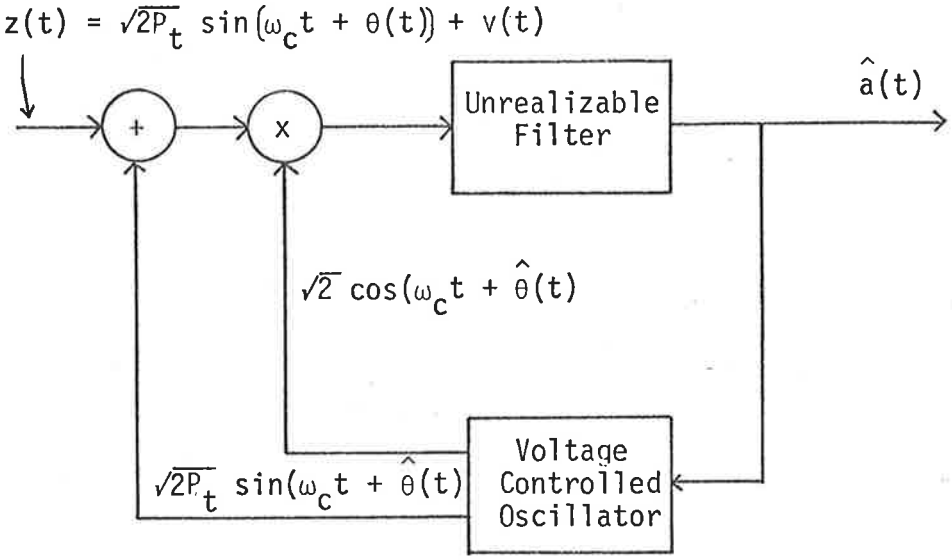

Fig. 1.1: Unrealizable optimum demodulator

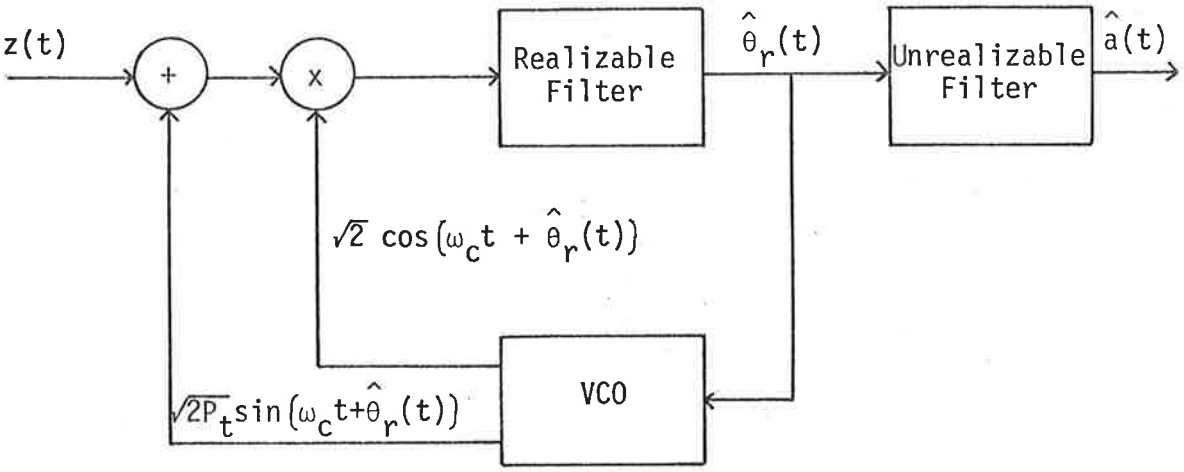

Fig. 1.2: Realizable (with delay) optimum demodulator

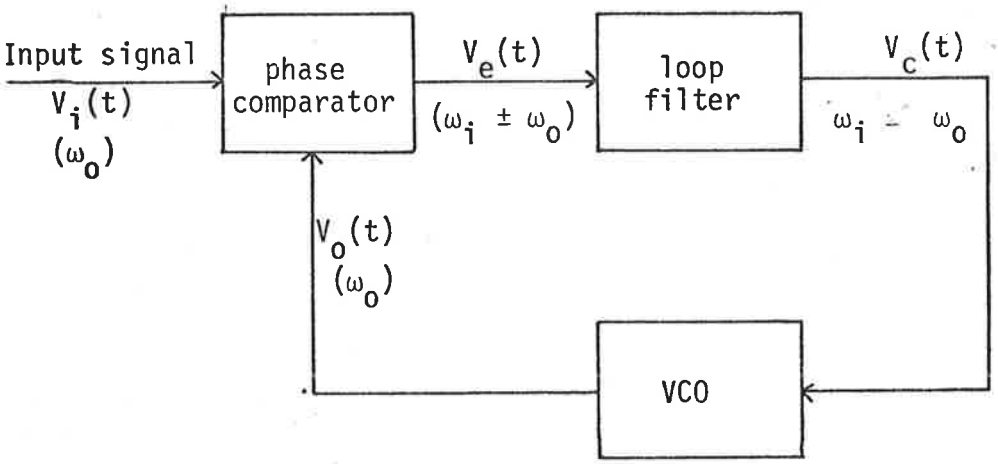

Fig. 1.3: Phase-locked loop

(i) easy formulation of the more complex systems, e.g. multiplicative noise channels or diversity systems, by the use of the augmented state vector, as will be done in this thesis,

(ii) direct application of results in modern estimation theory normally developed using state-variable models.

1.2.2. Digital Phase-locked Loops.

The requirements for compact and more accurate receivers has led investigators to consider digital realisations of the analog phase-locked loops. Advances in large-scale integrated (LSI) semiconductor technology has made digital processing of communication signals a much more attractive proposition with no more cost or power than some supoptimal analog demodulation methods. The voltage controlled oscillator (VCO) nonlinearities, inaccuracies in the phase detector, and the saturation problems due to noise spikes in the analog PLL, are eliminated by use of digital circuitry. The errors associated with digital systems, such as quantization, roundoff and overflow, are minor compared to the advantages of using digital processing.

The earlier works on digital phase-locked loops have been essentially heuristic approaches and can be broadly classified into three categories (as far as the phase-locked operation is concerned):

(i) hybrid PLL (Westlake, 1960; Gupta, 1968);

(ii) discrete PLL (Gill and Gupta, 1972; Weinberg and Liu, 1974); and

(iii) all-digital PLL (Natali, 1968; Pasternack and Whalin, 1968; Garodnick et al, 1972). These schemes are mainly concerned with the practical implementation of the phase-locked loop using digital techniques but there is no unified

theory equivalent to those developed for analog phase-locked loops. Kelly and Gupta (1972) made the first attempt to bridge the gap utilising recent developments in discrete estimation theory and state-variable approach. They extended the model of Snyder (1969) to a discrete-time observation sequence and applied Jazwinksi's (1970) continuous-discrete truncated and Gaussian second-order non-linear filters to obtain quasi-optimum digital demodulator structures. Their simulation results indicated performance comparable to the analog case. Polk and Gupta (1973) applied the discrete extended Kalman filter (EKF) and MAP estimation algorithms to obtain results identical to those of Kelly and Gupta (1972). Tam and Moore (1973) also extended the work to allow for fixed-lag smoothing. Under high SNR conditions, these filters are reduced to the form of a standard discrete Kalman filter. Employing quadrature sampling, McBride (1973) using the MAP algorithms, and Tam and Moore (1975) using a class of minimum variance algorithms, derived receiver structures whose performance are more readily simulated and are shown to be better than those using scalar sampling. By allowing for fixed-lag smoothing, Tam and Moore (1975) also achieved better performance.

1.3 Receivers for Fading Channels

In the framework of estimation theory, there have been a number of works studying the problem of demodulating an analog signal transmitting over fading channels, e.g. Schwartz (1964, 1966), Van Trees (1966, 1971), Boorstyn and Schwartz (1968), using the MAP approach of Youla (1954) as was done for the no fading case and result in a class of novel demodulator structures for linear and nonlinear modulation signals over various types of randomly time-varying channels. When specialised to the case of FM signals over Rayleigh fading channels, however, none of the above works contain any specific demodulator structures whose performance could be studied. To obtain an indication

of the effect of fading, the only results available seem to be from Schilling et.al. (1967) who considered the performance of an FM discriminator in a fading environment and found an irreducible error due to fading in the order of 3 - 7 dB for above threshold operation.

Recently, Dharamsi and Gupta (1975a, 1975b) extended the work by Kelly and Gupta (1972) for no fading to consider the problem of demodulating an FM signal transmitted over Rayleigh and Rician fading channels and obtained results for Rayleigh channels similar to those obtained independently in this thesis. Prasad and Mahalanabis (1974) also proposed fixed-lag receivers for fading channels but no result is obtained for FM signals. Painter, Gupta and Wilson (1973) developed a stochastic approximate model for the multipath channel for aeronautical communication and obtained simulation results (Painter and Wilson, 1974) for the recursive MAP detection of known M-ary signals. Takhar and Gupta (1976) also used this model to obtain results for analog FM signals. All the above results strongly suggest the feasibility of applying discrete estimation theory to derive a digital receiver for a wide class of communication systems. This thesis is an attempt to further explore in depth the performance of receivers for FM signal over Rayleigh fading channels in order to improve their performance.

1.4 Organization of the thesis

Chapter 2 will develop the analog communication model for an analog FM transmitted over Rayleigh fading channel using state-variable approach. The equivalent discrete model will be then derived. Chapter 3 will outline the developments of the EKF and the MAP filtering algorithms. Chapter 4 will discuss the use of computer simulation to study the performance of communication receivers. Chapter 5 will study the performance of receivers using scalar sampling. Chapter 6 will

consider receivers using quadrature sampling. Chapter 7 will discuss fixed-lag receivers and Chapter 8 will investigate the use of diversity techniques to combat fading. The thesis will conclude in Chapter 9 with a summary of the results obtained.

2. ANALOG AND DISCRETE COMMUNICATION MODELS

In this chapter, an analog communication model for frequency modulated (FM) signals transmitted over Rayleigh fading channel is developed using state variable formulation in Section 2.1. The equivalent discrete communication model is derived in Section 2.2. The last section (2.3) will discuss the sampling schemes to be employed.

2.1 Analog Communication Model

Figure 2.1 is the block diagram of a communication system in which the message $a(t)$ is frequency modulated resulted in a modulated signal $s(t)$ to be transmitted over a channel which introduces both multiplicative noise characterised by Rayleigh fading and additive noise. The received signal $z(t)$ is the sum of $h(t)$, the output from the Rayleigh channel and $n(t)$, the additive noise normally assumed to be a white gaussian process.

2.1.1 Message

The random analog message $a(t)$ is modelled as a stationary scalar gaussian process with a rational spectrum that approaches zero at high frequencies and can be represented by the differential equation

$$\frac{d^n}{dt} a(t) + \psi_1 \frac{d^{n-1}}{dt^{n-1}} a(t) + \ldots + \psi_n a(t)$$

$$= \lambda_1 \frac{d^{n-1}}{dt^{n-1}} u_a(t) + \lambda_2 \frac{d^{n-2}}{dt^{n-2}} u_a(t) + \ldots + \lambda_n u_a(t) \qquad (2.1)$$

where ψ_i's and λ_i's are constant coefficients and $u_a(t)$ is a zero-mean white gaussian process of unity variance. In other words, $a(t)$ can be represented as the output of a linear filter with the transfer function (Figure 2.2).

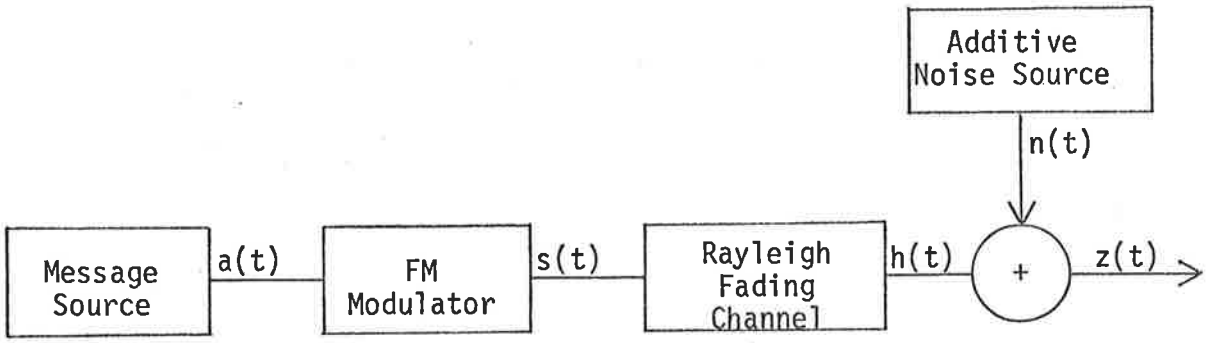

Figure 2.1. Analog FM Communication Model.

$$H(s) = \frac{\lambda_1 s^{n-1} + \lambda_2 s^{n-2} + \ldots + \lambda_n}{s^n + \psi_1 s^{n-1} + \ldots + \psi_n} \tag{2.2}$$

As an example is the class of Butterworth messages with the transfer function

$$H(s) = \frac{1}{s^n + \psi_1 s^{n-1} + \ldots + \psi_{n-1} s + 1} \tag{2.3}$$

such that the amplitude response is

$$|H(j\omega)| = \frac{k}{(1 + \omega^{2n})^{\frac{1}{2}}} \tag{2.4}$$

where k is a constant.

The equivalent state-variable realization of Equation 2.1 can be obtained by representing $a(t)$ by any one of several possible equations of state. A particular set of state equations is (Snyder, 1969)

$$\begin{aligned}
\frac{d}{dt} m_1(t) &= -\psi_1 m_1(t) + m_2(t) + \lambda_1 u_a(t) \\
\frac{d}{dt} m_2(t) &= -\psi_2 m_1(t) + m_3(t) + \lambda_2 u_a(t) \\
&\vdots \\
\frac{d}{dt} m_{n-1}(t) &= -\psi_{n-1} m_1(t) + m_n(t) + \lambda_{n-1} u_a(t) \\
\frac{d}{dt} m_n(t) &= -\psi_n m_1(t) + \lambda_n u_a(t)
\end{aligned} \tag{2.5}$$

where $a(t) = m_1(t)$. That this set of n first-order differential equations is equivalent to the n-th order differential Equation 2.1 for $a(t)$ can be verified by successively differentiating the first-order equations.

Equation 2.5 leads to the alternative realization of $a(t)$ as shown in Figure 2.3. Using matrix notation, Equation 2.5 can be written as a first-order vector state equation

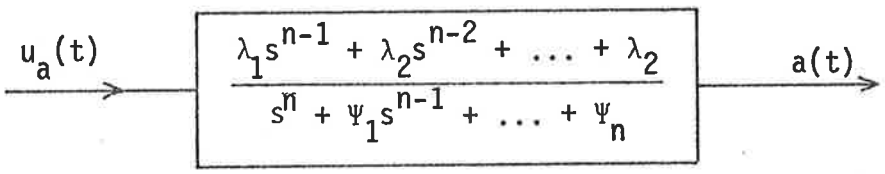

Figure 2.2: Transfer Function Realization of a(t).

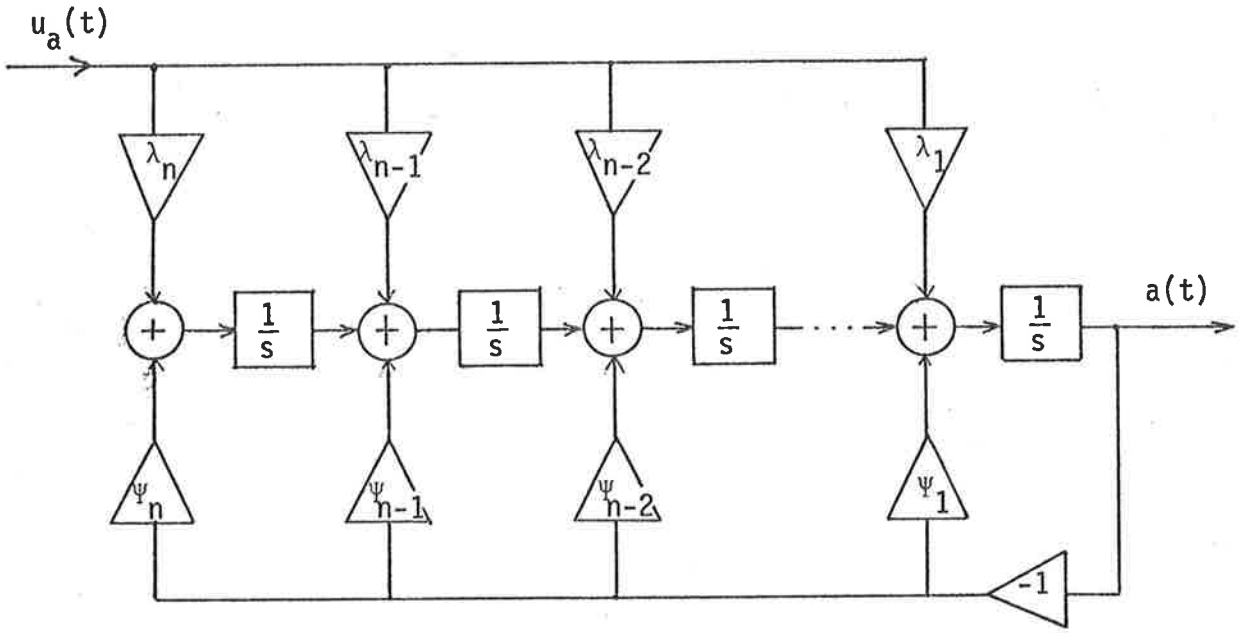

Figure 2.3: State Variable Realization of a(t).

$$\dot{\underline{m}}(t) = \underline{F}_a \, \underline{m}(t) + \underline{G}_a \, u_a(t) \tag{2.6}$$

where

$$\underline{m}(t) = \begin{pmatrix} m_1(t) \\ m_2(t) \\ \vdots \\ m_n(t) \end{pmatrix}$$

is an n-dimension message state vector with the first component being the scalar message $a(t)$ (2.6a)

$$\underline{F}_a = \left(\begin{array}{c|ccc} -\psi_1 & & & \\ -\psi_2 & & I_{n-1} & \\ \vdots & & & \\ \hline -\psi_n & 0 & \cdots & 0 \end{array}\right)$$

is an $n \times n$ matrix with I_{n-1} being an identity matrix of dimension $(n-1) \times (n-1)$ (2.6b)

$$\underline{G}_a = \begin{pmatrix} \lambda_1 \\ \lambda_2 \\ \vdots \\ \lambda_n \end{pmatrix}$$

is an n-dimension column vector (2.6c)

The message $a(t)$ is frequency modulated resulting in the output $s(t)$ of the FM modulator being written as

$$s(t) = \sqrt{2P_t}\sin(\omega_c t + \theta(t))$$

where

P_t is the average transmitted power

ω_c is the carrier frequency

$\theta(t)$ is the integral of the message

$$\theta(t) = d_f \int_0^t a(\tau)d\tau$$

and d_f is the frequency deviation (radians/sec).

We could incorporate $\theta(t)$ into the message state vector $\underline{m}(t)$ by defining $\theta(t)$ as an additional component resulting in

$$\underline{m}(t) = \begin{pmatrix} m_1(t) \\ m_2(t) \\ \vdots \\ m_{n+1}(t) \end{pmatrix} \qquad \begin{aligned} \text{with} \quad & m_1(t) \triangleq \theta(t) \quad \leftarrow \text{ phase} \\ & m_2(t) \triangleq a(t) \quad \leftarrow \text{ message} \\ \text{and} \quad & \dot{m}_1(t) \triangleq d_f\, m_2(t) \end{aligned} \tag{2.7a}$$

and now $\underline{m}(t)$ becomes an (n+1)-dimension state vector and Equation 2.6 now has

$$\underline{F}_a = \left(\begin{array}{c|c|ccc} 0 & d_f & 0 & \cdots & 0 \\ \hline 0 & -\psi_1 & & & \\ \vdots & \vdots & & I_{n-1} & \\ \hline 0 & -\psi_n & 0 & \cdots & 0 \end{array}\right) \qquad \text{an } (n+1) \times (n+1) \text{ matrix} \tag{2.7b}$$

$$\text{and} \quad \underline{G}_a = \begin{pmatrix} 0 \\ \lambda_1 \\ \vdots \\ \lambda_n \end{pmatrix} \qquad \text{an } (n+1) \text{ column vector.} \tag{2.7c}$$

2.1.2 Rayleigh fading channel

Fading of a signal is said to occur when the receive level varies from the free-space calculated level for a given far-end transmitter output. The mechanisms causing fading involves refraction, reflection, defraction, scattering, and other miscellaneous causes such as rainfall above 10 GHz (Freeman, 1975, Section 5.11) and result in various types of fading each having a different characteristic.

Multipath fading, often found in troposcatter (Fig. 2.4(a)) and mobile radio communications, is due to interference between a direct wave and another

wave, usually a reflected wave. The reflection may be from the ground, the buildings or from atmosphere layers. Detailed discussion of multipath fading phenomenon is to be found in Schwartz et al (1966) in which several chapters are devoted to the fading problems of radio signals. A more throughout treatment of fading dispersive channels is in Kennedy (1969) whose complete text is devoted to the subject. For the purpose of this study, it is sufficient to state here the assumptions behind a Rayleigh fading model.

Consider first a single sine wave tone being transmitted over a multipath medium in which the time differentials between the paths are smaller than the period of the sine wave tone. The received combined signal tends to have a Rayleigh fading envelope and a uniformly distributed phase.

When a packet of frequencies, i.e. a bandpass signal such as the one found in an FM modulated signal, is being transmitted over the same multipath fading medium, and, if

$$T_M << \frac{1}{W} \tag{2.9}$$

where T_M is a measure of the overall time delay spread in the multipath and W is the bandwidth of the bandpass signal, the fading effecting the various frequency components within the band is the same and is said to be non-selective. The maximum values of W for which relation 2.9 is valid is termed the coherence bandwidth.

The assumption of Rayleigh fading allows the output h(t) from the fading channel to be written as

$$h(t) = \sqrt{2P_t}\, r(t) \sin(\omega_c t + \theta(t) + \phi(t)) \tag{2.10}$$

where r(t), the envelope, has a Rayleigh distribution (Figure 2.4b)

$$p_r(r) = \frac{r}{\sigma^2} e^{-r^2/2\sigma^2} \tag{2.11}$$

with mean

$$E(r) = \sqrt{\frac{\pi}{2}}\,\sigma \tag{2.11a}$$

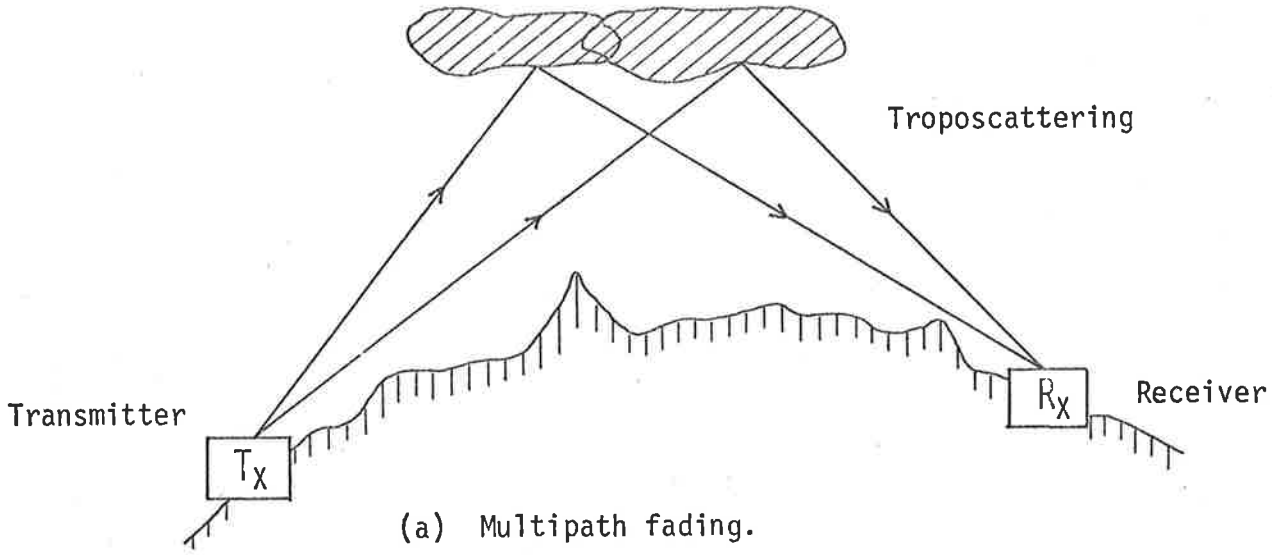

(a) Multipath fading.

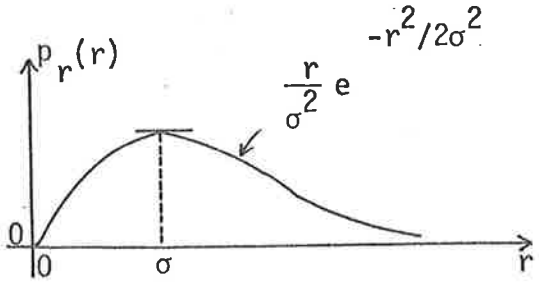

(b) Fading envelope distribution.

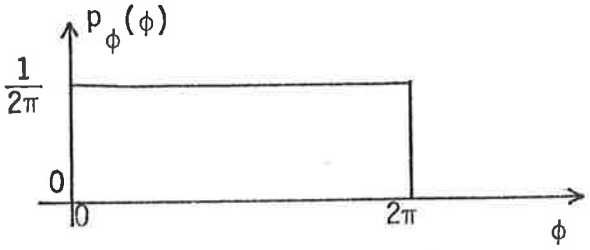

(c) Fading phase distribution.

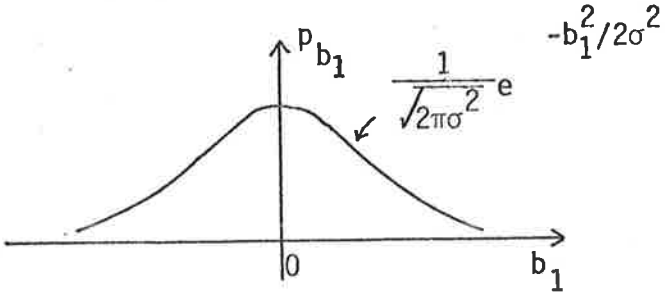

(d) Gaussian distribution.

Figure 2.4.

and mean square values

$$E(r^2) = 2\sigma^2 \tag{2.11b}$$

The random phase $\phi(t)$ is uniformly distributed between 0 and 2π (radians). (Figure 2.4c).

$$p_\phi(\phi) = \frac{1}{2\pi} \tag{2.12}$$

It can be further shown that h(t) can be resolved into a sum of an in-phase (or direct) and a quadrature component as follows

$$h(t) = \sqrt{2P_t}\,[b_1(t) \sin(\omega_c t + \theta(t)) + b_2(t) \cos(\omega_c t + \theta(t))] \tag{2.13}$$

where $b_1(t)$ and $b_2(t)$ are statistically independent gaussian process (Figure 2.4d) each having zero mean and variance σ^2. Furthermore they have identical "low-pass" power spectral densities and can be modelled as the output of linear dynamical systems in the same way as the modelling of the message process. These processes are to be called fading processes to distinguish them from the message process. The differential equations describing these processes are as follows:

$$\dot{\underline{p}}(t) = \underline{F}_{b_1}\,\underline{p}(t) + \underline{G}_{b_1}\,u_{b_1}(t) \tag{2.14}$$

$$\dot{\underline{q}}(t) = \underline{F}_{b_2}\,\underline{q}(t) + \underline{G}_{b_2}\,u_{b_2}(t) \tag{2.15}$$

$$\underline{p}(t) = \begin{pmatrix} p_1(t) \\ p_2(t) \\ \cdot \\ \cdot \\ \cdot \\ p_m(t) \end{pmatrix}$$

an m-dimension state vector with the first component being the in-phase fading process $b_1(t)$

$$b_1(t) \triangleq p_1(t)$$

$$\underline{q}(t) = \begin{pmatrix} q_1(t) \\ q_2(t) \\ . \\ . \\ . \\ q_m(t) \end{pmatrix}$$

an m-dimension state vector with the first component being the quadrature fading process $b_2(t)$

$$b_2(t) \triangleq q_1(t)$$

$\underline{F}_{b_1}$ and $\underline{F}_{b_2}$ are m x m matrices.
$\underline{G}_{b_1}$ and $\underline{G}_{b_2}$ are m-dimension column vectors.
$u_{b_1}(t)$ and u_{b_2} are scalar white gaussian processes with zero mean and unity variance.

2.1.3 Additive noise

The output h(t) from the Rayleigh fading channel is further contaiminated by additive noise v(t) caused by both man-made and natural sources. An example is the thermal or resistance noise at the front end of the receiver. The continuous received signal is then

$$z(t) = h(t) + v(t) \tag{2.16}$$

and v(t) is normally assumed to be gaussian and have a spectrum broad enough to be considered as white noise.

2.1.4 Augmented system state vector

Note that the output of the Rayleigh fading channel h(t) as given by Equation 2.13 is a function of the 3 state vectors $\underline{m}(t)$, $\underline{p}(t)$ and $\underline{q}(t)$, an augmented system state vector can be defined by adjoining the individual state vectors in any order. This technique, first used by Snyder (1969), permits a wide class of communication systems being represented as an estimation model and allows direct applications of modern stochastic estimation techniques.

By adjoining the (n+1)-dimension message state vector $\underline{m}(t)$ with the m-dimension fading state vectors $\underline{p}(t)$ and $\underline{q}(t)$ into an augmented system state vector $\underline{X}(t)$ as below:

$$\underline{X}(t) \triangleq \begin{pmatrix} \underline{m}(t) \\ - - - - \\ \underline{p}(t) \\ - - - - \\ \underline{q}(t) \end{pmatrix} = \begin{pmatrix} x_1(t) & \leftarrow \theta(t) \\ x_2(t) & \leftarrow a(t) \\ \cdot & \\ \cdot & \\ \cdot & \\ x_{n+2}(t) & \leftarrow b_1(t) \\ \cdot & \\ \cdot & \\ \cdot & \\ x_{n+m+2}(t) & \leftarrow b_2(t) \\ \cdot & \\ \cdot & \\ \cdot & \\ x_{n+2m+1}(t) & \end{pmatrix} \tag{2.17}$$

Then by combining Equations 2.6, 2.14 and 2.15, the state equation for the system vector $\underline{X}(t)$ is given by

$$\dot{\underline{X}}(t) = \underline{F}\,\underline{X}(t) + \underline{G}\,\underline{U}(t) \tag{2.18}$$

where

$$\underline{F} \triangleq \begin{pmatrix} \underline{F}_a & \phi & \phi \\ \phi & \underline{F}_{b_1} & \phi \\ \phi & \phi & \underline{F}_{b_2} \end{pmatrix} \quad \text{an } (n+2m+1)\text{-dimension square matrix} \tag{2.18a}$$

$$\underline{G} \triangleq \begin{pmatrix} \underline{G}_a & \phi & \phi \\ \phi & \underline{G}_{b_1} & \phi \\ \phi & \phi & \underline{G}_{b_2} \end{pmatrix} \quad \text{an } (n+2m+1)\text{x}3 \text{ matrix} \tag{2.18b}$$

ϕ is the null matrix of appropriate dimension.

and

$$\underline{U}(t) \triangleq \begin{bmatrix} u_a(t) \\ u_{b_1}(t) \\ u_{b_2}(t) \end{bmatrix} \quad \text{an 3-dimension column matrix} \qquad (2.18c)$$

Furthermore if we define

$$\begin{aligned} \underline{L}_1 &\triangleq [1\ 0\ 0\ \ldots\ 0\ \ 0\ 0\ 0\ \ldots\ 0\ \ 0\ 0\ 0\ \ldots\ 0] \\ \underline{L}_2 &\triangleq [0\ 0\ 0\ \ldots\ 0\ \ 1\ 0\ 0\ \ldots\ 0\ \ 0\ 0\ 0\ \ldots\ 0] \\ \underline{L}_3 &\triangleq [0\ 0\ 0\ \ldots\ 0\ \ 0\ 0\ 0\ \ldots\ 0\ \ 1\ 0\ 0\ \ldots\ 0] \end{aligned} \qquad (2.19)$$

↑ 1st column; ↑ $(n+2)^{th}$ column; ↑ $(n+m+2)^{th}$ column; ↑ $(2m+n+1)^{th}$ column

Then written in terms of $\underline{X}(t)$

phase: $\theta(t) \triangleq x_1(t) = \underline{L}_1\underline{X}(t)$

in-phase fading component: $b_1(t) \triangleq x_{n+2}(t) = \underline{L}_2\underline{X}(t)$

quadrature fading component: $b_2(t) \triangleq x_{n+m+2}(t) = \underline{L}_3\underline{X}(t)$

The received signal $z(t)$ can then be written as

$$z(t) = h[\underline{X}(t)] + v(t) \qquad (2.20)$$

where

$$h[\underline{X}(t)] = \sqrt{2P_t}\ [\underline{L}_2\underline{X}(t) \sin(\omega_c t + \underline{L}_1\underline{X}(t)) + \underline{L}_3\underline{X}(t) \cos(\omega_c t + \underline{L}_1\underline{X}(t))] \qquad (2.21)$$

The formulation of the analog communication system using state-variable as described by Equations 2.18 - 2.20 is then complete and a block diagram of the system is shown in Figure 2.5.

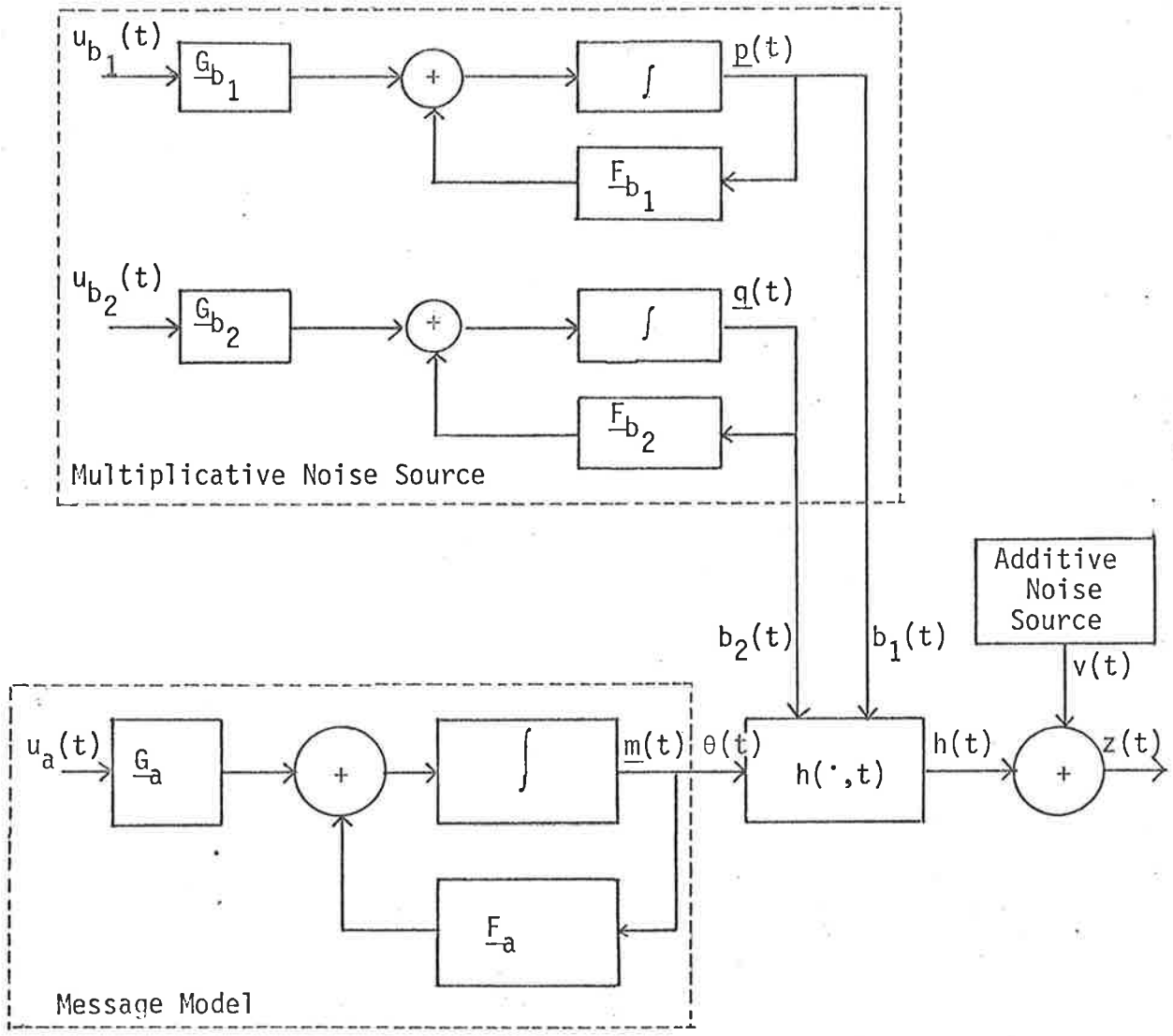

(a) Analog models for message and channel disturbances

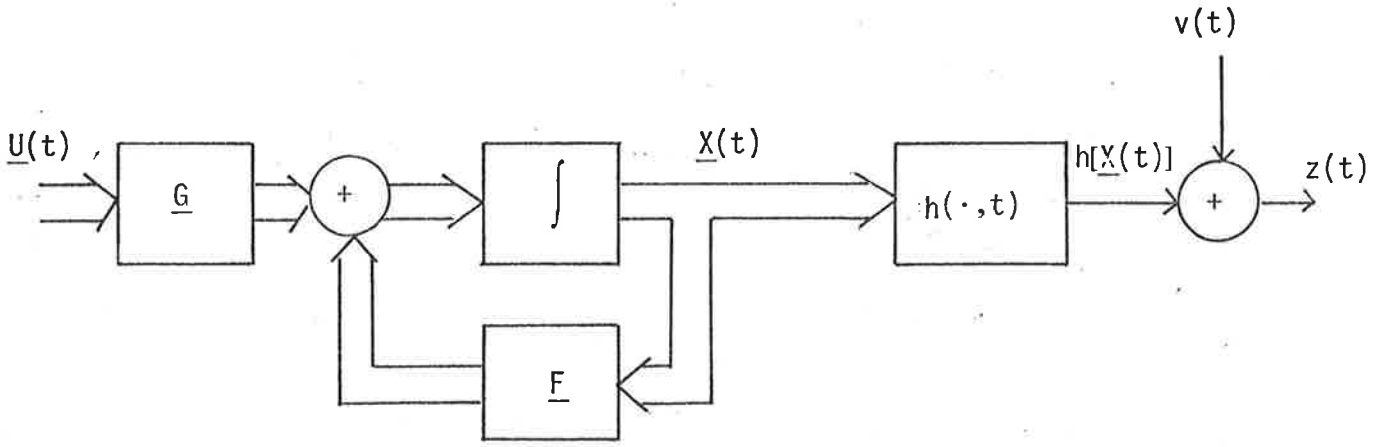

(b) General analog FM communication model

Figure 2.5

2.2 Discrete communication model

In order to generate and simulate the system state vector $\underline{X}(t)$ using digital techniques, the system model as described by the continuous differential equation 2.18 is to be converted into an equivalent discrete state-variable model. The common method for doing this is to convert Equation 2.18 into a difference equation. This involves the uses of various integration procedures and detailed descriptions can be found in many standard texts, e.g. Peikari (1974, Chapter 7). Another method (Mehra, 1969) is to discretize Equation 2.18 in such a way that the output of the discretized system possesses the same statistical properties at the sampling instants as the output of the continuous system. This method gives the same result as the one described below.

Consider the solution of Equation 2.18 (Peikari, 1974) which is

$$\underline{X}(t) = \Phi(t,t_o)\underline{X}(t_o) + \int_{t_o}^{t} \Phi(t,\tau)\underline{G}\,\underline{U}(\tau)dt \tag{2.22}$$

where $\Phi(t,t_o)$ is the transition matrix associated with the continuous system represented by Equation 2.18 and is the solution of the homogenous linear differential equation

$$\frac{d}{dt}\Phi(t,t_o) = \underline{F}\Phi(t,t_o) \tag{2.23}$$

with the boundary condition

$$\Phi(t_o,t_o) = \underline{I} \tag{2.23a}$$

As the system has been assumed to be stationary, $\underline{F}$ is a constant matrix and the solution of Equation 2.23 is given by

$$\Phi(t,t_o) = \Phi(t-t_o)$$

$$= e^{\underline{F}(t-t_o)} \tag{2.24}$$

By letting

$$t = t_k$$

$$t_o = t_{k-1}$$

The transition matrix $\Phi(t_k,t_{k-1})$ is dependent only on the sampling interval T

$$T \triangleq t_k - t_{k-1}$$

and is given by

$$\Phi(t_k,t_{k-1}) \triangleq \Phi(k,k-1)$$

$$= e^{\underline{F}T} \tag{2.25}$$

The solution (2.22) can then be put into a recursive form

$$\underline{X}_{k+1} = \Phi(k,k-1)\underline{X}(k) + \underline{W}(k) \tag{2.26}$$

$$\underline{W}(k) \triangleq \int_{t_{k-1}}^{t_k} \Phi(t_k,\tau)\,\underline{G}\,\underline{U}(\tau)\,d\tau \tag{2.27}$$

Since $\underline{U}(t)$ is a zero-mean white gaussian vector process, $\underline{W}(k)$ is a white gaussian sequence with zero-mean

$$E\,\underline{W}(k) = 0 \tag{2.28}$$

and variance

$$E\,\underline{W}(k)\underline{W}^T(j) = \underline{Q}(k)\delta_{kj} \tag{2.29}$$

where the covariance matrix is symmetrical and is given by

$$\underline{Q}(k) = \int_{t_{k-1}}^{t_k} \Phi(t_k,\tau)\underline{G}\underline{G}^T\Phi^T(t_k,\tau)\,d\tau \tag{2.29a}$$

Table I is a summary of the discrete model for the general analog for communication system. Equation I.1 is equivalent to the continuous message model (Equation 2.6) together with the definitions given by Equation 2.7a, 2.7b and 2.7c) whereas Equations I.2 and I.3 are equivalent to Equation 2.14 and 2.15 representing the continuous fading processes. The equivalent discrete system model (Figure 2.7) is derived directly from Equation 2.18 as was done above (Equation 2.26) or by adjoining the discrete models of the individual components (Equations I.4a, I.4b and I.4c).

The initial distribution of $\underline{X}(0)$ is assumed to be gaussian with mean $\underline{\mu}_{X_0}$ (normally assumed to be zero) and variance $\underline{V}_{X_0}$ as given by Equations I.5a and I.5b.

2.3 Scalar and quadrature sampling

The continuous received signal as given by Equation 2.20 is to be sampled and processed by a digital receiver. Two sampling techniques are used to obtain discrete samples suitable for digital processing. The first employs uniform or scalar sampling (Kohlenberg, 1953) and the second employs quadrature or second-order sampling (Kohlenberg, 1953, Grace and Pitt, 1968; and also Grace, 1970). McBride (1973) first applied the quadrature sampling

TABLE I

GENERAL DISCRETE MODEL FOR ANALOG FM COMMUNICATION SYSTEM OVER RAYLEIGH FADING CHANNELS

Message Model (n+1 dimensional)

$$\underline{m}(k) = \underline{\Phi}_a(k,k-1)\underline{m}(k-1)+\underline{W}_m(k) \tag{I.1}$$

Channel model (m dimensional)

$$\underline{p}(k) = \underline{\Phi}_{b1}(k,k-1)\underline{p}(k-1)+\underline{W}_p(k), \tag{I.2}$$

$$\underline{q}(k) = \underline{\Phi}_{b2}(k,k-1)\underline{q}(k-1)+\underline{W}_q(k) \tag{I.3}$$

Equivalent system model (2m+n+1 dimensional)

$$\underline{X}(k) = \underline{\Phi}(k,k-1)\underline{X}(k-1)+\underline{W}(k) \tag{I.4}$$

where

$$\underline{X}(k) = \begin{pmatrix} \underline{m}(k) \\ \hline \underline{p}(k) \\ \hline \underline{q}(k) \end{pmatrix} \quad \text{with} \quad \begin{cases} m_1(k) = \theta(k) \\ m_2(k) = a(k) \end{cases} \quad \text{with} \quad p_1(k) = b_1(k) \quad \text{with} \quad q_1(k) = b_2(k) \tag{I.4a}$$

$$\underline{\Phi}(k,k-1) = \left(\begin{array}{c|c|c} \underline{\Phi}_a(k,k-1) & \phi & \phi \\ \hline \phi & \Phi b_1(k,k-1) & \phi \\ \hline \phi & \phi & \Phi b_2(k,k-1) \end{array}\right) \tag{I.4b}$$

$$\underline{W}(k) = \begin{pmatrix} \underline{W}_m(k) \\ \hline \underline{W}_p(k) \\ \hline \underline{W}_q(k) \end{pmatrix} \quad \text{with } E[\underline{W}(k)\underline{W}^T(j)] = \underline{Q}(k)\delta_{kj} \tag{I.4c}$$

Initial conditions

$$E[\underline{X}(0)] = \mu_{\underline{X}_0} \tag{I.5a}$$

$$E[\underline{X}(0)\underline{X}^T(0)] = \underline{V}_{\underline{X}_0} \tag{I.5b}$$

Observation model

$$\underline{Z}(k) = \underline{h}[\underline{X}(k)]+\underline{V}(k) \tag{I.6}$$

with

$$E[\underline{V}(k)\underline{V}^T(j)] = \underline{R}(k)\delta_{kj} \tag{I.7}$$

For uniform sampling

$$h[\underline{X}(k)] = \sqrt{2P_t}[\underline{L}_2\underline{X}(k)\sin(\omega_c t_k+\underline{L}_1\underline{X}(k))+\underline{L}_3\underline{X}(k)\cos(\omega_c t_k+\underline{L}_1\underline{X}(k))] \tag{I.8}$$

For quadrature sampling

$$\underline{h}[\underline{X}(k)] = \sqrt{2P_t}\begin{pmatrix} \underline{L}_2\underline{X}(k) & \underline{L}_3\underline{X}(k) \\ -\underline{L}_3\underline{X}(k) & \underline{L}_2\underline{X}(k) \end{pmatrix}\begin{pmatrix} \sin(\underline{L}_1\underline{X}(k)) \\ \cos(\underline{L}_1\underline{X}(k)) \end{pmatrix} \tag{I.9}$$

Definitions

$$\begin{aligned} \underline{L}_1 &= [1\ 0\ 0\ \ldots\ 0\ \ 0\ 0\ 0\ \ldots\ 0\ \ 0\ 0\ 0\ \ldots\ 0] \\ \underline{L}_2 &= [0\ 0\ 0\ \ldots\ 0\ \ 1\ 0\ 0\ \ldots\ 0\ \ 0\ 0\ 0\ \ldots\ 0] \\ \underline{L}_3 &= [0\ 0\ 0\ \ldots\ 0\ \ 0\ 0\ 0\ \ldots\ 0\ \ 1\ 0\ 0\ \ldots\ 0] \end{aligned} \tag{I.10}$$

1st column; $(n+2)^{th}$ column; $(n+m+2)^{th}$ column; $(2m+n+1)^{th}$ column

$$\Phi_a(k,k-1) = e^{\underline{F}_a T} \tag{I.11a}$$

$$\Phi_{b1}(k,k-1) = e^{\underline{F}_{b1} T} \tag{I.11b}$$

$$\Phi_{b2}(k,k-1) = e^{\underline{F}_{b2} T} \tag{I.11c}$$

$$\underline{Q}(k) = \int_{t_{k-1}}^{t_k} \Phi(t_k,\tau)\underline{G}\underline{G}^T\Phi(t_k,\tau)d\tau \tag{I.12}$$

technique to derive optimum sampled-data FM demodulators (MAP filter, no fading) and it was later used by Tam and Moore (1975) to derive receivers using the extended Kalman filter, the modified truncated second-order filter and the modified Gaussian second-order filter. They considered the non-fading case only but extended their study to include fixed-lag demodulators. Prasad (1974) also used quadrature sampling technique in his study of fixed-lag receivers for fading channels. Apart from the resulting better performance of receivers using quadrature sampling techniques as reported in the studies mentioned above, another motivation for the use of quadrature sampling technique in the present study is that the filtering algorithms do not have carrier frequency terms and can be simulated directly without having to derive a baseband model as would be done for the uniform sampling case.

An important parameter to be considered is the minimum sampling rate required to sample a bandpass signal. The frequency-modulated bandpass signal is assumed to have a bandwidth of B (cycles/sec) centred at $\pm f_c$ (cycles/sec). (Figure 2.6a.)

2.3.1 Sampling rate for uniform sampling

The permissible values of the sampling period are given by (Kohlenberg, 1953)

$$\frac{m}{2 f_{min}} \leqslant T \leqslant \frac{m+1}{2 f_{max}} , \quad m = 0, 1, 2, \ldots \tag{2.30}$$

where

$$f_{min} = f_c - \frac{B}{2} \tag{2.30a}$$

$$f_{max} = f_c + \frac{B}{2} \tag{2.30b}$$

are assumed to be the minimum and maximum frequencies respectively of the FM bandpass signals (noting that the spectrum of an FM signal is strictly non-bandlimited).

Using the above relationship, Panter (1965) derived the minimum sampling frequency in terms of f_{max}, the highest frequency component as shown in Figure 2.6b. It can be seen that the minimum permissible sampling rate required always lies between 2B and 4B samples/sec

$$2B \leqslant (f_s)_{min} \leqslant 4B \text{ (samples/sec)} \tag{2.31}$$

Let t_k denote the discrete time sampling instants, the sampled received signal using uniform sampling is given by

$$z(t_k) \triangleq z(k)$$

$$= h\left[\underline{X}(t_k)\right] + v(t_k) \triangleq h\left[\underline{X}(k)\right] + v(k)$$

$$= \sqrt{2P_t}\left[\underline{L}_2\underline{X}(k)\sin(\omega_c t_k + \underline{L}_1\underline{X}(k)) + \underline{L}_3\underline{X}(k)\cos(\omega_c t_k + \underline{L}_1\underline{X}(k))\right] + v(k) \tag{2.32}$$

where v(k) is the sampled white-noise having zero mean and variance R(k) appropriately determined from r.

2.3.2 Sampling rate for quadrature sampling

The maximum sampling interval for quadrature sampling is given by (Grace and Pitt, 1968)

$$T_{max} = \frac{1}{f_c}\left[\frac{f_c}{B}\right] \leqslant \frac{1}{B} \tag{2.33}$$

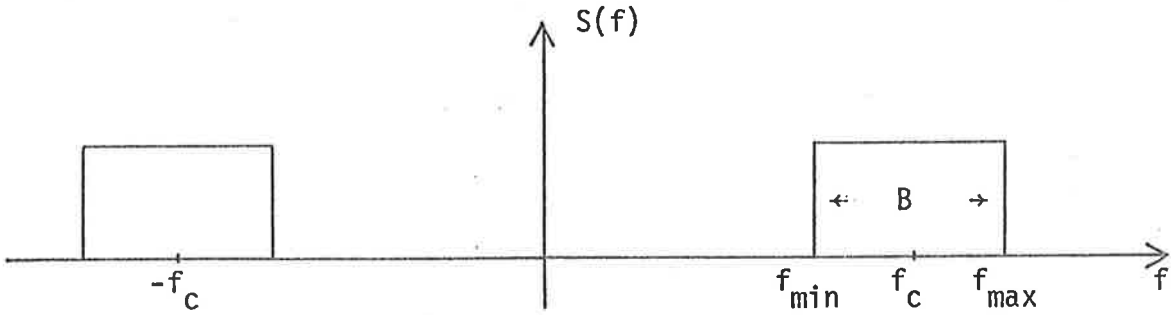

(a) FM bandpass spectrum

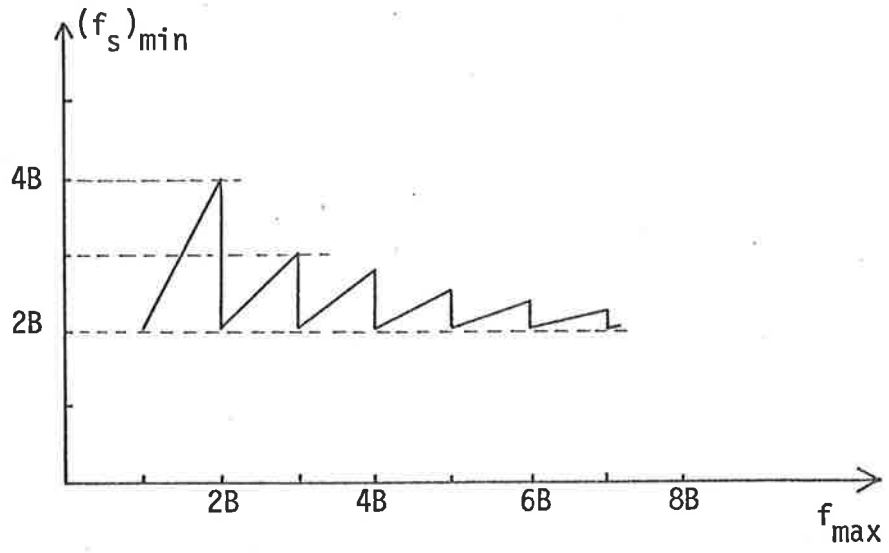

(b) Minimum Sampling Frequency for Band of Width B

(from Panter, 1965, p. 527)

FIGURE 2.6

where the symbol [·] denotes the greatest integer function.

To obtain the in-phase sample the FM bandpass signal z(t) as given by Equation 2.20 is sampled at time instant

$$t_k = k \frac{I}{f_c} \tag{2.34}$$

where k is the sample time index (k = 1, 2, 3 ...) and I is an integer such that

$$I \leqslant \frac{f_c}{B} \tag{2.34a}$$

then

$$z(t_k) = h\left(\underline{X}(t_k)\right) + v(t_k)$$

$$\triangleq h\left(\underline{X}(k)\right) + v(t_k)$$

$$= \sqrt{2P_t}\left(\underline{L}_2\underline{X}(k)\sin(\underline{L}_1\underline{X}(k)) + \underline{L}_3\underline{X}(k)\cos(\underline{L}_1\underline{X}(k))\right) + v_c(k) \tag{2.35}$$

The quadrature sample is obtained by sampling z(t) at time instant

$$t_k^* = t_k + \frac{1}{4f_c} \tag{2.36}$$

i.e. a quarter of a carrier cycle later (and hence the term "quadrature") and we obtain

$$z(t_k^*) = h\left(\underline{X}(t_k^*)\right) + v(t_k^*)$$

Since the carrier frequency f_c is usually much greater than the bandwidth of the components of $\underline{X}(t)$ so

$$\underline{X}(t_k^*) \doteq X(t_k) \tag{2.37}$$

and the quadrature component can be written as

$$z(t_k^*) = \sqrt{2P_t}\left[-\underline{L}_3\underline{X}(k)\sin(\underline{L}_1\underline{X}(k))+\underline{L}_2\underline{X}(k)\cos(\underline{L}_1\underline{X}(k))\right] + v(t_k^*) \tag{2.38}$$

The sampled noises $v(t_k)$ and $v(t_k^*)$ are independent white gaussian sequences having zero-mean and variance $R(k)$ appropriately determined from r.

$$E[v^2(t_k)] = E[v^2(t_k^*)] = R(k)$$

By defining the discrete observation and sampled noise vectors as

$$\underline{Z}(k) = \begin{bmatrix} z_1(k) \\ z_2(k) \end{bmatrix} \triangleq \begin{bmatrix} z(t_k) \\ z(t_k^*) \end{bmatrix}$$

$$\underline{V}(k) = \begin{bmatrix} v_1(k) \\ v_2(k) \end{bmatrix} \triangleq \begin{bmatrix} v(t_k) \\ v(t_k^*) \end{bmatrix}$$

and combine Equations 2.35 and 2.38 to give

$$\begin{aligned} \underline{Z} &= \underline{h}[\underline{X}(k)] + \underline{V}(k) \\ &= \sqrt{2P_t}\begin{bmatrix} \underline{L}_2\underline{X}(k) & \underline{L}_3\underline{X}(k) \\ -\underline{L}_3\underline{X}(k) & \underline{L}_2\underline{X}(k) \end{bmatrix}\begin{bmatrix} \sin(\underline{L}_1\underline{X}(k)) \\ \cos(\underline{L}_1\underline{X}(k)) \end{bmatrix}+\begin{bmatrix} v_1(k) \\ v_2(k) \end{bmatrix} \end{aligned} \tag{2.39}$$

with the covariance matrix of $\underline{V}(k)$ given by

$$\underline{R}(k) = \begin{pmatrix} R(k) & 0 \\ 0 & R(k) \end{pmatrix}$$

The derivation of the discrete communication model is complete and will be used as the estimation model for the derivation of the nonlinear filtering algorithms in Chapter 3. A block diagram of the discrete model showing the message model together with the observation models is shown in Figure 2.7.

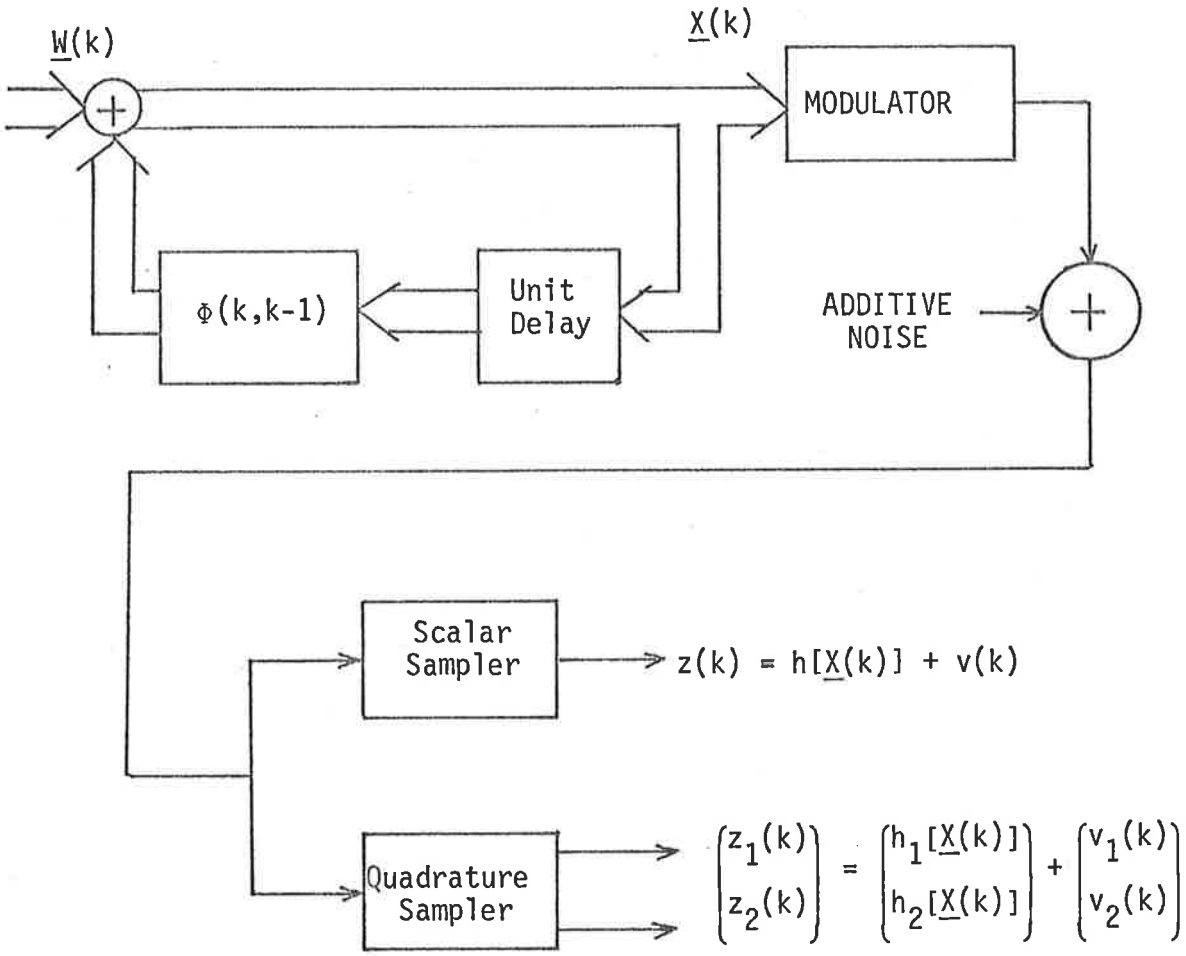

Figure 2.7: Discrete FM Communication Model

3. DISCRETE NON-LINEAR FILTERING ALGORITHMS

Having formulated the FM communication model as an estimation model in Chapter 2, this chapter will briefly discuss the derivations of the most well known nonlinear filtering algorithms that have found applications in a wide range of practical problems, notably in the dominant aerospace areas and also in other diverse fields such as electric power systems (e.g. Miller and Lewis, 1971), speech processing (e.g. Gibson and Melsa, 1976), and of course communication systems as already discussed in Chapter 1. Section 3.1 will give a brief historical account of estimation theory in connection with the thesis. The estimation problem is formulated in Section 3.2 and will consider the class of linear system model and nonlinear discrete observations. Sections 3.3 and 3.4 will outline the developments of the extended Kalman filter (EKF) algorithm and the maximum *a posterior* probability (MAP) filtering algorithms. Section 3.5 will conclude with a discussion on the merits of these two algorithms as have been found in the literature.

3.1 Introduction

The problem of obtaining an optimum estimate of a message contaminated by noise was formulated and solved by Wiener (1949) and independently by Kolmogorov (1941). They used as the optimal estimate a linear combination of the observed signal that would minimise the mean square error of the estimate. The end result was the specification of the weighting function of the optimal linear filter as a solution of the Wiener-Hopf equation. This is an integral equation which relates the correlation functions of the message and noise with the impulse response of the optimum linear filter (called Wiener filter). The solution is dependent on the assumptions of

(i) stationarity of the message and noise processes, and

(ii) knowledge of the entire past of the observed process.

The Wiener filter is thus limited to linear processing of stationary processes involving the use of the correlation functions of the processes. Kalman (1960) developed an alternative approach for the general nonstationary filtering problem by representing the message and noise processes with differential equations. The optimum linear estimate is then specified as the solution to a differential equation whose coefficients are determined by the statistics of the message and noise processes. The resulting Kalman filter can be considered as a true time-varying Wiener filter (Anderson and Moore, 1971) and is easier to solve using analog or digital techniques.

If the message and/or observation models are non-linear then the Kalman filter does not apply. However, by linearising the models (using a Taylor series expansion about the current predicted estimate and assuming that the estimation error is small), the Kalman filter algorithm can be used to give an approximate nonlinear filter. This is the extended Kalman filter (Jazwinski, 1970) and will be discussed further in Section 3.3.

The general nonlinear problem was first studied by Kushner (1964) using the probalistic approach in which stochastic differential equations were used to model the message and observations. Kushner (1967) also shows that the optimum nonlinear minimum variance filter is infinite dimensional in that all the moments of the conditional probability density function are required in order to solve for the optimal estimate. Approximation techniques are thus required and Section 3.4 will consider the maximum *a posterior* approach in which the conditional probability density function is maximised.

3.2 Problem formulation

The discrete communication model developed in Chapter 2 can be considered as a special class if more general estimation models in which the system and observation models are given by

$$\underline{X}(k) = \underline{f}\,[\underline{X}(k-1)] + \underline{W}(k) \tag{3.1}$$

$$\underline{Z}(k) = \underline{h}\,[\underline{X}(k)] + \underline{V}(k) \tag{3.2}$$

In this thesis, the message model is assumed to be linear time-invariant system described by

$$\underline{X}(k) = \Phi(k,k-1)\underline{X}(k-1)+\underline{W}(k) \tag{3.3}$$

where $\Phi(k,k-1)$ is the transition matrix and $\underline{W}(k)$ is assumed to be white gaussian noise sequence with zero mean and covariance

$$E[\underline{W}(k)\underline{W}^{T}(j)] = \underline{Q}(k)\delta_{kj} \tag{3.4}$$

The initial state $\underline{X}(0)$ is assumed to be gaussian with mean

$$E[\underline{X}(0)] = \underline{\mu}_{\underline{X}_0} \tag{3.5a}$$

and covariance

$$E[\underline{X}(0)\underline{X}^{T}(0)] = \underline{V}_{\underline{X}_0} \tag{3.5b}$$

The observation function $\underline{h}$ (.) depends on the type of modulation used. In an FM system, $\underline{h}$(.) is a nonlinear function of $\underline{X}(k)$.

The additive noise $\underline{V}(k)$ is also assumed to be white gaussian noise sequence with zero mean and covariance

$$E[\underline{V}(k)\underline{V}^T(j)] = \underline{R}(k)\delta_{kj} \tag{3.6}$$

Furthermore, it is assumed that $\underline{W}(k)$, $\underline{V}(k)$ and $\underline{X}(0)$ are uncorrelated.

The filtering problem is defined as the problem of determining "in some optimum sense" an estimate of the system state vector $\underline{X}(k)$, say $\hat{\underline{X}}(k)$, given the set of observations

$$\underline{Z}^k \triangleq \{\underline{Z}(1), \underline{Z}(2), \ldots, \underline{Z}(k)\} \tag{3.7}$$

Consistent with the above definition is a widely accepted definition which states that the data $\underline{Z}^k$ are to be used to determine the *a posterior* density function $p[\underline{X}(k)|\underline{Z}^k]$. This density function provides the most complete description of the system that is possible.

The "optimum sense" is defined in terms of an error criterion and two of the most important criteria are

(i) Minimum mean-square (MMSE) error criterion: the estimate $\hat{\underline{X}}(k)$ is chosen so that the mean square error

$$E\left[(\underline{X}(k)-\hat{\underline{X}}(k))\ (\underline{X}(k)-\hat{\underline{X}}(k))^T\right] \tag{3.8}$$

is minimised.

(ii) Maximum *a posterior* probability (MAP) criterion: The estimate $\hat{\underline{X}}(k)$ is chosen so that the *a posterior* density is maximised

$$p\left(\hat{\underline{X}}(k)|\underline{Z}^k\right) = \max\left(p(\underline{X}(k)|\underline{Z}^k)\right) \tag{3.9}$$

3.3 MMSE Filters: Extended Kalman Filtering Algorithm

It is well known (Jazwinski, 1970) that the minimum variance estimate is given by the conditional mean

$$\hat{\underline{X}}(k) = E(\underline{X}(k)|\underline{Z}^k) \tag{3.10}$$

A recursive algorithm in which the solution for the *(k-1)* stage is used to obtain the solution for the *kth* stage can be obtained through the used of Bayes' rule to show (Ho and Lee, 1964) that the *a posterior* density evolves in the following manner

$$p(\underline{X}(k)|\underline{Z}^k) = c_k p(\underline{X}(k)|\underline{Z}^{k-1})\ p(\underline{Z}^k|\underline{X}(k)) \tag{3.11}$$

$$p(\underline{X}(k)|\underline{Z}^{k-1}) = \int p(\underline{X}(k-1)|\underline{Z}^{k-1}) p(\underline{X}(k)|\underline{X}(k-1)) d\underline{X}(k-1) \tag{3.12}$$

where the normalizing constant c_k is given by

$$1/c_k = p(\underline{Z}(k)|\underline{Z}^{k-1})$$

$$= \int p(\underline{X}(k)|\underline{Z}^{k-1}) p(\underline{Z}(k)|\underline{X}(k)) d\underline{X}(k) \tag{3.13}$$

The initial condition for Equation (3.11) is

$$p(\underline{X}(0)|\underline{Z}^0) = p(\underline{X}(0)) \tag{3.14}$$

The densities $p[\underline{Z}(k) \mid \underline{X}(k)]$ and $p[\underline{X}(k) \mid \underline{X}(k-1)]$ are gaussian as a result of $\underline{V}(k)$ and $\underline{W}(k)$ being gaussian and when used in conjunction with the initial conditions $p[\underline{X}(0)]$ provide a general solution to the nonlinear filtering problem. The actual evaluation of the Bayesian recursive relation (3.11) is not easy and various techniques have been developed (Sorenson, 1974) to compute (3.11) for specific nonlinear systems. The only exception is the case when the observation model is linear (having assumed that the message model is linear in Equation 3.3) then the *a posterior* density is gaussian and the conditional mean and variance are described by the well known Kalman filter equations (Kalman 1960, see also Sage and Melsa 1971, Table 7.2-2, p. 268).

The extended Kalman filtering algorithm used in this thesis is developed by expanding the nonlinear observation function $h[\underline{X}(k)]$ into a Taylor series about a nominal trajectory $\overline{\underline{X}}(k)$ and the series is truncated after the linear term to obtain

$$\begin{aligned} \underline{Z}(k) &= \underline{h}[\underline{X}(k)]+\underline{V}(k) \\ &= \underline{h}[\overline{\underline{X}}(k)]+ \frac{\partial \underline{h}[\overline{\underline{X}}(k)]}{\partial \overline{\underline{X}}(k)} \; [\underline{X}(k)-\overline{\underline{X}}(k)]+\underline{V}(k) \end{aligned} \tag{3.15}$$

By letting

$$\underline{X}^*(k) \triangleq \underline{X}(k)-\overline{\underline{X}}(k) \tag{3.16}$$

and

$$\underline{Z}^*(k) \triangleq \underline{Z}(k)-\underline{h}[\overline{\underline{X}}(k)] \tag{3.17}$$

Then Equation 3.15 can be written as

$$\underline{Z}^*(k) = \frac{\partial \underline{h}[\overline{\underline{X}}(k)]}{\partial \overline{\underline{X}}(k)} \underline{X}^*(k) + \underline{V}(k) \tag{3.18}$$

Furthermore, if the trajectory $\overline{\underline{X}}(k)$ is assumed to be such that, with given

$$\overline{\underline{X}}(0) \triangleq E[\underline{X}(0)] \tag{3.19}$$

then $\overline{\underline{X}}$ is generated by

$$\overline{\underline{X}}(k) = \Phi(k,k-1)\overline{\underline{X}}(k-1) \tag{3.20}$$

Equation 3.3 can then be put into the form

$$\underline{X}^*(k) = \Phi(k,k-1)\underline{X}^*(k-1) + \underline{W}(k) \tag{3.21}$$

which represents a linear system describing the "state deviation" $\underline{X}^*(k)$. The "observation deviation" $\underline{Z}^*(k)$ is thus processed by a Kalman filter to give an estimate of $\underline{X}^*(k)$, denoted as $\hat{\underline{X}}^*(k)$, and the estimate of the state vector $\underline{X}(k)$ is then given by

$$\hat{\underline{X}}(k) = \overline{\underline{X}}(k) + \hat{\underline{X}}^*(k) \tag{3.22}$$

The resulting algorithm using the above linearised model is known as the discrete extended Kalman filter (EKF) algorithm (Jazwinski, 1970, pp. 272-278) and is summarised in Table II with the trajectory $\overline{\underline{X}}(k)$ chosen as the propagated conditional mean $\hat{\underline{X}}(k|k-1)$ and given by the one-stage prediction algorithm (Equation

TABLE II

GENERAL DISCRETE EXTENDED KALMAN FILTER (EKF) FILTERING ALGORITHM

System model

$$\underline{X}(k) = \Phi(k,k-1)\underline{X}(k-1)+\underline{W}(k) \qquad \text{(II.1)}$$

Observation model

$$\underline{Z}(k) = \underline{h}[\underline{X}(k)]+\underline{V}(k) \qquad \text{(II.2)}$$

Statistical parameters

$$E[\underline{X}(0)] = \underline{\mu}_{\underline{X}_0} \qquad \text{(II.3a)}$$

$$E[\underline{X}(0)\underline{X}^T(0)] = \underline{V}_{\underline{X}_0} \qquad \text{(II.3b)}$$

$$E[\underline{W}(k)] = E[\underline{V}(k)] = 0 \qquad \text{(II.3c)}$$

$$E[\underline{W}(k)\underline{W}^T(j)] = \underline{Q}(k)\delta_{kj} \qquad \text{(II.3d)}$$

$$E[\underline{V}(k)\underline{V}^T(j)] = \underline{R}(k)\delta_{kj} \qquad \text{(II.3e)}$$

One stage prediction algorithm

$$\hat{\underline{X}}(k|k-1) = \Phi(k,k-1)\hat{\underline{X}}(k-1) \qquad \text{(II.4)}$$

$$\hat{\underline{X}}(0) = \underline{\mu}_{\underline{X}_0} \qquad \text{(II.4a)}$$

Prior error variance algorithm

$$\underline{V}_{\tilde{\underline{X}}}(k|k-1) = \Phi(k,k-1)\underline{V}_{\tilde{\underline{X}}}(k-1)\Phi^T(k,k-1)+\underline{Q}(k) \qquad \text{(II.5)}$$

$$\underline{V}_{\tilde{\underline{X}}}(0) = \underline{V}_{\underline{X}_0} \qquad \text{(II.5a)}$$

Error variance algorithm

$$\underline{V}_{\tilde{X}}(k) = \underline{V}_{\tilde{X}}(k|k-1) - \underline{V}_{\tilde{X}}(k|k-1)\underline{H}^T(k)\underline{M}^{-1}(k)\underline{H}(k)\underline{V}_{\tilde{X}}(k|k-1) \qquad \text{(II.6)}$$

where

$$\underline{H}(k) \triangleq \frac{\partial \underline{h}[\hat{\underline{X}}(k|k-1)]}{\partial \hat{\underline{X}}(k|k-1)} \qquad \text{(II.7)}$$

$$\underline{M}(k) \triangleq \underline{H}(k)\underline{V}_{\tilde{X}}(k|k-1)\underline{H}^T(k) + \underline{R}(k) \qquad \text{(II.8)}$$

Filtering algorithm

$$\hat{\underline{X}}(k) = \hat{\underline{X}}(k|k-1) + \underline{G}(k)\underline{\nu}(k) \qquad \text{(II.9)}$$

where

$$\underline{G}(k) \triangleq \underline{V}_{\tilde{X}}(k)\underline{H}^T(k)\underline{R}^{-1}(k) \qquad \text{(filter gain)} \qquad \text{(II.10)}$$

$$\underline{\nu}(k) \triangleq \underline{Z}(k) - \underline{h}[\hat{\underline{X}}(k|k-1)] \qquad \text{(innovation process)} \qquad \text{(II.11)}$$

II.2) corresponding to Equation 3.20 above. Discussions of the derivation of the EKF algorithm are also found in Sage and Melsa (1971, Table 9.4-3, p. 462) from which Table II was formed.

3.4 MAP Filtering Algorithm

It can be shown (Sage and Melsa, 1971, p. 443) that maximizing $p[\underline{X}(k_f)|\underline{Z}^{k_f}]$ (with k_f defined as another discrete time index) is equivalent to minimizing a scalar J given by

$$J = \frac{1}{2}\|\underline{X}(0)-\underline{\mu}_{\underline{X}_0}\|^2_{\underline{V}_{\underline{X}_0}^{-1}} + \frac{1}{2}\sum_{k=1}^{k_f}\|\underline{Z}(k)-\underline{h}[\underline{X}(k)]\|^2_{\underline{R}(k)^{-1}} + \frac{1}{2}\sum_{k=1}^{k_f}\|\underline{W}(k)\|^2_{\underline{Q}(k)^{-1}} \tag{3.23}$$

subject to the equality constraint (3.3) and the associated initial conditions (3.5).

Equation (3.23) suggests the application of the discrete maximum principle (Sage, 1968, Chapter 6) with the Hamiltonian defined as

$$H[\underline{X}(k),\underline{W}(k),\underline{\lambda}(k),k] \triangleq \frac{1}{2}\|\underline{Z}(k)-\underline{h}[\underline{X}(k)]\|^2_{\underline{R}(k)^{-1}} + \frac{1}{2}\|\underline{W}(k)\|^2_{\underline{Q}(k)^{-1}} + \underline{\lambda}^T(k)\underline{X}(k) \tag{3.24}$$

The canonic equations are given by

$$\hat{\underline{X}}(k|k_f) = \frac{\partial H}{\partial \underline{\lambda}(k)} \tag{3.25}$$

$$\underline{\lambda}(k|k_f) = \frac{\partial H}{\partial \underline{X}(k)} \Bigg| \underline{X}(k) = \hat{\underline{X}}(k|k_f) \tag{3.26}$$

$$\frac{\partial H}{\partial \underline{W}(k)} = 0 \tag{3.27}$$

with the two-point boundary conditions given by

$$\underline{\lambda}(k_o|k_o) = \underline{V}_{\underline{X}_0}^{-1} [\underline{\mu}_{\underline{X}_0} - \hat{\underline{X}}(0)] \tag{3.28}$$

and

$$\underline{\lambda}(k_f|k_f) = 0 \tag{3.29}$$

These canonic equations and the associated boundary conditions specify a nonlinear two-point boundary-value problem whose solution yield a fixed-interval "smoothing" solution $\hat{\underline{X}}(k|k_f)$ to stage k_f. If only the filtering solution $\hat{\underline{X}}(k_f|k_f)$ is desired then k_f is to be treated as a running variable and an approximate recursive solution may be obtained by using the discrete invariant imbedding techniques (Sage, 1968). The resulting algorithms are shown in Table III where it can be seen that the difference between the discrete EKF algorithm of Table II and the discrete MAP filtering algorithm is in the error variance equation. For the MAP filtering algorithm, the error variance equations involves the innovation process

TABLE III

GENERAL DISCRETE NONLINEAR MAP FILTERING ALGORITHMS

Systems model

$$\underline{X}(k) = \Phi(k,k-1)\underline{X}(k-1)+\underline{W}(k) \qquad \text{(III.1)}$$

Observation model

$$\underline{Z}(k) = \underline{h}[\underline{X}(k)]+\underline{V}(k) \qquad \text{(III.2)}$$

Statistical parameters

$$E[\underline{X}(0)] = \underline{\mu}_{\underline{X}_0} \qquad \text{(III.3a)}$$

$$E[\underline{X}(0)\underline{X}^T(0)] = \underline{V}_{\underline{X}_0} \qquad \text{(III.3b)}$$

$$E[\underline{W}(k)] = E[\underline{V}(k)] = 0 \qquad \text{(III.3c)}$$

$$E[\underline{W}(k)\underline{W}^T(j)] = \underline{Q}(k)\delta_{kj} \qquad \text{(III.3d)}$$

$$E[\underline{V}(k)\underline{V}^T(j)] = \underline{R}(k)\delta_{kj} \qquad \text{(III.3e)}$$

One stage prediction algorithm

$$\hat{\underline{X}}(k|k-1) = \Phi(k,k-1)\hat{\underline{X}}(k-1) \qquad \text{(III.4)}$$

$$\hat{\underline{X}}(0) = \underline{\mu}_{\underline{X}_0} \qquad \text{(III.4a)}$$

Prior error variance algorithm

$$\underline{V}_{\tilde{\underline{X}}}(k|k-1) = \Phi(k,k-1)\underline{V}_{\tilde{\underline{X}}}(k-1)\Phi^T(k,k-1)+\underline{Q}(k) \qquad \text{(III.5)}$$

$$\underline{V}_{\tilde{\underline{X}}}(0) = \underline{V}_{\underline{X}_0} \qquad \text{(III.5a)}$$

Error variance algorithm

Either

$$\underline{V}_{\tilde{X}}(k) = \underline{V}_{\tilde{X}}(k|k-1) - \underline{V}_{\tilde{X}}(k|k-1)\underline{J}^{T}(k)\underline{N}^{-1}(k)\underline{J}(k)\underline{V}_{\tilde{X}}(k|k-1) \qquad \text{(III.6)}$$

where

$$\underline{J}(k)\underline{R}^{-1}(k)\underline{J}(k) \triangleq -\frac{\partial}{\partial \hat{\underline{X}}(k|k-1)}\left(\frac{\partial \underline{h}^{T}[\hat{\underline{X}}(k|k-1)]}{\partial \hat{\underline{X}}(k|k-1)}\underline{R}^{-1}(k)\underline{\nu}(k)\right) \qquad \text{(III.6a)}$$

$$\underline{N}(k) \triangleq \underline{J}(k)\underline{V}_{\tilde{X}}(k|k-1)\underline{J}^{T}(k) + \underline{R}(k) \qquad \text{(III.6b)}$$

---

or

$$\underline{V}_{\tilde{X}}(k) = \left[\underline{I} + \underline{V}_{\tilde{X}}(k|k-1)\underline{M}[\hat{\underline{X}}(k|k-1),k]\right]^{-1}\underline{V}_{\tilde{X}}(k|k-1) \qquad \text{(III.7)}$$

$$= \underline{V}_{\tilde{X}}(k|k-1) - \underline{V}_{\tilde{X}}(k|k-1)\underline{M}[\hat{\underline{X}}(k|k-1),k] \cdot \left[\underline{I} + \underline{V}_{\tilde{X}}(k|k-1)\underline{M}[\hat{\underline{X}}(k|k-1),k]\right]^{-1}\underline{V}_{\tilde{X}}(k|k-1)$$

where

$$\underline{M}[\hat{\underline{X}}(k|k-1),k] \triangleq -\frac{\partial}{\partial \hat{\underline{X}}(k|k-1)}\left(\underline{H}(k)\underline{R}^{-1}(k)\underline{\nu}(k)\right) \qquad \text{(III.8)}$$

$$\underline{H}(k) \triangleq \frac{\partial \underline{h}^{T}[\hat{\underline{X}}(k|k-1)]}{\partial \hat{\underline{X}}(k|k-1)} \qquad \text{(III.9)}$$

$$\underline{\nu}(k) \triangleq \underline{Z}(k) - \underline{h}[\hat{\underline{X}}(k|k-1)] \quad \text{(innovation process)} \qquad \text{(III.10)}$$

Filtering algorithm

$$\hat{\underline{X}}(k) = \hat{\underline{X}}(k|k-1) + \underline{G}(k)\underline{\nu}(k) \qquad \text{(III.11)}$$

where

$$\underline{G}(k) \triangleq \underline{V}_{\tilde{X}}(k)\underline{H}^{T}(k)\underline{R}^{-1}(k) \quad \text{(filter gain)} \qquad \text{(III.12)}$$

$$\underline{\nu}(k) \triangleq \underline{Z}(k)-\underline{h}[\hat{\underline{X}}(k|k-1)] \tag{3.30}$$

and take two alternative forms. The first form (Equation III.6) is convenient to use when the Hessian matrix

$$-\frac{\partial}{\partial\hat{\underline{X}}(k|k-1)}\left\{\frac{\partial\underline{h}^T[\hat{\underline{X}}(k|k-1)]}{\partial\hat{\underline{X}}(k|k-1)}\right\}\underline{R}^{-1}(k)\underline{\nu}(k)$$

is positive definite and can be factorised as $\underline{J}(k)\underline{R}^{-1}(k)J(k)$. As will be seen later in Chapter 5, this is not the case for the problem considered in this thesis so the alternative form (Equation III.7) is used.

3.5 EKF versus MAP Algorithms

At the outset, the choice between the EKF algorithm and the MAP algorithm is not obvious. The EKF algorithm is the most popular one and has been found to performance satisfactorily provided that the assumptions inherent its development are verified by practical experience to be valid. There are also well-known disadvantages and difficulties associated with the application of the extended Kalman filter. The manifestation of these difficulties is commonly referred to as the diverjence problem (Nahi, 1976) which is said to occur when the actual error in the estimate becomes inconsistent with the error variance matrix approximation provided by the filter algorithms. In the application to be considered in this thesis, this is likely to occur when the signal goes into a deep fade and results in an instantaneous SNR level below threshold and render the estimation scheme to be invalid for the duration of the deep fade. Further discussions on the EKF algorithm can be found in Nahi (1976) and two comprehensive survey papers by Sorenson (1974a,

1974b).

The MAP algorithm is more complex and requires more computation time but has been found (McBride 1973; Pyle, 1974) to perform well in a situation when phase locking is required and thus the ability of the estimator to reach steady state operation is intimately connected with the initial set of observation data.

Due to lack of comparison results based on the experiences of other workers, it was however decided that both algorithms are employed and results are compared. It was found that the MAP algorithm is better than the EKF in terms of performance for the problems considered in this thesis.

4. SIMULATION METHODOLOGY

The filtering algorithms described in Chapter 3 will be applied to the communication model developed in Chapter 2 to derive the receiver structures whose performances are to be investigated by computer simulations. To reduce the dimension of the system state vector and render the simulation possible in terms of execution time, a simple 4-dimension model using the Ornstein-Ublenbeck stochastic processes (Ornstein and Ublenbeck, 1954) for the message and fading components will be developed in Section 4.1. These processes result when Gaussian white noise is passed through a low-pass filter described by a first-order transfer function and have a first-order Butterworth spectrum. Section 4.2 will give some theoretical considerations on the use of computer simulation to study receiver performance. Section 4.3 will set out the procedure followed in organising the simulation programs together with a description of the parameter set used in the programs. The latter is very important in interpreting and reproducing the results.

4.1 Example of an FM communication system

Consider a scalar message a(t) having a first-order Butterworth spectrum and represented by a first-order differential equation

$$\dot{a}(t) = -\alpha a(t) + \sqrt{2\alpha P_a}\, u_a(t) \qquad (4.1)$$

where $u_a(t)$ is a zero-mean white gaussian process having unity variance

$$E[u_a(t)\, u_a(\tau)] = \delta_D(t-\tau) \qquad (4.2)$$

$\delta_D(t)$ is the Dirac delta function

α and P_a are constants having special meanings as can be seen by first determining the transfer function corresponding to Equation 4.1.

$$H(s) = \frac{\sqrt{2\alpha P_a}}{s+\alpha} \tag{4.3}$$

The power spectrum of a(t) is then

$$S_a(\omega) = |H(j\omega)|^2 = \frac{2\alpha P_a}{\omega^2+\alpha^2} \tag{4.4a}$$

It can be verified from Equations 4.3 and 4.4a that α measured in radians/sec is the one-sided 3-dB bandwidth and is also the half-power frequency of the message power spectral density.

The autocorrelation function of a(t) is given by the Fourier transform of $S_a(\omega)_\infty$

$$R_a(\tau) = \frac{1}{2\pi}\int_{-\infty} S_a(\omega)e^{j\omega\tau}\, d\omega = P_a e^{-\alpha|\tau|} \tag{4.4b}$$

$1/\alpha$ is thus the correlation time and P_a is the average power of the message. Note that a(t) is a gaussian process with zero mean and variance P_a.

Figure 4.1 shows the plots of the frequency response $|H(j\omega)|$, the power spectrum $S_a(\omega)$ and the correlation function $R_a(\tau)$ for such a first-order Butterworth process.

If we define

$$\underline{m}(t) \triangleq \begin{bmatrix} m_1(t) \\ m_2(t) \end{bmatrix} \begin{matrix} \leftarrow \text{ phase} \\ \leftarrow \text{ message} \end{matrix}$$

where $m_2(t)$ is the message a(t) and $m_1(t)$ is the phase $\Theta(t)$

$$\Theta(t) = d_f \int_0^t a(\tau)d\tau$$

Then the state variable model for the message being FM modulated can be written as

$$\begin{bmatrix} \dot{m}_1(t) \\ \dot{m}_2(t) \end{bmatrix} = \begin{bmatrix} 0 & d_f \\ 0 & -\alpha \end{bmatrix} \begin{bmatrix} m_1(t) \\ m_2(t) \end{bmatrix} + \begin{bmatrix} 0 \\ \sqrt{2\alpha P_a} \end{bmatrix} u_a(t) \tag{4.5}$$

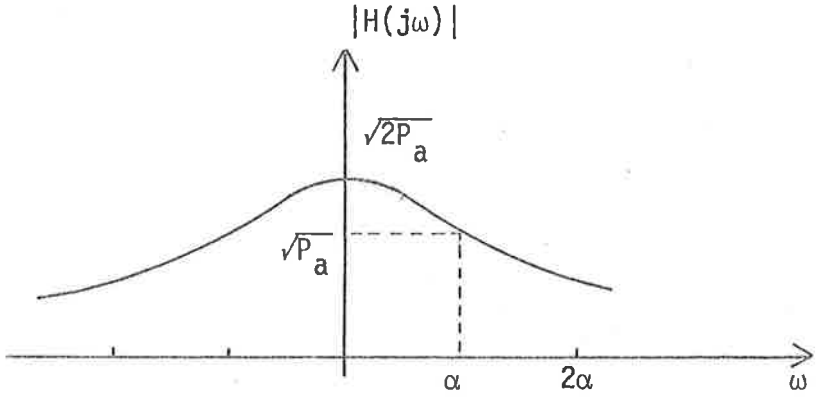

(a) Amplitude ratio

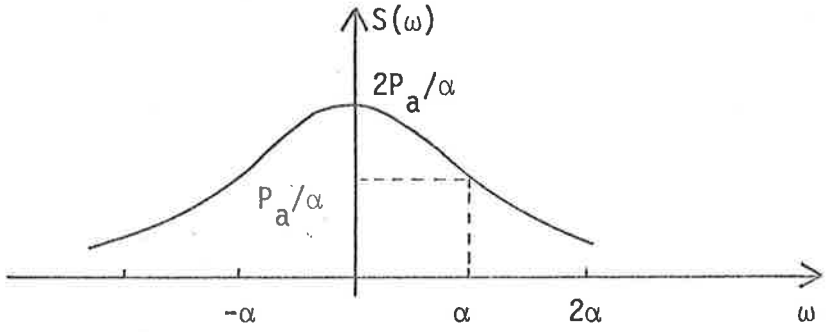

(b) Power spectrum

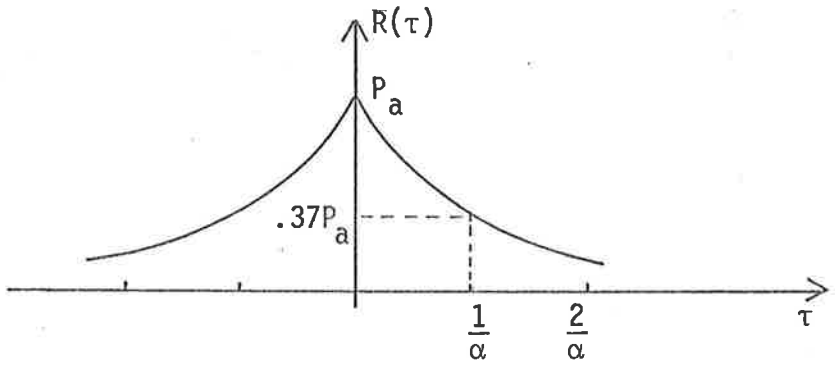

(c) Correlation function

Figure 4.1. Characteristics of a first-order Butterworth Process

The channel processes characterising the Rayleigh fading channel are also to be modelled as first-order Butterworth processes

$$\dot{b}_1(t) = -\gamma b_1(t) + \sqrt{2\gamma P_f}\, u_{b_1}(t) \tag{4.6}$$

$$\dot{b}_2(t) = -\gamma b_2(t) + \sqrt{2\gamma P_f}\, u_{b_2}(t) \tag{4.7}$$

where

$u_{b_1}(t)$ and $u_{b_2}(t)$ are zero-mean white gaussian processes having unity variances

$$E[u_{b_1}(t)\, u_{b_1}(\tau)] = E[u_{b_2}(t)\, u_{b_2}(\tau)] = \delta_D(t-\tau) \tag{4.8}$$

γ is the half-power frequency and P_f is the average power of the fading processes. Recall that $b_1(t)$ and $b_2(t)$ are supposed to be independent processes having identical statistics and thus $u_{b_1}(t)$ and $u_{b_2}(t)$ are independent of each other and are also independent of $u_a(t)$.

Now if we define

$$\underline{X}(t) = \begin{pmatrix} x_1(t) \\ x_2(t) \\ x_3(t) \\ x_4(t) \end{pmatrix} \triangleq \begin{pmatrix} \Theta(t) \\ a(t) \\ b_1(t) \\ b_2(t) \end{pmatrix} \begin{matrix} \leftarrow \text{ phase} \\ \leftarrow \text{ message} \\ \leftarrow \text{ in-phase fading component} \\ \leftarrow \text{ quadrature fading component} \end{matrix}$$

Then by combining Equations 4.5, 4.6 and 4.7 we get for the system state vector $\underline{X}(t)$ the following state differential equation:

$$\dot{\underline{X}}(t) = \underline{F}\underline{X}(t) + \underline{G}\underline{U}(t) \tag{4.9}$$

where

$$\underline{F} = \begin{pmatrix} 0 & d_f & 0 & 0 \\ 0 & -\alpha & 0 & 0 \\ 0 & 0 & -\dot{\gamma} & 0 \\ 0 & 0 & 0 & -\gamma \end{pmatrix} \tag{4.9a}$$

$$\underline{G} = \begin{pmatrix} 0 & 0 & 0 \\ \sqrt{2\gamma P_a} & 0 & 0 \\ 0 & \sqrt{2\gamma P_f} & 0 \\ 0 & 0 & \sqrt{2\gamma P_f} \end{pmatrix} \tag{4.9b}$$

$$\underline{U}(t) = \begin{pmatrix} u_a(t) \\ u_{b_1}(t) \\ u_{b_2}(t) \end{pmatrix} \tag{4.9c}$$

Using the relations between the analog and the corresponding discrete models developed in Chapter 2, the discrete model for the FM system considered in this example is derived and summarised in Table IV (Equations IV.3 - IV.5) together with the observation model using both the uniform and quadrature sampling techniques (Equations IV.6 - IV.9).

The transition matrix $\Phi(k,k-1)$ is derived by using the Laplace Transform method (Peikari, 1974, p. 246) to compute $e^{\underline{F}t}$ as the inverse Laplace Transform of the resolvent matrix $(sI - \underline{F})^{-1}$

$$e^{\underline{F}t} = \mathcal{L}^{-1}(s\underline{I} - \underline{F})^{-1} \tag{4.10}$$

Figure 4.2 is a block diagram of the discrete communication model in this example.

TABLE IV

AN EXAMPLE OF AN FM COMMUNICATION SYSTEM WITH RAYLEIGH FADING

Message model (2-dimensional)

$$\underline{m}(k) = \Phi_a(k,k-1)\underline{m}(k-1)+\underline{W}_m(k) \qquad \text{(IV.1)}$$

Channel model (1-dimensional)

$$b_i(k) = \Phi_{bi}(k,k-1)b_i(k-1)+w_{bi}(k), \qquad i = 1,2 \qquad \text{(IV.2)}$$

Equivalent system model (4-dimensional)

$$\underline{X}(k) = \Phi(k,k-1)\underline{X}(k-1)+\underline{W}(k) \qquad \text{(IV.3)}$$

where

$$\underline{X}(k) \triangleq \begin{pmatrix} x_1(k) \\ x_2(k) \\ x_3(k) \\ x_4(k) \end{pmatrix} \begin{matrix} \leftarrow \text{ phase} \\ \leftarrow \text{ message} \\ \leftarrow \text{ in-phase fading component} \\ \leftarrow \text{ quadrature fading component} \end{matrix}$$

$$\underline{W}(k) \triangleq \begin{pmatrix} w_1(k) \\ w_2(k) \\ w_3(k) \\ w_4(k) \end{pmatrix} \quad \text{with } E[\underline{W}(k)\underline{W}^T(j)] = \underline{Q}(k)\delta_{kj} \qquad \text{(IV.4)}$$

$$\Phi(k,k-1) \triangleq \begin{pmatrix} 1 & \beta(1-e^{-\alpha T}) & 0 & 0 \\ 0 & e^{-\alpha T} & 0 & 0 \\ 0 & 0 & e^{-\gamma T} & 0 \\ 0 & 0 & 0 & e^{-\gamma T} \end{pmatrix} \qquad \text{(IV.5)}$$

Observation model

$$\underline{Z}(k) = \underline{h}[\underline{X}(k)]+\underline{V}(k) \qquad \text{(IV.6)}$$

with

$$E[\underline{V}(k)\underline{V}^T(j)] = \underline{R}(k)\delta_{kj} \qquad \text{(IV.7)}$$

For uniform sampling

$$h[\underline{X}(k)] = \sqrt{2P_t}\,[\underline{L}_2\underline{X}(k)\sin(\omega_c t_k + \underline{L}_1\underline{X}(k)) + \underline{L}_3\underline{X}(k)\cos(\omega_c t_k + \underline{L}_1\underline{X}(k))]$$

$$R(k) = \frac{r}{T} \qquad \text{(IV.8)}$$

For quadrature sampling

$$\underline{h}[\underline{X}(k)] = \sqrt{2P_t}\begin{pmatrix} \underline{L}_2\underline{X}(k) & \underline{L}_3\underline{X}(k) \\ -\underline{L}_3\underline{X}(k) & \underline{L}_2\underline{X}(k) \end{pmatrix}\begin{pmatrix} \sin(\underline{L}_1\underline{X}(k)) \\ \cos(\underline{L}_1\underline{X}(k)) \end{pmatrix}$$

$$\underline{R}(k) = \begin{pmatrix} \frac{r}{T} & 0 \\ 0 & \frac{r}{T} \end{pmatrix} \qquad \text{(IV.9)}$$

Definitions

$$\left.\begin{aligned} \underline{L}_1 &\triangleq [1 \quad 0 \quad 0 \quad 0] \\ \underline{L}_2 &\triangleq [0 \quad 0 \quad 1 \quad 0] \\ \underline{L}_3 &\triangleq [0 \quad 0 \quad 0 \quad 1] \end{aligned}\right\} \qquad \text{(IV.10)}$$

$$\beta = \frac{d_f}{\alpha} = \frac{\text{frequency deviation (constant)}}{\text{3-db frequency of message (radians/sec)}}$$

$T = t_k - t_{k-1}$ (sampling interval) (secs)

P_t = average transmitted power (watts/sec)

ω_c = Carrier frequency (radians/sec)

$$\underline{Q}(k) = \begin{pmatrix} Q_{11} & Q_{12} & 0 & 0 \\ Q_{12} & Q_{22} & 0 & 0 \\ 0 & 0 & Q_{33} & 0 \\ 0 & 0 & 0 & Q_{44} \end{pmatrix}$$

$$Q_{11} = P_a\beta^2(2\alpha T - 3 + 4e^{-\alpha T} - e^{-2\alpha T})$$

$$Q_{12} = Q_{21} = P_a\beta(1-e^{-\alpha T})^2$$

$$Q_{22} = P_a(1-e^{-2\alpha T})$$

$$Q_{33} = Q_{44} = P_f(1-e^{-2\gamma T}) \qquad \text{(IV.11)}$$

γ = 3-db frequency of fading components (radians/sec)

P_a = average message power (watts/sec)

P_f = average fading component power (watts/sec)

r = two-sided spectral height of continuous additive white gaussian noise (watts/cycle)

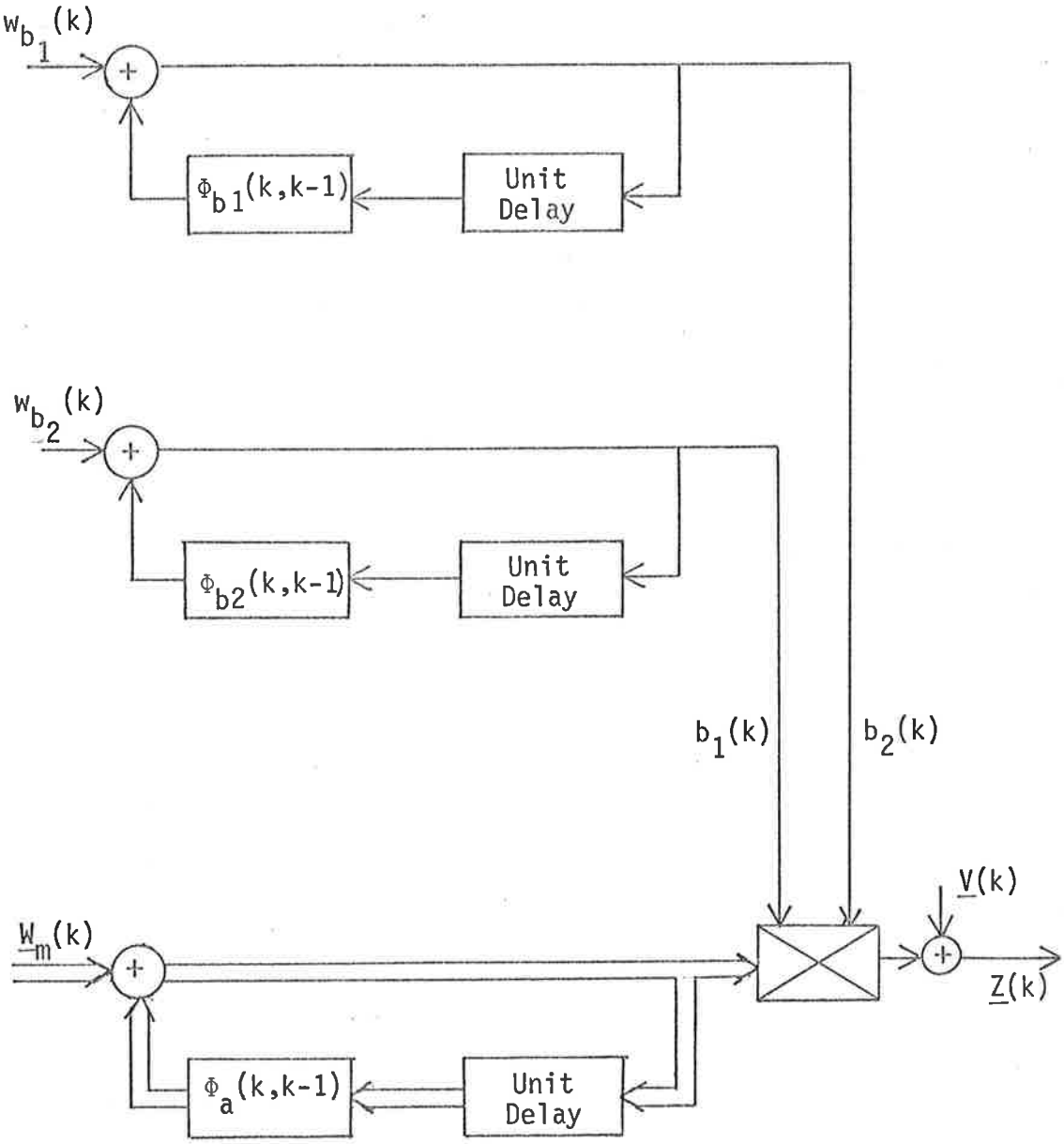

Figure 4.2. Discrete FM Communication Model

4.1.1 Definition of terms

Several terms relating to the communication model as formulated in this study require some clarifications.

(i) Bandwidth expansion ratio

Van Trees (1971, p. 88) defines the bandwidth expansion ratio as

$$\beta = \frac{d_f}{\alpha}$$

and this is the same as the modulation index (Schwartz et al, 1966, p. 164) defined as the ratio of the rms frequency deviation $\Delta\omega$ to the rms bandwidth $B_{\dot{\theta}}$ of $\dot{\theta}(t)$ as can be seen below

Recall that

$$\theta(t) = d_f \int_0^t a(\tau)d\tau$$

It can be verified that the rms bandwidth of $\dot{\theta}(t)$ given by

$$(B_{\dot{\theta}})^2 \triangleq \frac{\int_{-\infty}^{\infty} f^2 S_{\dot{\theta}}(f)df}{\int_{-\infty}^{\infty} S_{\dot{\theta}}(f)df}$$

with $S_{\dot{\theta}}(f)$ derived from Equation 4.4a
is

$$B_{\dot{\theta}} = \alpha \quad \text{(radians/sec)}$$

Furthermore, the rms frequency deviation of $\dot{\theta}(t)$ given by (Schwartz, ibid.)

$$(\Delta\omega)^2 \triangleq \int_{-\infty}^{\infty} S_{\dot{\theta}}(f)\, df$$

is

$$\Delta\omega = d_f \quad \text{(radians/sec)}$$

and thus

$$\beta = \frac{\Delta\omega}{B_{\dot{\theta}}} = \frac{d_f}{\alpha} \tag{4.11}$$

(ii) Average received power.

The received signal

$$z(t) = \sqrt{2P_t}(b_1(t) \sin[\omega_c t + \theta(t)] + b_2(t) \cos[\omega_c t + \theta(t)]) + v(t)$$

has the average received power P given by

$$P = 2P_t P_f \tag{4.12}$$

where P_t is the average transmitter power (and would be also the average received power in the non-fading case) and P_f is the average power of the fading processes.

(iii) Variance of continuous additive noise.

The continuous additive noise v(t) is assumed to be a scalar white gaussian process having zero mean and variance

$$E[v(t)v(\tau)] = r\delta(t-\tau) \tag{4.13}$$

and r is thus the two-sided spectral height measured in watts/cycle.

(iv) Variance of sampled additive noise.

The measured noise, i.e. the sampled white noise sequence, $\underline{V}(k)$ have also zero mean and variance (Sage and Melsa, 1971, p. 83).

$$E[\underline{V}(k)\underline{V}(j)] = \underline{R}(k)\delta_{kj} \tag{4.14}$$

where

$$\underline{R}(k) = \frac{r}{T} \quad \text{for uniform sampling}$$

$$\underline{R}(k) = \begin{bmatrix} r/T & 0 \\ 0 & r/T \end{bmatrix} \quad \text{for quadrature sampling}$$

4.1.2. Signal-to-noise ratio and fading rate

Before leaving this section, there are two important parameters to be defined for later discussions. The first is the signal-to-noise in the message bandwidth defined as

$$\Lambda \triangleq \frac{\text{average received power}}{\text{noise power in the message bandwidth}}$$

The noise power in the message bandwidth is given in terms of the (one-sided) noise equivalent bandwidth of the message power spectral density (Carlson, 1975, p. 125).

$$B_n = \frac{\frac{1}{2\pi}\int_0^\infty |H(j\omega)|^2 \, d\omega}{|H(j\omega)|^2_{max}}$$

$$= \frac{\frac{1}{2\pi}\int_0^\infty \frac{2\alpha}{\omega^2+\alpha^2} \, d\omega}{(2/\alpha)}$$

$$= \frac{\pi}{2}\alpha \text{ (radians/sec)} = \frac{\alpha}{4} \text{ (cycles/sec)} \qquad (4.15)$$

and therefore

$$\Lambda = \frac{P}{2B_n r}$$

$$= \frac{2P}{\alpha r} \qquad (4.16)$$

This definition of the signal to noise ratio in the message bandwidth agrees with those used by Polk and Gupta (1973), McBride (1973), for the non-fading case and also by Dharamsi and Gupta (1975b) for the fading case and thus allows direct comparison of their results with those obtained in this thesis.

In his study of fading channels, Van Trees (1971, p. 258) also defines an "effective" signal-to-noise ratio in the message bandwidth as

$$\Lambda_e \triangleq \Lambda_a[1- \frac{1}{\Lambda_b} \ln (1+\Lambda_b)] \tag{4.17}$$

where Λ_a is the signal-to-noise ratio in the message bandwidth as defined in Equation 4.15 and Λ_b is the signal-to-noise ratio in the channel bandwidth given by

$$\Lambda_b = \frac{2P}{\gamma r} \tag{4.18}$$

The second parameter, to be called the "fading rate", is defined by:

$$f_r \triangleq \frac{\text{3-db bandwidth of fading component}}{\text{3-db bandwidth of message}}$$

$$= \frac{\gamma}{\alpha} \tag{4.19}$$

and is a measure of the rate of variation of the carrier signal amplitude compared to the changing rate of the random message. If $f_r = 0$, the carrier signal amplitude is constant and no fading is said to occur. If $f_r = 0.01$, the amplitude is varying but at a much slower rate than the message. A rather artificial value $f_r = 0.05$ is to be chosen as an intermediate value and the fading is said to be "fast" if

$$f_r >> 0.05$$

and "slow" if

$$f_r << 0.05$$

4.2 Computer simulation - Theoretical considerations

The discrete model for the example of an FM communication system as described in Section 4.1 will be used in conjunction with the algorithms in Chapter 3 to develop receiver structures in the remaining chapters. The performance of the receivers will be studied using Monte Carlo simulation. As discussed by Bucy, et al (1972, Chapter IV) the term "Monte Carlo simulation" is subjected to a great number of alternative and sometimes misleading interpretations. Quite often, the simulation results are presented in the literature with no explanations regarding the procedure followed and the degree of confidence associated with the results obtained. Many types of errors can occur in a simulation study and great care must be taken in attempting to draw meaningful conclusions about the validity, significance and accuracy of the results. In the following subsections, some of the important topics on computer simulation relevant to this thesis will be discussed.

4.2.1 Generation of gaussian random variables

Most digital computers have at least one uniform pseudo-random number generator in their system library. These generate numbers which are uniformly distributed between 0 and 1. Usually they are based on the mixed congruential method of generation and some control of the algorithm is available by allowing the user to choose the seed for initiating the sequence (Fishman, 1972). For example, RANF(.), available from the CDC 6400, is a modified form of the mixed congruent generator and the initialisation is done by calling RANSET(.) with any chosen seed.

From these prime sources of uniform random numbers, random variables of other distribution can be generated. Of particular interest is the gaussian distribution associated with many types

of signals encountered in communication systems. The generation of gaussian variables can be done using either:

(i) Sum of uniform random numbers:

As a consequence of the central limit theorem, the distribution of a linear combination of random processes with similar first and second order statistics tends to that of a gaussian distribution. By summing N variables uniformly distributed in the interval (0, 1), the resultant variable would have a gaussian distribution with mean N/2 and a variance N/12. This method has been found to have a bad gaussian "tail" and is only marginally more efficient in terms of execution time than the more exact direct transformation method as below.

(ii) The exact transform method.

Let U_1 and U_2 be independent random variables uniformly distributed in the interval (0, 1). By transforming U_1 and U_2 using the relationships

$$V_1 = (-2\ln U_1)^{\frac{1}{2}}\cos 2\pi U_2$$
$$V_2 = (-2\ln U_1)^{\frac{1}{2}}\sin 2\pi U_2 \qquad (4.20)$$

The random variables V_1 and V_2 are independent and normally distributed with zero mean and unity variance. To verify this, it is noted that (Sage and Melsa, 1971, page 25)

$$p_{V_1,V_2}(v_1,v_2) = |\det \underline{J}|\, p_{U_1,U_2}(U_1,U_2) \qquad (4.21)$$

where $|\det \underline{J}|$ is the magnitude of the determinant of the Jacobian matrix

$$\underline{J} \triangleq \begin{pmatrix} \frac{\partial U_1}{\partial V_1} & \frac{\partial U_1}{\partial V_2} \\ \frac{\partial U_2}{\partial V_1} & \frac{\partial U_2}{\partial V_2} \end{pmatrix}$$

$$= \begin{pmatrix} -v_1 e^{-(v_1^2+v_2^2)/2} & -v_2 e^{-(v_1^2+v_2^2)/2} \\ \frac{-v_2}{2\pi(v_1^2+v_2^2)} & \frac{v_1}{2\pi(v_1^2+v_2^2)} \end{pmatrix}$$

$$= \frac{-1}{2\pi} e^{-(v_1^2+v_2^2)/2}$$

thus

$$p_{V_1,V_2}(v_1,v_2) = \frac{1}{2} e^{-(v_1^2+v_2^2)/2} \tag{4.22}$$

and

$$p_{V_1}(v_1) = \int_{-\infty}^{\infty} p(v_1,v_2)dv_2 = \frac{1}{\sqrt{2\pi}} e^{-v_1^2/2} \tag{4.23}$$

$$p_{V_2}(v_2) = \int_{-\infty}^{\infty} p(v_1,v_2)dv_1 = \frac{1}{\sqrt{2\pi}} e^{-v_2^2/2} \tag{4.24}$$

Generation of gaussian random variables N of mean m and variance σ^2 requires further transformation

$$N = \sigma V + m \tag{4.25}$$

where V is gaussian variable of zero mean and unity variance generated by Equation 4.20.

In generating white gaussian noise as required in the simulation of the received signal being contaminated by additive noise of two-sided spectral height r and sampled at the sampling rate $f_s = \frac{1}{T}$, the variance of the white noise sequence is said to be appropriately determined from r. As simulated white process cannot contain frequencies higher than one half the sampling frequency so the total power in the power spectrum must be equal to the variance R of the generated noise samples, i.e.

$$R = rf_s = \frac{r}{T} \tag{4.26}$$

and this agrees with Equation 4.14 given earlier.

4.2.2 Multivariate normal distribution

The simulation of the system model as given in Equation IV.3 (Table IV) requires the generation of $\underline{W}(k)$, a multivariate normal random vector with zero mean and covariance matrix.

$$\underline{Q}(k) = \begin{pmatrix} Q_{11} & Q_{12} & 0 & 0 \\ Q_{12} & Q_{22} & 0 & 0 \\ 0 & 0 & Q_{33} & 0 \\ 0 & 0 & 0 & Q_{33} \end{pmatrix} \qquad \text{(See IV.11)}$$

By first generating a multivariate normal random vector $\underline{\Gamma}(k)$ with zero mean and unity covariance matrix, $\underline{W}(k)$ can be given by

$$\underline{W}(k) = \underline{C}\,\underline{\Gamma}(k) \tag{4.27}$$

where $\underline{C}$ is a unique lower triangular matrix satisfying (Anderson, 1958, p. 19)

$$\underline{Q}(k) = \underline{C}\,\underline{C}^T \tag{4.28}$$

In particular, with $\underline{Q}(k)$ as given by Equation IV.11, the matrix $\underline{C}$ is computed to be

$$\underline{C} = \begin{bmatrix} \sqrt{Q_{11}} & 0 & 0 & 0 \\ \frac{Q_{12}}{\sqrt{Q_{11}}} & \sqrt{Q_{22} - \frac{Q_{12}^2}{Q_{11}}} & 0 & 0 \\ 0 & 0 & \sqrt{Q_{33}} & 0 \\ 0 & 0 & 0 & \sqrt{Q_{44}} \end{bmatrix} \quad (4.29)$$

4.2.3 Sources of Error

There are several types of errors involved in a simulation study and can be classified broadly as

(i) Modelling errors in the model of the communication systems under study. This includes the errors occuring in modelling real random signals as the output of dynamical systems excited by white noise as was done for the message and fading processes. The statistics of these random signals may not be known accurately. To reduce the modelling errors, extensive experimental data have to be collected to determine the validity of the model used or else the unknown parameters can be augmented into the system state vector to be adaptively identified before they can be used in the estimation model. This problem is not attempted here, however, and the model is assumed to be accurate enough to render modelling errors insignificant.

(ii) Discretization errors due to the discrete representation of continuous processes as was done in Section 2.2.

(iii) Statistical errors due to the finite observation time. The simulation normally consists of N_r number of runs of length N_p simulation points each. For each run the total observation time τ is given by

$$\tau = N_p T$$

where T is the sampling interval. As a guideline, this product must be at least several times the dominant time constant of the system which is the time constant (also called the correlation time) $\frac{1}{\gamma}$ of the fading processes $b_1(t)$ and $b_2(t)$ in the example considered in Section 4.1.

4.2.4 Sample size requirements

The performance of the receiver is measured in terms of the mean square error ξ_i between the state estimate (at time instant t_k) $\hat{x}_i(k)$ and the true state $x_i(k)$. The subscript "i" indicates the particular state to be estimated and

i = 1 : phase	}	Corresponds to the system state vector defined in Section 4.1
i = 2 : message		
i = 3 : in-phase fading component		
1 = 4 : quadrature fading component		

The mean square error ξ_i (also called the error covariance for zero-mean processes) is computed as

$$\xi_i = \frac{1}{N} \sum_{k=1}^{N} \tilde{x}_i^2(k) \tag{4.30}$$

where N is the sample size

$$N = N_r N_p \tag{4.31}$$

and

$$\tilde{x}_i \triangleq x_i(k) - \hat{x}_i(k)$$

is the error in the estimates at time t_k and is assumed to be Gaussian distributed. ξ_i is thus the sum of N squared Gaussian

random variables and would follow a χ^2 - distribution (Papoulis, 1965, p. 250) with an effective number of degrees of freedom given by (Bucy and Mallinckrodt, 1973)

$$N_{eff} = \frac{N}{1 + \frac{2F^2}{1 + 2F}} \tag{4.32}$$

$$\rightarrow \frac{N}{F} \text{ for large F} \tag{4.32a}$$

where F is defined as

$$F = \frac{1}{2BT} \tag{4.32b}$$

with B being the FM bandwidth (cycles/sec) and T is the sampling period. Equation 4.32a thus becomes

$$N_{eff} = 2BTN \tag{4.32c}$$

and is interpreted as the total number of independent samples obtained over the total observation time (TN) which agrees with the assumption behind the χ^2 - distribution.

If N_{eff} is greater than 30; the χ^2 - distribution is asymtotically normal with variance (Appendix C, Equation C.4)

$$\sigma^2 = \frac{2}{N_{eff}} \mu_2^2 \tag{4.33}$$

where

$$\mu_2 \triangleq E[\tilde{x}_i^2(k)] \tag{4.34}$$

and it can be further shown (Appendix C, Equation C.7) that the probability of ξ_i to be within some fraction s of the true mean square value μ_2 is given by

$$P_s[|\xi_i - \mu_2| \leq s\mu_2] = 1 - 2Q\left(s\sqrt{\frac{N_{eff}}{2}}\right) \tag{4.35}$$

where Q(.) is the "error probability" function (Carlson, 1975, Table D, p. 474).

Consequently if we require, for example, 5% accuracy ($s = 0.05$) with 98% confidence ($P_s = .98$), the minimum required N_{eff} is given approximately

$$(N_{eff})_{min} = 4000 \tag{4.36}$$

4.3 Computer simulation - Procedure

Having discussed the theoretical considerations for the use of computer simulation to study performance of communication systems, the actual procedure is to be developed in this section and will be followed throughout the rest of the studies.

4.3.1 Program organisation

The simulation programs are organised according to the flow chart depicted in Figure 4.3 and brief descriptions of the various steps are given below.

Step 1. Input parameters

Various parameters are to be specified at the beginning of the simulation programs. A short summary of these parameters is given below:

Parameter		Definitions
(i)	α	3-dB one-sided bandwidth of message
(ii)	P_a	average power of message
(iii)	γ	3-dB one-sided bandwidth of fading process
(iv)	P_f	average power of fading process
(v)	β	bandwidth expansion ratio (Equation 4.11)
(vi)	P_t	average transmitter power
(vii)	Λ	signal-to-noise ratio in the message bandwidth
(viii)	T	sampling interval
(ix)	N_r	number of simulation runs
(x)	N_p	number of simulation points for each run

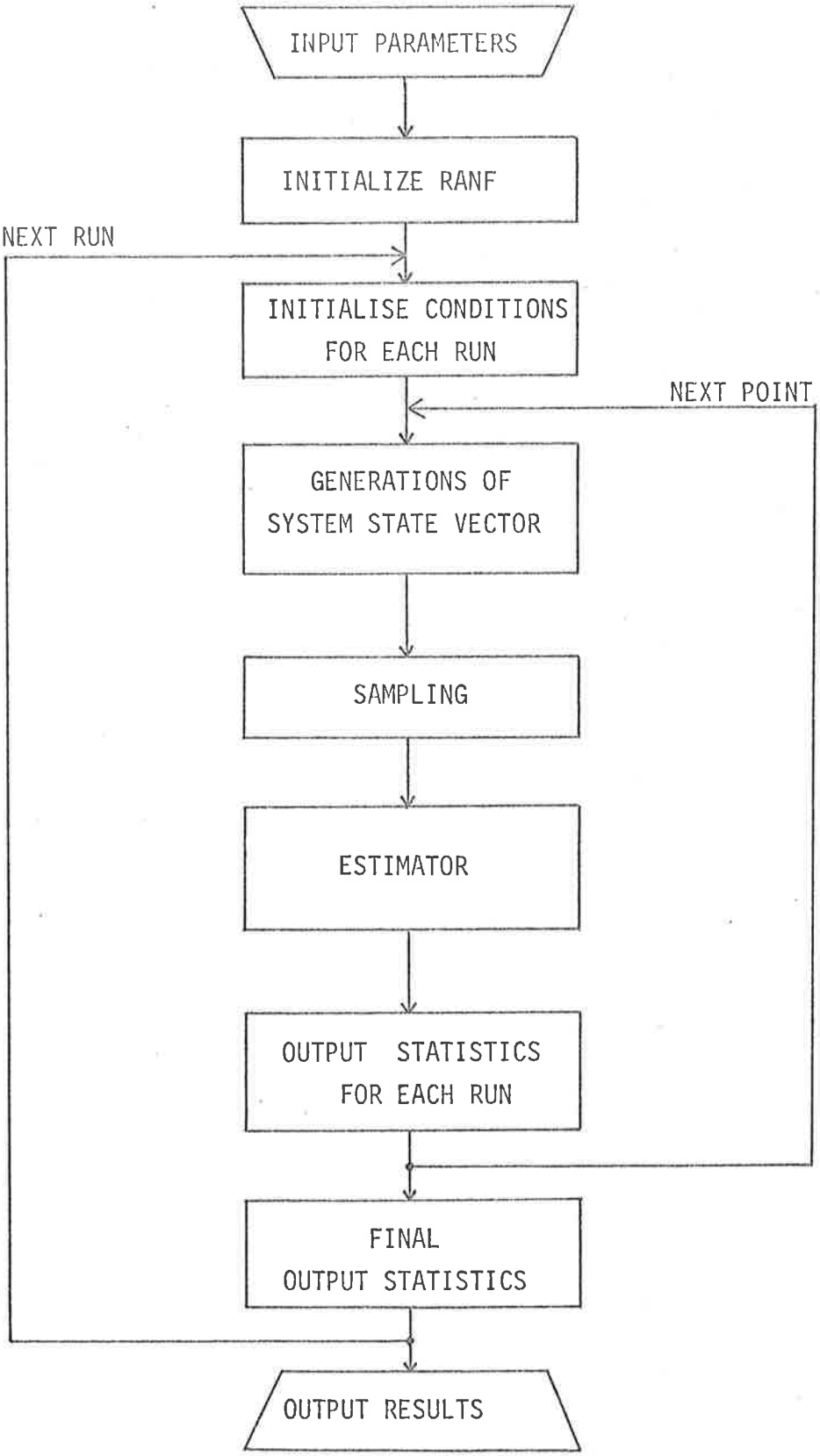

Figure 4.3. Flowchart of General Simulation Program

The actual parameter set used in the simulation programs is discussed further in Section 4.3.2.

Step 2. Initialise RANF

This is required only if the sequence of uniform random numbers generated by the RANF(.) function on the CDC 6400 computer is desired to be the same for various parameter sets.

Step 3. Initial conditions for each run

When several runs each of length N_p points are to be made, they are made independent of each other by randomly selecting the initial conditions giving the initial state vector $\underline{X}(0)$ with the assumption that $\underline{X}(0)$ is normally distributed with mean $\underline{\mu}_{\underline{X}_0}$, normally assumed to be zero, and variance $\underline{V}_{\underline{X}_0}$. Note that these statistical parameters are later used as initial conditions for the estimation algorithms.

Step 4. Generation of the system state vector

This requires the evaluation of the transition matrix (Equation IV.5) which is constant for this example and then

(i) generation of $\underline{W}(k)$ by Equation 4.27.

(ii) generation of $\underline{X}(k)$ by Equation IV.3.

Step 5. Sampling

This requires the generation of the sampled white Gaussian noise sequence having zero mean and variance

$$R(k) = \frac{r}{T}$$

$$= \frac{2P}{\alpha \Lambda T} \qquad (4.37)$$

For uniform sampling, only one sequence is required to form the discrete observation signal as given by Equation IV.8.

For quadrature sampling, two independent noise samples are required to form the discrete inphase and quadrature observation signal as given by Equation IV.9.

Step 6. Estimation

This is the main step in the program and employs a chosen filtering algorithm (EKF or MAP as discussed in Chapter 3) to process the observed signals to obtain the optimum estimates for the system state vector.

Step 7. Output statistics for each run

For the j^{th} run, the partial statistics ξ_i^j is computed as

$$\xi_i^j = \frac{1}{N_p} \sum_{k=1}^{N_p} \tilde{x}_i^2(k) \tag{4.38}$$

for the desired state estimate, namely the phase (i = 1) and the message (i = 2).

Step 8. Final output statistics

The simulation is repeated for N_r number of runs, each time with a different set of initial conditions (chosen in Step 3) and the final output statistics is computed as

$$\xi_i = \frac{1}{N_r} \sum_{j=1}^{N_r} \xi_i^j \tag{4.39}$$

Step 9. Output results

After having run the simulation for several set of parameters, the results consist of plots of the inverse simulated error covariance ($1/\xi_i$) versus the signal-to-noise in the message bandwidth (Λ) for a certain combination of the input parameters

(i) β, to investigate the effects of bandwidth expansion ratio

(ii) f_r, to investigate the effects of the "fading rate" as defined in Equation 4.19

(iii) T, to investigate the effects of the sampling rate

and, of course, for both the EKF and the MAP algorithms used in the single channel case. As for the MAP receivers using quadrature sampling for fixed-lag smoothing (Chapter 7) and for diversity reception (Chapter 8), the number of lags allowed and the number of diversity branches would be the relevant parameters.

Often found plotted on the same graph are simulation results obtained by Polk (1973) and McBride (1973). These results are for comparison and also serve as an indication of how well the results for the Rayleigh fading could be expected to improve.

4.3.2. A typical parameter set

Unless explicitly stated, the input parameter set has the values chosen below

$$\left.\begin{matrix}\alpha \\ P_a \\ P_f\end{matrix}\right\} \text{ normalised to unity } \begin{cases}\alpha = 1 \text{ (radians/sec)} \\ P_a = 1 \\ P_f = 1\end{cases}$$

$$f_r \triangleq \frac{\gamma}{\alpha} = \gamma \quad (\text{for } \alpha = 1)$$

$$\gamma = \begin{cases} .1 & \text{"fast" fading} \\ .01 & \text{"slow" fading (typical)} \\ .001 & \text{"very slow" fading} \end{cases}$$

$P_t = \frac{1}{2}$ (allowing P normalised to unity)

$$\beta = \begin{cases} 10 \\ 25 \text{ (typical)} \\ 50 \end{cases}$$

Λ = 20-45 dB (in steps of 5 dB)

The choice of the remaining parameters (T, N_r, N_p) require some further discussions.

Choice of sampling rate ($f_s = \frac{1}{T}$): dependent on the bandwidth B of the FM bandpass signal. Van Trees (1971, p. 100 ff) shows that for wideband FM ($\beta \geq 5$), the spectrum of the frequency modulated signal can be approximated by a gaussian-shaped spectrum

$$G_s(f) = \frac{\sqrt{2\pi P_t}}{\sqrt{P_a}\, d_f} e^{-(2\pi f)^2/2P_a d_f^2} \tag{4.40}$$

The root-mean-square bandwidth B_s (cycles/sec) defined by

$$B_s^2 \triangleq \frac{4}{(2\pi)^2 P_t} \int_{-\infty}^{\infty} f^2 (G_s(f))_{LP} df \tag{4.41}$$

and is evaluated to be (see Figure 4.4)

$$B_s = 2\sqrt{P_a}\, d_f \text{ (cycles/sec)} \tag{4.42}$$

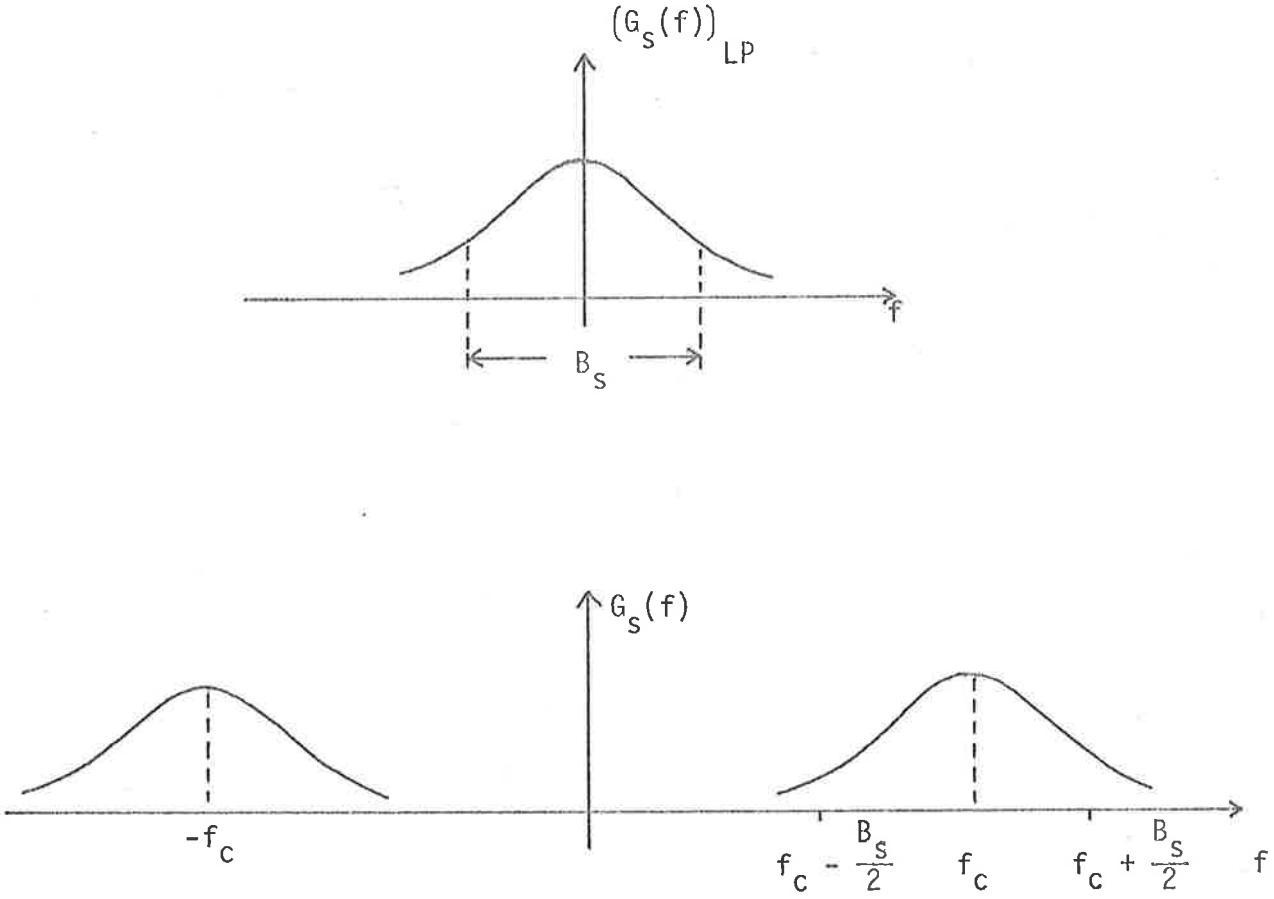

Fig. 4.4: FM modulated signal spectrum and equivalent low-pass spectrum.

the approximate modulated bandwidth is then given by

$$B = kB_s \tag{4.43}$$

where k is a constant chosen by the designer. For example, if k = 2, 95% of the power is contained in B.

Having determined B, the minimum sampling frequency is chosen as required in Section 2.3. For example, for $\beta = 25$

$$d_f = \alpha\beta = 25 \text{ (radians/sec)}$$
$$B_s = 2\sqrt{P_a}\, d_f$$
$$= 50 \text{ (cycles/sec)}$$
$$B = kB_s$$
$$= 100 \text{ (cycles/sec)} \qquad \text{for } k = 2$$

(a) For scalar sampling, choose

$$(f_s)_{min} = 4B \tag{Eq. 2.31}$$

and allow for a safe factor of 10 then the required sampling frequency is

$$f_s = 40B \tag{4.44}$$

(b) For quadrature sampling, assuming

$$f_c = 10^6 \text{ (cycles/sec)}$$
$$\frac{f_c}{B} = 10^4$$

Minimum sampling frequency is

$$(f_s)_{min} = \frac{f_c}{[f_c/B]}$$

$$= 100 \quad \text{(cycles/sec)}$$

By allowing for a safe factor of 10, the required sampling frequency is

$$f_s = 10^3 \quad \text{(cycles/sec)} \tag{4.45}$$

Choice of N_r and N_p

Having determined the sampling frequency, the minimum total of simulation points is given by

$$(N)_{min} = \frac{(N_{eff})_{min}}{2BT} \qquad \text{(Eqs. 4.32(c) and 4.36)}$$

$$= \begin{cases} 8 \times 10^4 & \text{scalar sampling} \\ 2 \times 10^4 & \text{quadrature sampling} \end{cases}$$

The actual choice is

$$N = \begin{cases} 10^5 & \text{scalar sampling} \\ 2.5 \times 10^4 & \text{quadrature sampling} \end{cases} \tag{4.46}$$

To obtain the total number of simulation points as given by Equation (4.46) N_r and N_p are chosen so that

$$N_r N_p = N$$

and allow for a minimum number of 10 runs to sample the initial distribution, N_p is then given by

$$N_p = \begin{cases} 10^4 & \text{for scalar sampling} \\ 2.5 \times 10^3 & \text{for quadrature sampling} \end{cases} \qquad (4.47)$$

Each simulation study thus consists of a minimum number of 10 runs each of minimum lengths 10,000 or 2,500 points depending on the sampling scheme.

5. RECEIVERS USING UNIFORM SAMPLING

Employing uniform (or scalar) sampling, the filtering algorithms of Chapter 3 are to be applied to the communication model of Section 4.1 to obtain various set of algorithms from which receiver structures can be identified and their performances are studied by using computer simulation.

Section 5.1 will consider receivers using the EKF algorithm. These receivers are further simplified for very slow fading channel using a "quasi-stationary" analysis in Section 5.2. Section 5.3 consider receivers using the MAP algorithm and a "quasi-stationary" version is compared with the EKF receivers. The last section is a summary of the development in this chapter. The effect of sampling rate and comparison of results for no fading will be postponed until Chapter 6 after considering receivers using quadrature sampling.

5.1 Discrete EKF Receivers

5.1.1 Algorithm

The discrete EKF algorithm developed in Chapter 3 (Table II) is applied to the example of an FM communication system discussed in Section 4.1 and summarised in Table IV. Uniform sampling is employed and the resulting algorithms are tabulated in Table V. To illustrate the recursive nature of these algorithms, a flowchart is shown in Figure 5.1 and will be used in conjunction with the flowchart for the General Simulation Program discussed in Section 4.3 to simulate the system.

The development of these algorithms is summarised below.

Equations V.1 through V.4 corresponds to the communication model in Table IV. Equations V.5 and V.6 are the direct application of Equations II.4 and II.5 to the above model. The initial

TABLE V

DISCRETE EKF FILTERING ALGORITHM FOR FM COMMUNICATION SYSTEM WITH RAYLEIGH FADING (UNIFORM SAMPLING)

System model $\quad \underline{X}(k) = \Phi(k,k-1)\underline{X}(k-1)+\underline{W}(k)$

$$\begin{pmatrix} x_1(k) \\ x_2(k) \\ x_3(k) \\ x_4(k) \end{pmatrix} = \begin{pmatrix} 1 & \beta(1-e^{-\alpha T}) & 0 & 0 \\ 0 & e^{-\alpha T} & 0 & 0 \\ 0 & 0 & e^{-\gamma T} & 0 \\ 0 & 0 & 0 & e^{-\gamma T} \end{pmatrix} \begin{pmatrix} x_1(k-1) \\ x_2(k-1) \\ x_3(k-1) \\ x_4(k-1) \end{pmatrix} + \begin{pmatrix} w_1(k) \\ w_2(k) \\ w_3(k) \\ w_4(k) \end{pmatrix} \tag{V.1}$$

Observation model (uniform sampling): $\quad z(k) = h[X(k)]+v(k)$

$$z(k) = \sqrt{2P_t}[x_3(k)\sin(\omega_c t_k+x_1(k))+x_4(k)\cos(\omega_c t_k+x_1(k))]+v(k) \tag{V.2}$$

Statistical parameters

$$E[\underline{W}(k)\underline{W}^T(j)] = \underline{Q}(k)\delta_{kj} \tag{V.3}$$

$$E[v(k)v(j)] = R(k)\delta_{kj} \tag{V.4}$$

} See Table IV

One stage prediction algorithm

$$\hat{\underline{X}}(k|k-1) = \underline{\Phi}(k,k-1)\hat{\underline{X}}(k-1) \tag{V.5}$$

$$\hat{\underline{X}}(0) = \underline{\mu}_{\underline{X}_0} \tag{V.5a}$$

Prior error variance algorithm

$$\underline{V}_{\tilde{\underline{X}}}(k|k-1) = \Phi(k,k-1)\underline{V}_{\tilde{\underline{X}}}(k-1)\Phi^T(k,k-1)+\underline{Q}(k) \tag{V.6}$$

$$\underline{V}_{\tilde{\underline{X}}}(0) = \underline{V}_{\underline{X}_0} \tag{V.6a}$$

Filtering algorithm

$$\hat{\underline{X}}(k) = \hat{\underline{X}}(k|k-1)+\underline{G}(k)\nu(k) \tag{V.7}$$

where

$$\underline{G}(k) \triangleq \frac{\underline{V}_{\tilde{\underline{X}}}}{(r/T)} \sum_{i=1}^{3} H_i L_i^T \qquad \text{(filter gain)} \tag{V.8}$$

$$\nu(k) \triangleq z(k)-h[\hat{\underline{X}}(k|k-1)] \qquad \text{(innovation process)} \tag{V.9}$$

Error variance algorithm

$$\underline{V}_{\tilde{X}}(k) = \underline{V}_{\tilde{X}}(k|k-1) - \sum_{i,j=1}^{3} \frac{H_i H_j}{M(k)} \underline{V}_{\tilde{X}}(k|k-1) \underline{L}_i^T \underline{L}_j \underline{V}_{\tilde{X}}(k|k-1) \tag{V.10}$$

where

$$\begin{pmatrix} \underline{L}_1 \\ \underline{L}_2 \\ \underline{L}_3 \end{pmatrix} \triangleq \begin{pmatrix} 1 & 0 & 0 & 0 \\ 0 & 0 & 1 & 0 \\ 0 & 0 & 0 & 1 \end{pmatrix} \tag{V.11}$$

$$H_1 \triangleq \frac{\partial h[\hat{\underline{X}}(k|k-1)]}{\partial \hat{x}_1(k|k-1)} = \sqrt{2P_t}[\hat{x}_3(k|k-1)\cos\hat{\Omega}(k|k-1) - \hat{x}_4(k|k-1)\sin\hat{\Omega}(k|k-1)] \tag{V.12a}$$

$$H_2 \triangleq \frac{\partial h[\hat{\underline{X}}(k|k-1)]}{\partial \hat{x}_3(k|k-1)} = \sqrt{2P_t}\sin\hat{\Omega}(k|k-1) \tag{V.12b}$$

$$H_3 \triangleq \frac{\partial h[\hat{\underline{X}}(k|k-1)]}{\partial \hat{x}_4(k|k-1)} = \sqrt{2P_t}\cos\hat{\Omega}(k|k-1) \tag{V.12c}$$

$$\hat{\Omega}(k|k-1) \triangleq \omega_c t_k + \hat{x}_1(k|k-1) \tag{V.13}$$

$$M(k) \triangleq m_o + m_s \sin 2\hat{\Omega}(k|k-1) + m_c \cos 2\hat{\Omega}(k|k-1) \tag{V.14}$$

$$m_0 = \left(\frac{r}{T}\right) + P_t\{(\hat{x}_3^2(k|k-1) + \hat{x}_4^2(k|k-1))V_{\tilde{x}_1}(k|k-1) + V_{\tilde{x}_3}(k|k-1) + V_{\tilde{x}_4}(k|k-1) \tag{V.14a}$$

$$+2(V_{\tilde{x}_1\tilde{x}_4}(k|k-1)\hat{x}_3(k|k-1) - V_{\tilde{x}_1\tilde{x}_3}(k|k-1)\hat{x}_4(k|k-1))\}$$

$$m_s = 2P_t\{-\hat{x}_3(k|k-1)\hat{x}_4(k|k-1)V_{\tilde{x}_1}(k|k-1) + \hat{x}_3(k|k-1)V_{\tilde{x}_1\tilde{x}_3}(k|k-1) \tag{V.14b}$$

$$-\hat{x}_4(k|k-1)V_{\tilde{x}_1\tilde{x}_4}(k|k-1) + V_{\tilde{x}_3\tilde{x}_4}(k|k-1)\}$$

$$m_c = P_t\{(\hat{x}_3^2(k|k-1) - \hat{x}_4^2(k|k-1))V_{\tilde{x}_1}(k|k-1) - V_{\tilde{x}_3}(k|k-1) + V_{\tilde{x}_4}(k|k-1) \tag{V.14c}$$

$$+2(\hat{x}_4(k|k-1)V_{\tilde{x}_1\tilde{x}_3}(k|k-1) + \hat{x}_3(k|k-1)V_{\tilde{x}_1\tilde{x}_4}(k|k-1))\}$$

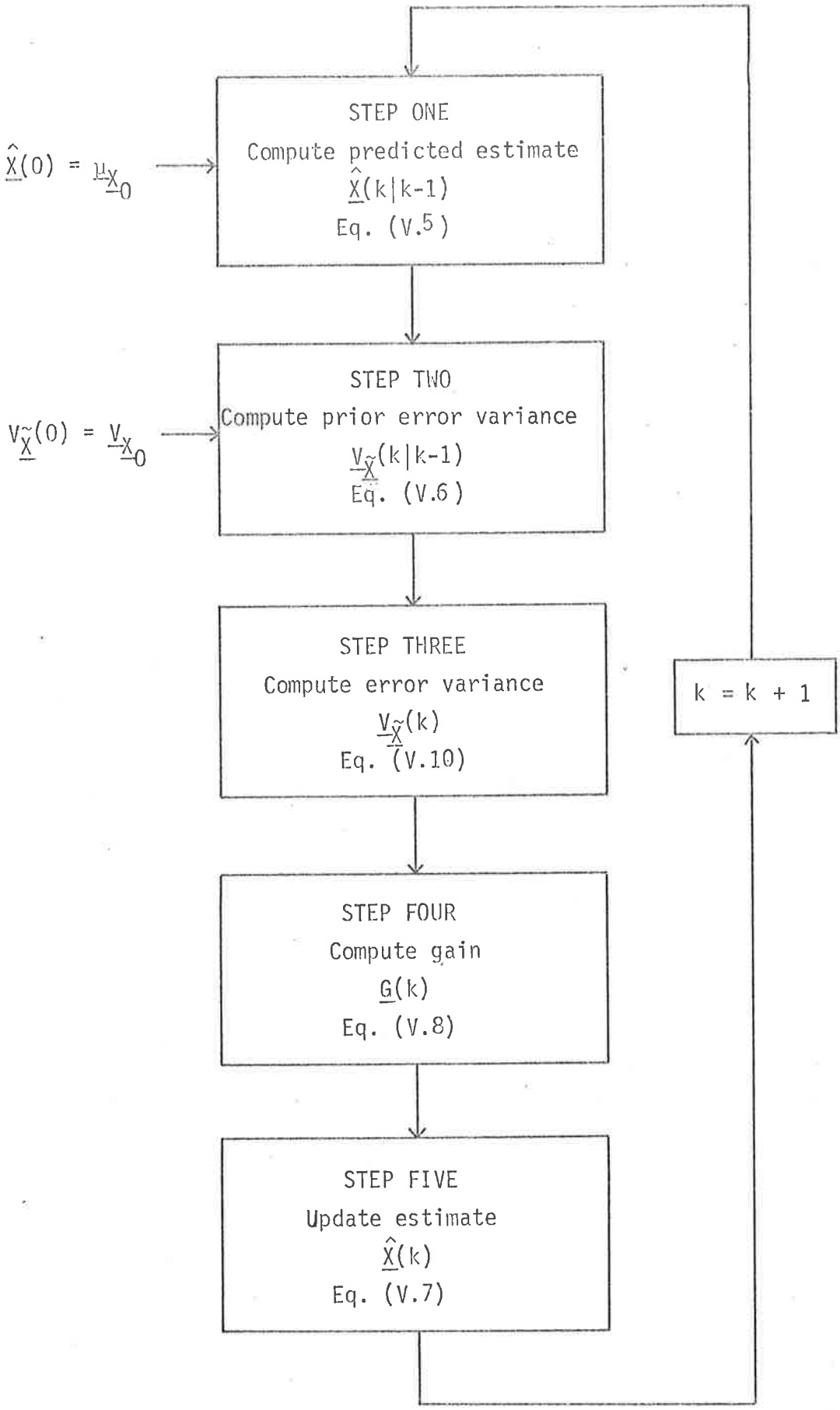

Fig. 5.1: Flowchart of EKF algorithm (Table V.)

conditions required for these equations are given in terms of the mean and variance of the distribution assumed normal of the initial state $\underline{X}(0)$

$$\hat{\underline{X}}(0) = \underline{\mu}_{\underline{X}_0} \triangleq E[\underline{X}(0)]$$

$$\underline{\tilde{V}}_{\underline{X}}(0) = \underline{V}_{\underline{X}_0} \triangleq E[\underline{X}(0)\underline{X}^T(0)]$$

In applying Equations II.6 and II.9 to derive the corresponding Equations V.10 and V.7 for the error variance algorithm and the filtering algorithm respectively, it is observed that the Jacobian matrix

$$\underline{H}(k) \triangleq \frac{\partial h[\hat{\underline{X}}(k|k-1)]}{\partial \hat{\underline{X}}(k|k-1)}$$

$$= \begin{bmatrix} \dfrac{\partial h[\hat{\underline{X}}(k|k-1)]}{\partial \hat{x}_1(k|k-1)} \\ \dfrac{\partial h[\hat{\underline{X}}(k|k-1)]}{\partial \hat{x}_2(k|k-1)} \\ \dfrac{\partial h[\hat{\underline{X}}(k|k-1)]}{\partial \hat{x}_3(k|k-1)} \\ \dfrac{\partial h[\hat{\underline{X}}(k|k-1)]}{\partial \hat{x}_4(k|k-1)} \end{bmatrix}^T$$

where the observation function $h[\hat{\underline{X}}(k|k-1)]$ is a function of $\hat{x}_1(k|k-1)$, $\hat{x}_3(k|k-1)$, $\hat{x}_4(k|k-1)$ only so

$$\frac{\partial h[\hat{\underline{X}}(k|k-1)]}{\partial \hat{x}_2(k|k-1)} = 0$$

and thus

$$\underline{H}(k) = \sum_{i=1}^{3} H_i \underline{L}_i^T$$

where

$$H_1 \triangleq \frac{\partial h[\hat{\underline{X}}(k|k-1)]}{\partial \hat{x}_1(k|k-1)} \qquad \text{(Eq. V.12a)}$$

$$H_2 \triangleq \frac{\partial h[\hat{\underline{X}}(k|k-1)]}{\partial \hat{x}_3(k|k-1)} \qquad \text{(Eq. V.12b)}$$

$$H_3 \triangleq \frac{\partial h[\hat{\underline{X}}(k|k-1)]}{\partial \hat{x}_4(k|k-1)} \qquad \text{(Eq. V.12c)}$$

and

$$\begin{pmatrix} \underline{L}_1 \\ \underline{L}_2 \\ \underline{L}_3 \end{pmatrix} \triangleq \begin{pmatrix} 1 & 0 & 0 & 0 \\ 0 & 0 & 1 & 0 \\ 0 & 0 & 0 & 1 \end{pmatrix} \qquad \text{(Eq. V.11)}$$

Using these shorthand notations and after some tedious but straightforward calculations, the term

$$\underline{M}(k) \triangleq \underline{H}(k)\underline{V}_{\tilde{X}}(k|k-1)\underline{H}^T(k)+\underline{R}(k) \qquad \text{(Eq. II.8)}$$

is shown to be

$$\underline{M}(k) = m_o+m_s\sin 2\hat{\Omega}(k|k-1)+m_c\cos 2\hat{\Omega}(k|k-1) \qquad \text{(Eq. V.14)}$$

where

$$\hat{\Omega}(k|k-1) \triangleq \omega_c t_k + \hat{x}_1(k|k-1) \qquad \text{(Eq. V.13)}$$

and m_o, m_s and m_c are given by Equations V.14a, V.14b and V.14c respectively.

Similarly, the filter gain

$$\underline{G}(k) \triangleq \underline{V}_{\tilde{X}}(k)\underline{H}^T(k)\underline{R}^{-1}(k) \qquad \text{(Eq. II.10)}$$

is shown to be

$$\underline{G}(k) = \frac{\underline{V}_{\tilde{X}}(k)}{(r/T)} \sum_{i=1}^{3} H_i \underline{L}_i^T \qquad \text{(Eq. V.8)}$$

where R(k) has been intentionally substituted by

$$R(k) = r/T$$

to indicate the discrete nature of the receiver.

Figure 5.2 is a block diagram of the receiver structure as depicted by the above algorithms.

5.1.2 Baseband Model

In order to facilitate the simulation of the receiver, further simplifications are required to derive a "baseband" model. To illustrate the meaning of the term "baseband" and the procedure to obtain it, consider the filtering algorithm

$$\hat{\underline{X}}(k) = \hat{\underline{X}}(k|k-1) + \underline{G}(k)\nu(k) \qquad \text{(Eq. V.7)}$$

$$= \Phi(k,k-1)\hat{\underline{X}}(k-1) + G(k)\nu(k) \qquad (5.1)$$

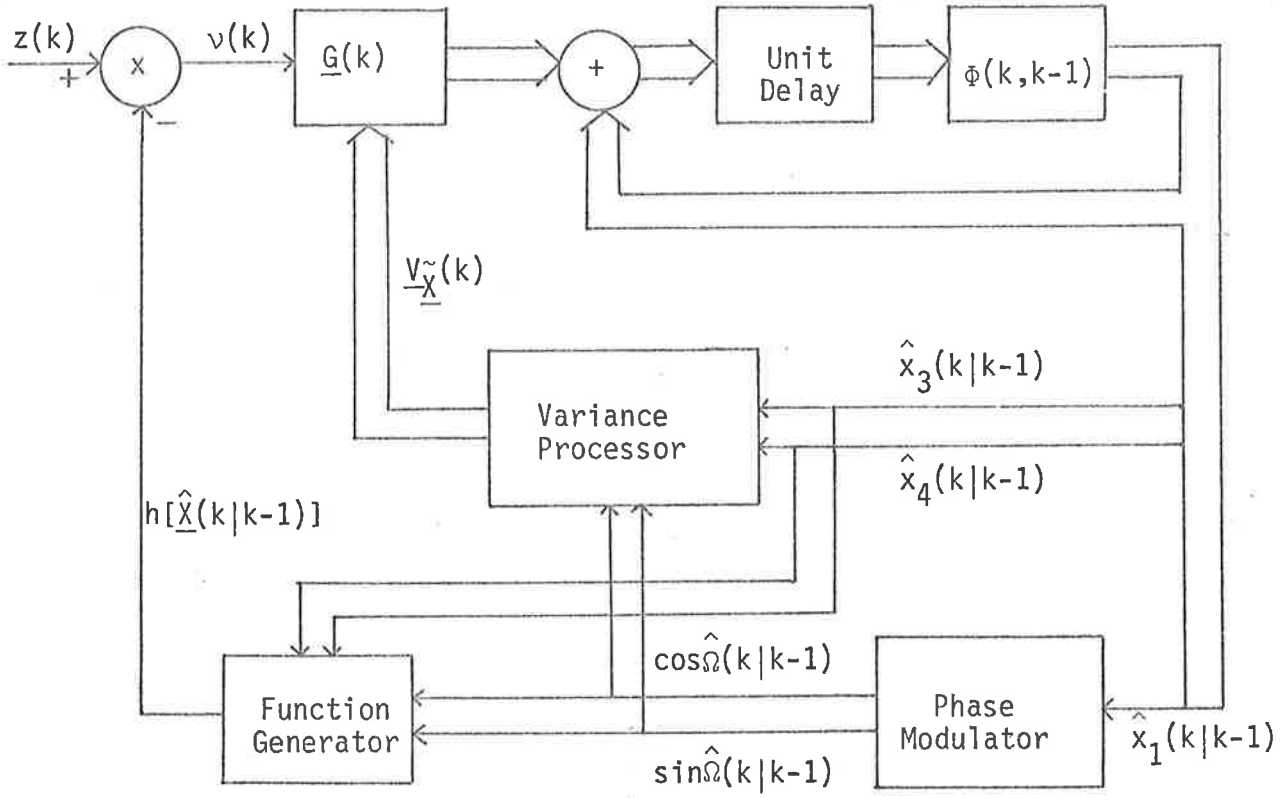

Figure 5.2: EKF Receiver Structure.

which can be implemented as a digital filter excited by the innovation process (see Figure 5.2).

$$\nu(k) \triangleq z(k)-h[\underline{\hat{X}}(k|k-1)]$$

which is equivalent to a random forcing term normally approximated as white gaussian noise.

The desired estimate $\underline{X}(k)$ is expected to have a low-pass (baseband) spectrum and the filtering operation, implicit in Equation 5.1 will tend to filter out any high frequency component associated with the carrier frequency as implied in the error variance Equation V.10. This can be done explicitly by

(i) Determine the baseband form of the error variance equation

$$\underline{V}_{\underline{X}}^{\sim}(k) = \underline{V}_{\underline{X}}^{\sim}(k|k-1)- \sum_{i,j=1}^{3} \frac{H_i H_j}{M(k)} \underline{V}_{\underline{X}}^{\sim}(k|k-1)\underline{L}_i^T \underline{L}_j \underline{V}_{\underline{X}}^{\sim}(k|k-1) \quad \text{(Eq. V.10)}$$

by noting that the term

$$F_{ij} = \frac{H_i H_j}{M(k)}, \qquad \begin{matrix} i = 1, 2, 3 \\ j = 1, 2, 3 \end{matrix} \qquad (5.2)$$

can be put in a general form

$$F_{ij} = \frac{n_o+n_s\sin 2\hat{\Omega}(k|k-1)+n_s\cos 2\hat{\Omega}(k|k-1)}{m_o+m_s\sin 2\hat{\Omega}(k|k-1)+m_c\cos 2\hat{\Omega}(k|k-1)} \qquad (5.2a)$$

where the coefficients in the numerator are evaluated readily from the expressions for H_i's (Eqs. V.12(a), V.12(b) and V.12(c).)

All of these coefficients are time-varying and assumed to vary very slowly compared with the double carrier frequency term to be considered as constants when expanding F_{ij} into a Fourier series with the d.c. component given by

$$D_{ij} = \frac{1}{T_p} \int_{-T_p/2}^{T_p/2} F_{ij}(t)dt \tag{5.3}$$

where T_p is the period of the continuous function $F_{ij}(t)$ obtained from F_{ij} by letting t_k to be a continuous time variable (t).

The evaluation of the integral (5.3) is given in Appendix A and the results are given by Equation VI.4 (see Table VI).

One difficulty occurs here in ascertaining that

$$m_o^2 - m_s^2 - m_c^2 > 0 \tag{5.4}$$

and this was later checked and confirmed by simulation.

(ii) Consider the correction term

$$\underline{G}(k)\nu(k) = \underline{G}(k)\{z(k)-h[\hat{\underline{X}}(k|k-1)]\}$$

$$= \underline{G}(k)z(k)-\underline{G}(k)h[\hat{\underline{X}}(k|k-1)] \tag{5.5}$$

where

$$\underline{G}(k) = \frac{\tilde{\underline{V_X}}(k)}{(r/T)} \sum_{i=1}^{3} H_i \underline{L}_i^T \tag{Eq. VI.6}$$

with $\underline{V}_{\underline{X}}(k)$ being the solution of the baseband error variance equation VI.3 and with H_i's given by

$$\begin{pmatrix} H_1 \\ H_2 \\ H_3 \end{pmatrix} = \sqrt{2P_t} \begin{pmatrix} \hat{x}_3(k|k-1)\cos\hat{\Omega}(k|k-1) - \hat{x}_4(k|k-1)\sin\hat{\Omega}(k|k-1) \\ \sin\hat{\Omega}(k|k-1) \\ \cos\hat{\Omega}(k|k-1) \end{pmatrix} \quad \text{(Eq. VI.7) (See also Eqs. V.12)}$$

As $z(t)$ contains carrier frequency term so the product $\underline{G}(k)z(k)$ will contribute a baseband term.

The second product $\underline{G}(k)\underline{h}[\hat{\underline{X}}(k|k-1)]$ is expanded and by retaining only the baseband term we get

$$\{\underline{G}(k)\underline{h}[\hat{\underline{X}}(k|k-1)]\}_{\text{baseband}} = \frac{\hat{\underline{V}_{\underline{X}}}(k)}{(r/T)} P_t(\hat{x}_3(k|k-1)\underline{L}_2^T + \hat{x}_4(k|k-1)\underline{L}_3^T) \qquad (5.5)$$

The resulting baseband filtering algorithm is then given by Equation VI.5.

Table VI is a summary of the baseband form of the discrete EKF filtering algorithms for FM communication system with Rayleigh fading and Figure 5.3 is the corresponding flowchart.

5.1.3. Baseband receiver structures

Figure 5.4 is a block diagram of the baseband receiver structure resulted from the algorithms of Table VI. On the diagram, the thick line indicate vector quantities whereas the thinner line is used to indicate scalar quantities. The receiver can be recognised as a feedback system similar in form to those of the well-known phase-locked loop (Gupta, 1975) except for the time-varying gain $\underline{G}(k)$ given in terms of the solution of the variance processor driven by the estimates of the channel fading processes.

TABLE VI.

BASEBAND FORM OF THE DISCRETE EKF FILTERING ALGORITHMS FOR FM COMMUNICATION SYSTEM WITH RAYLEIGH FADING

One stage prediction algorithm

$$\hat{\underline{X}}(k|k-1) = \Phi(k,k-1)\hat{\underline{X}}(k-1) \tag{VI.1}$$

$$\hat{\underline{X}}(0) = \underline{\mu}_{X_0} \tag{VI.1a}$$

Prior error variance algorithm

$$\underline{V}_{\tilde{X}}(k|k-1) = \Phi(k,k-1)\underline{V}_{\tilde{X}}(k-1)\Phi^T(k,k-1)+\underline{Q}(k) \tag{VI.2}$$

$$\underline{V}_{\tilde{X}}(0) = \underline{V}_{X_0} \tag{VI.2a}$$

Error variance algorithm

$$\underline{V}_{\tilde{X}}(k) = \underline{V}_{\tilde{X}}(k|k-1) - \sum_{i,j=1}^{3} D_{ij}\underline{V}_{\tilde{X}}(k|k-1)\underline{L}_i^T\underline{L}_j\underline{V}_{\tilde{X}}(k|k-1) \tag{VI.3}$$

where

$$[D_{ij}] = P_t\Delta\begin{bmatrix} \hat{x}_3^2(k|k-1)+\hat{x}_4^2(k|k-1) & -\hat{x}_4(k|k-1) & \hat{x}_3(k|k-1) \\ -\hat{x}_4(k|k-1) & 1 & 0 \\ \hat{x}_3(k|k-1) & 0 & 1 \end{bmatrix}$$

$$+\frac{m_s(1-m_0\Delta)}{m_s^2+m_c^2}P_t\begin{bmatrix} -2\hat{x}_3(k|k-1)\hat{x}_4(k|k-1) & \hat{x}_3(k|k-1) & -\hat{x}_4(k|k-1) \\ \hat{x}_3(k|k-1) & 0 & 1 \\ -\hat{x}_4(k|k-1) & 1 & 0 \end{bmatrix}$$

$$+\frac{m_c(1-m_0\Delta)}{m_s^2+m_c^2}P_t\begin{bmatrix} \hat{x}_3^2(k|k-1)-\hat{x}_4^2(k|k-1) & \hat{x}_4(k|k-1) & \hat{x}_3(k|k-1) \\ \hat{x}_4(k|k-1) & -1 & 0 \\ \hat{x}_3(k|k-1) & 0 & 1 \end{bmatrix}$$

$$\Delta \triangleq \frac{1}{\sqrt{m_0^2-m_s^2-m_c^2}} \tag{VI.4}$$

L_i's, m_0, m_s and m_c are as defined in Table V.

Filtering algorithm

$$\underline{\hat{X}}(k) = \underline{\hat{X}}(k|k-1)+\underline{G}(k)z(k)-\frac{P_t}{(r/T)}\underline{V}_{\underline{\tilde{X}}}(k)[\hat{x}_3(k|k-1)\underline{L}_2^T+\hat{x}_4(k|k-1)\underline{L}_3^T] \quad \text{(VI.5)}$$

where

$$\underline{G}(k) = \frac{\underline{V}_{\underline{\tilde{X}}}(k)}{(r/T)} \sum_{i=1}^{3} H_i \underline{L}_i^T \quad \text{(VI.6)}$$

and H_i's are as defined in Table V.

$$\begin{pmatrix} H_1 \\ H_2 \\ H_3 \end{pmatrix} = \sqrt{2P_t} \begin{pmatrix} \hat{x}_3(k|k-1)\cos\hat{\Omega}(k|k-1)-\hat{x}_4(k|k-1)\sin\hat{\Omega}(k|k-1) \\ \sin\hat{\Omega}(k|k-1) \\ \cos\hat{\Omega}(k|k-1) \end{pmatrix} \quad \text{(VI.7)}$$

$$\hat{\Omega}(k|k-1) = \omega_c t_k+\hat{x}_1(k|k-1) \quad \text{(VI.8)}$$

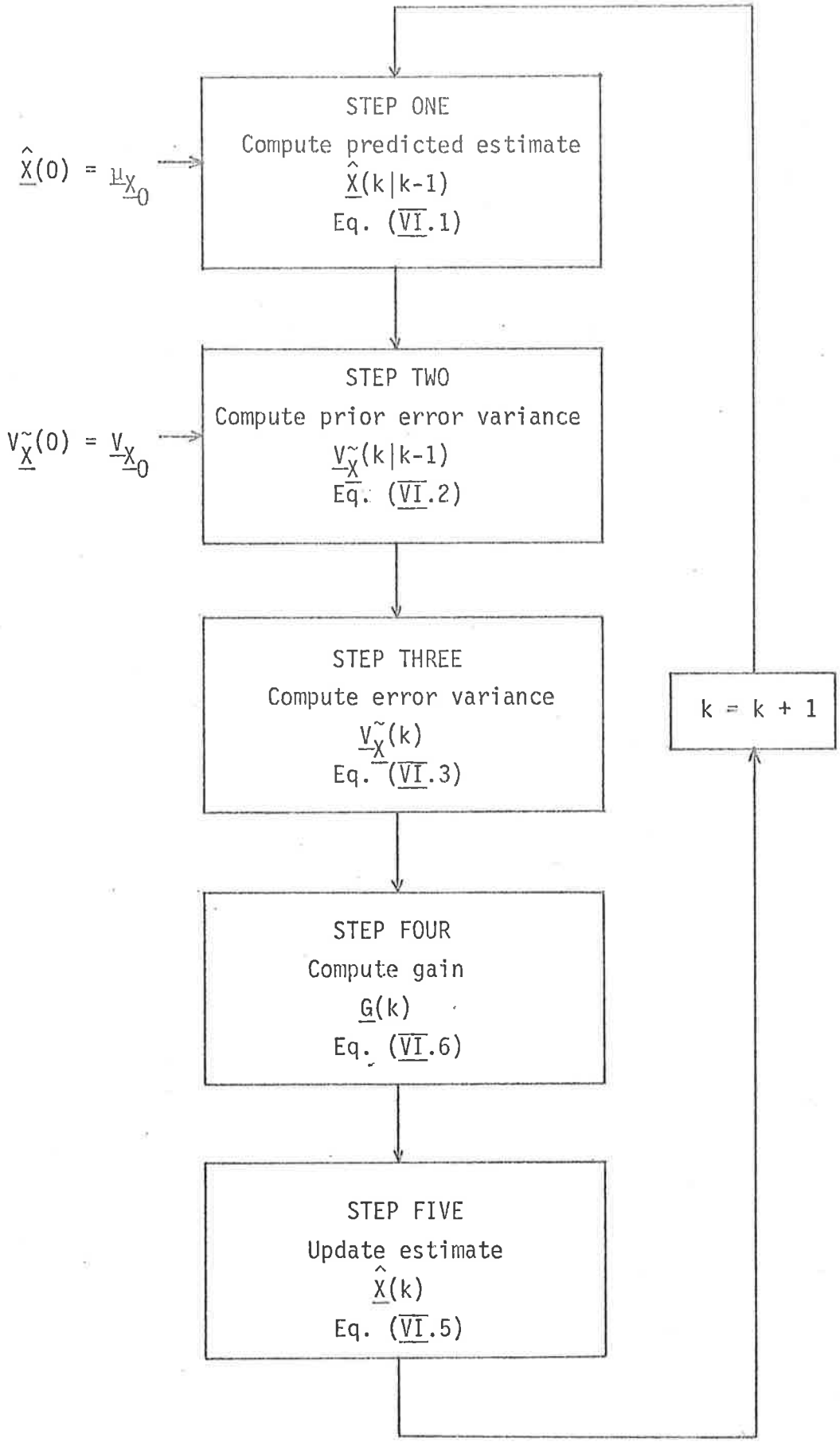

Figure 5.3. Flow chart for baseband EKF algorithm (Table VI).

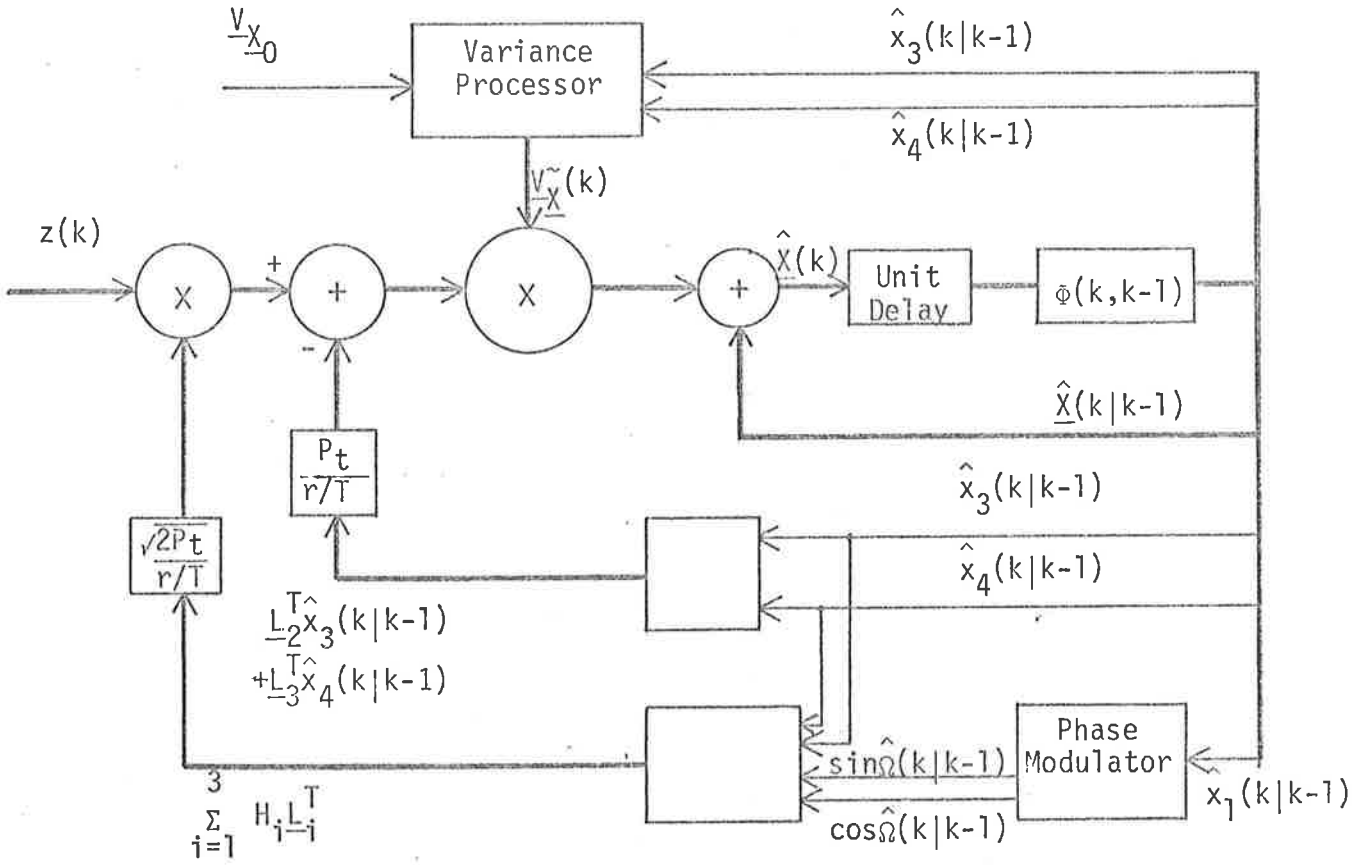

Figure 5.4. Baseband EKF Receivers

5.1.4. Performance

Computer simulation is used to study the performance of the receivers. The procedure and the parameter set used have been described in Chapter 4 and the results are summarised below.

Figures 5.5(a) and 5.5(b): Inverse Error Variance for various values of the bandwidth expansion ratio (β).

Each graph consists of two sets of curves showing the predicted inverse error variances and the simulated inverse error variances against the signal to noise ratio in the message bandwidth (Λ) as defined in Equation 4.16. As already discussed in Chapter 4, the predicted error variances are obtained as the steady-state value of the error variance equations

$$\lim_{k\to\infty} V_{\tilde{x}_1}(k) \qquad \text{for phase}$$

$$\lim_{k\to\infty} V_{\tilde{x}_2}(k) \qquad \text{for message}$$

and the simulated error variances are calculated as

$$\sum_{k=1}^{N} [x_1(k)-\hat{x}_1(k)]^2 \qquad \text{for phase}$$

$$\sum_{k=1}^{N} [x_2(k)-\hat{x}_2(k)]^2 \qquad \text{for message}$$

where N is total number of simulation points determined in Chapter 4.

Also plotted on the same graph are the simulated results of Polk (1973) for no fading using the EKF algorithm and uniform sampling with $\beta = 25$.

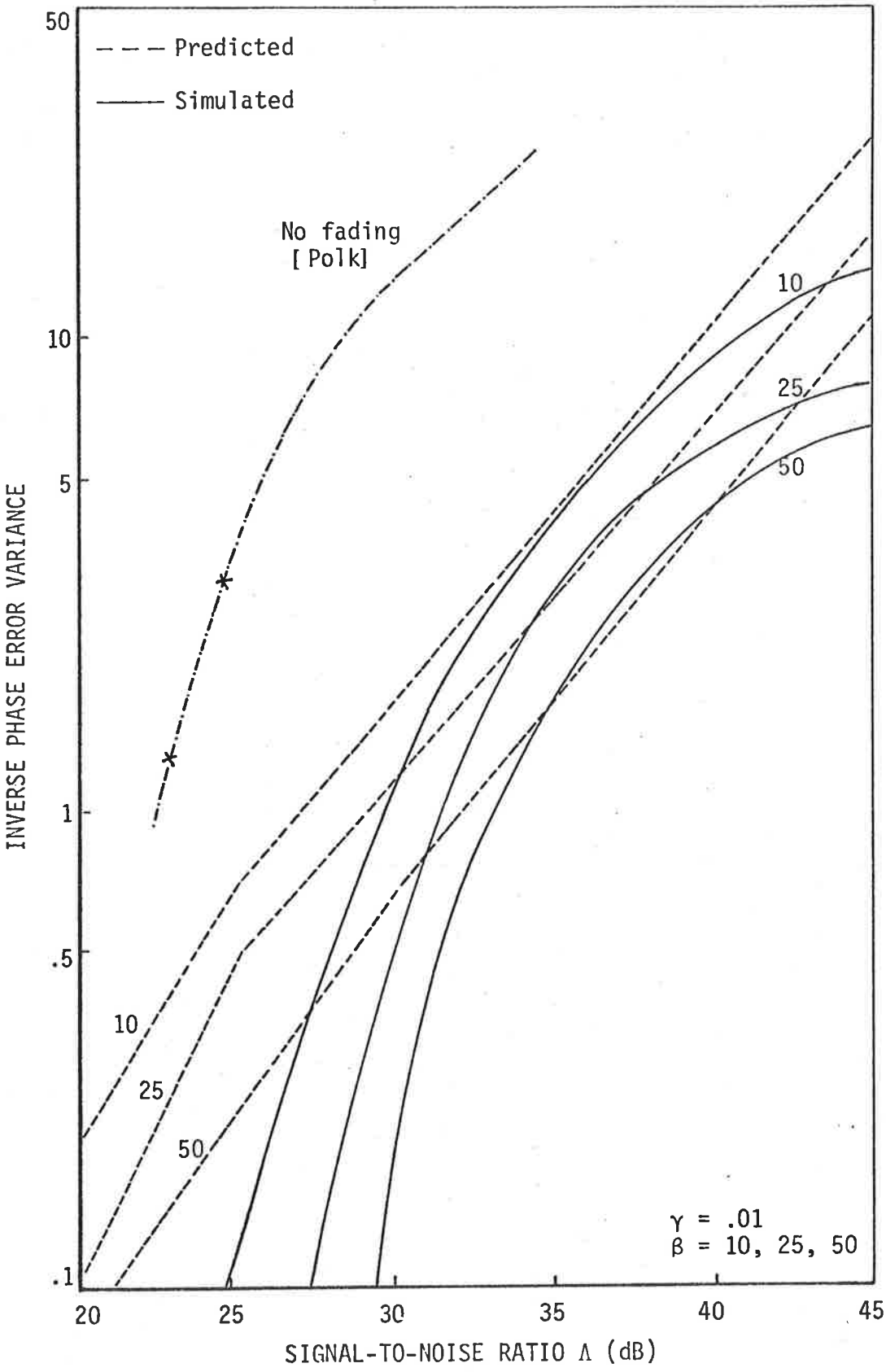

Fig. 5.5(a): Inverse phase error variance (EKF, uniform, β varying)

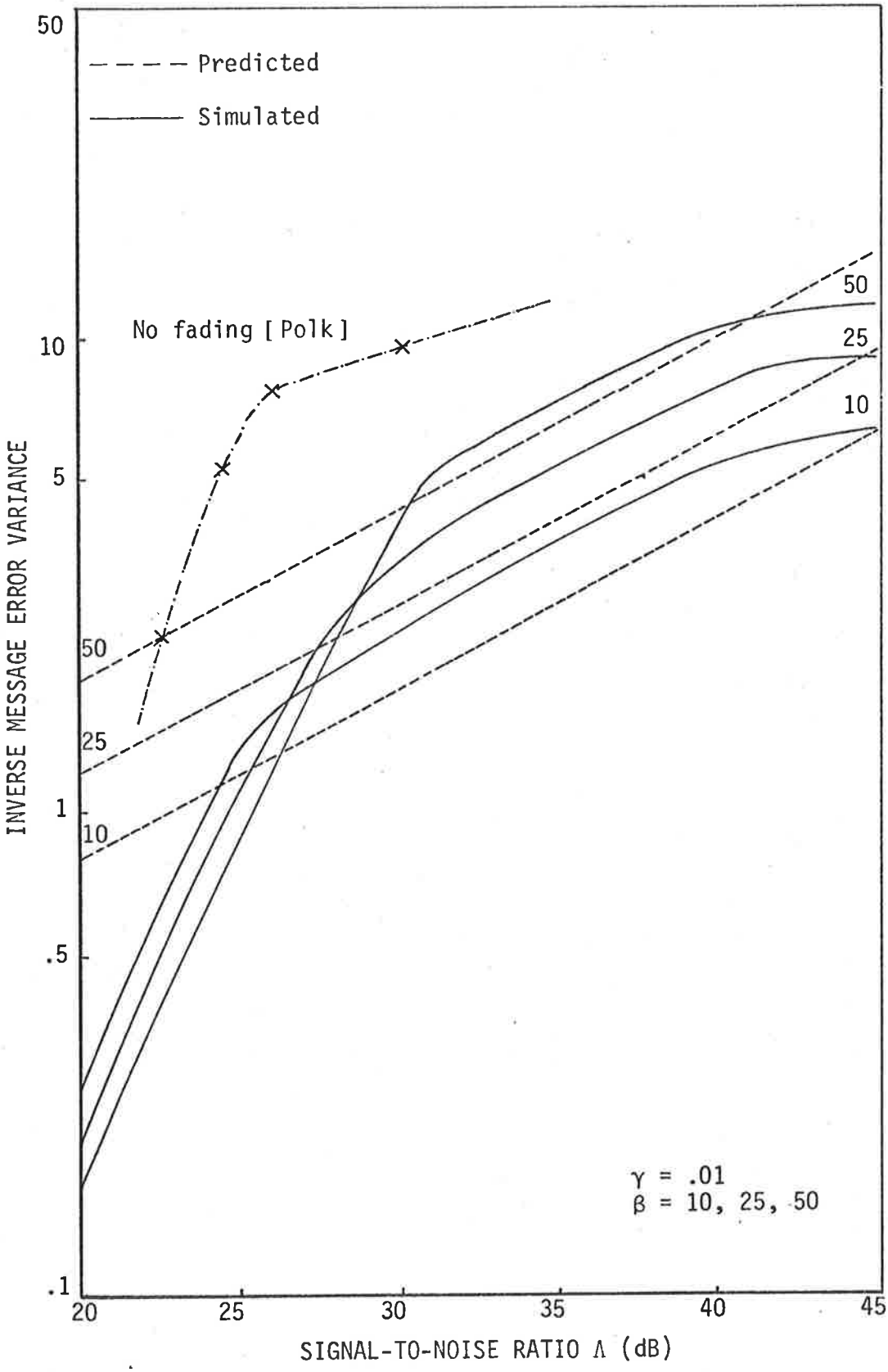

Fig. 5.5(b): Inverse Message Error Variance (EKF, uniform, β varying)

The results exhibits the features characteristic of an FM system, namely,

(i) Threshold behaviour: following Polk (1973), threshold is said to occur when the phase error variance exceeds

$$\left(V_{x_1}(k)\right)_{\text{threshold}} = .25 \qquad (5.6)$$

and it can be seen (Figure 5.5(a)) that threshold occurs at approximately 11dB higher than the no fading case (for $\beta = 25$).

(ii) Bandwidth versus signal-to-noise ratio tradeoff: By increasing β and therefore increasing the bandwidth required for transmission, the error variance of the phase also increases as expected but the message error variance (Figure 5.5(b)) decreases and results in better output signal-to-noise ratio at the expense of higher threshold.

Another observation is the agreement between the predicted and the simulated values of the error variances which seems to be very good around threshold region and becomes very bad below threshold. This is due to the approximate nature inherent in the derivation of the algorithm which renders it valid only for low noise conditions.

Figures 5.6(a) and 5.6(b): Inverse Error Variance for various values of the "fading rate".

The "fading rate" f_r defined as

$$f_r = \frac{\gamma}{\alpha} = \gamma \quad (\text{for } \alpha = 1)$$

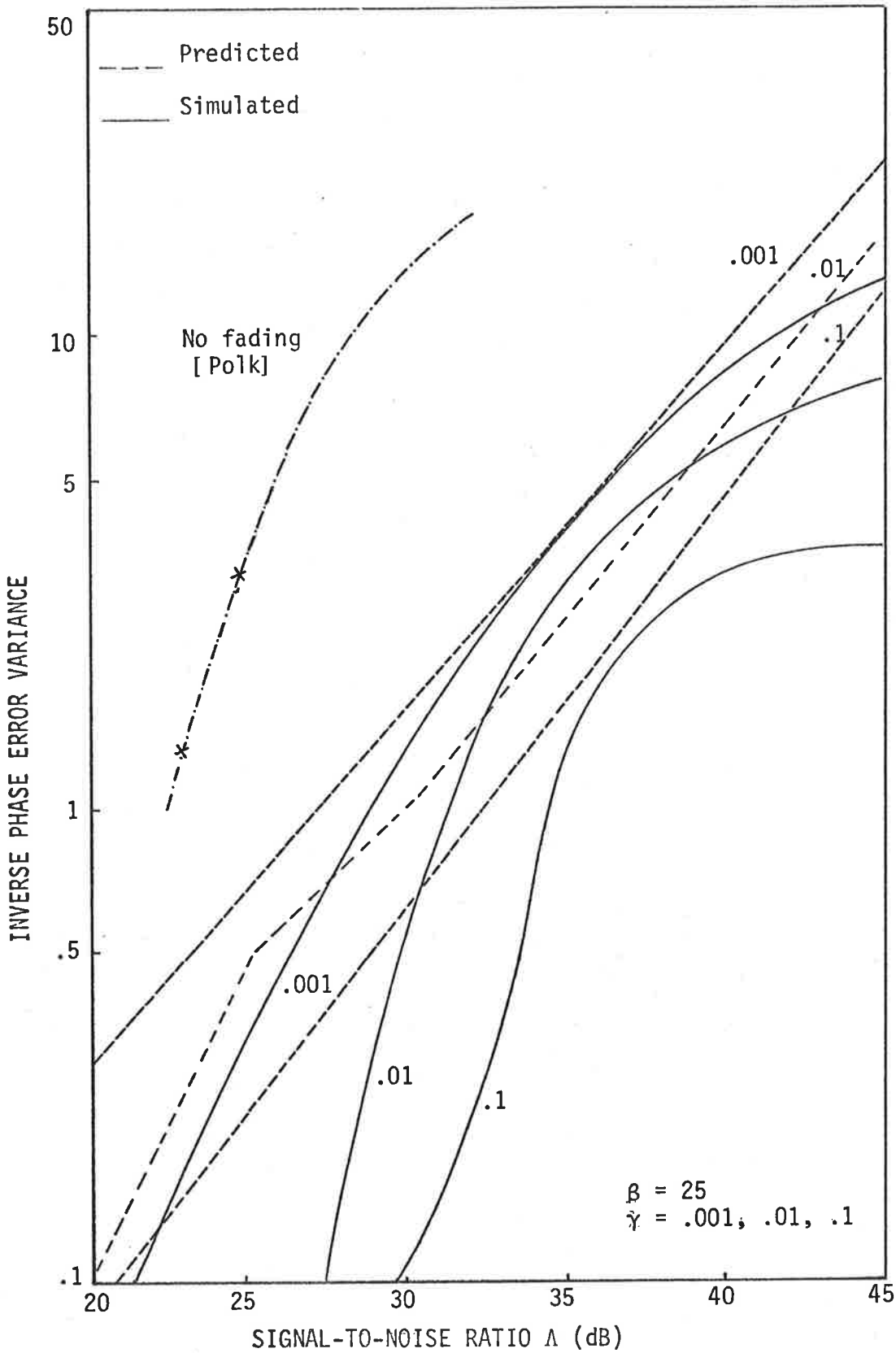

Fig. 5.6(a): Inverse Phase Error Variance (EKF, Uniform, γ varying)

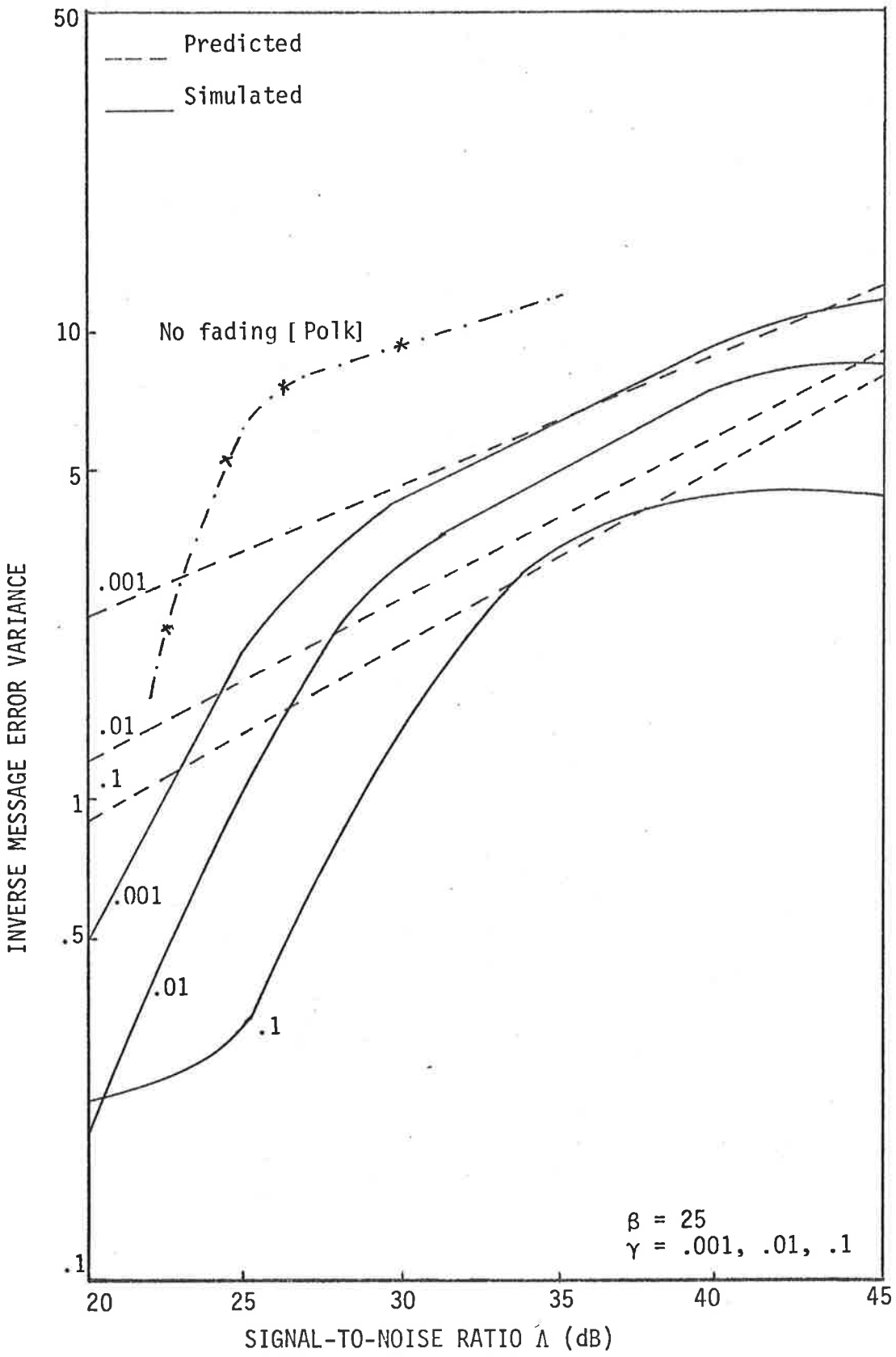

Fig. 5.6(b): Inverse Message Error Variance (EKF, Uniform, γ varying)

is varied to study the effect of "slow" or "fast" fading by which the rates of variation of the fading components $b_1(t)$ and $b_2(t)$ is compared to the rate of variation of the message. As can be seen, the performance of the receiver improvesboth in terms of threshold and of signal-to-noise ratio when γ decreases from $\gamma = 0.01$ (slow fading) to $\gamma = .001$ (very slow fading). On the other hand, with $\gamma = .1$, the receiver seems to be operating below threshold all the times.

5.1.5. Comparison with Dharamsi results

Dharamsi and Gupta (1975a) considered an identical problem of discrete-time demodulation of analog FM signals transmitted over Rayleigh fading channels using the EKF algorithm and uniform sampling as was done in this section. They also consider Rician channels by allowing one of the fading processes to have a non-zero mean equal to the specular component of the Rician channel. Furthermore, they also considered other estimation algorithms and the performance results are presented in another paper (Dharamsi and Gupta, 1975b). Their results for the EKF algorithm are compared with those obtained in this section. Figure 5.7 shows the results for the inverse message error variance with $\beta = 25$ and $\gamma = .01$ (the quantity γ used here corresponds to α in Dharamsi and Gupta paper) which seems to agree well with respect to the simulated error variance but differ significantly for the predicted error variance. This is despite the fact that the algorithms have been checked to be identical and in fact, some of the notations used in this thesis have been borrowed from their work and made as identical as possible. For the case when $\gamma = .1$, their results indicated that the performance is better than those for the case when $\gamma = .01$ which is exactly the opposite of those obtained and presented in Figure 5.6(a) and 5.6(b).

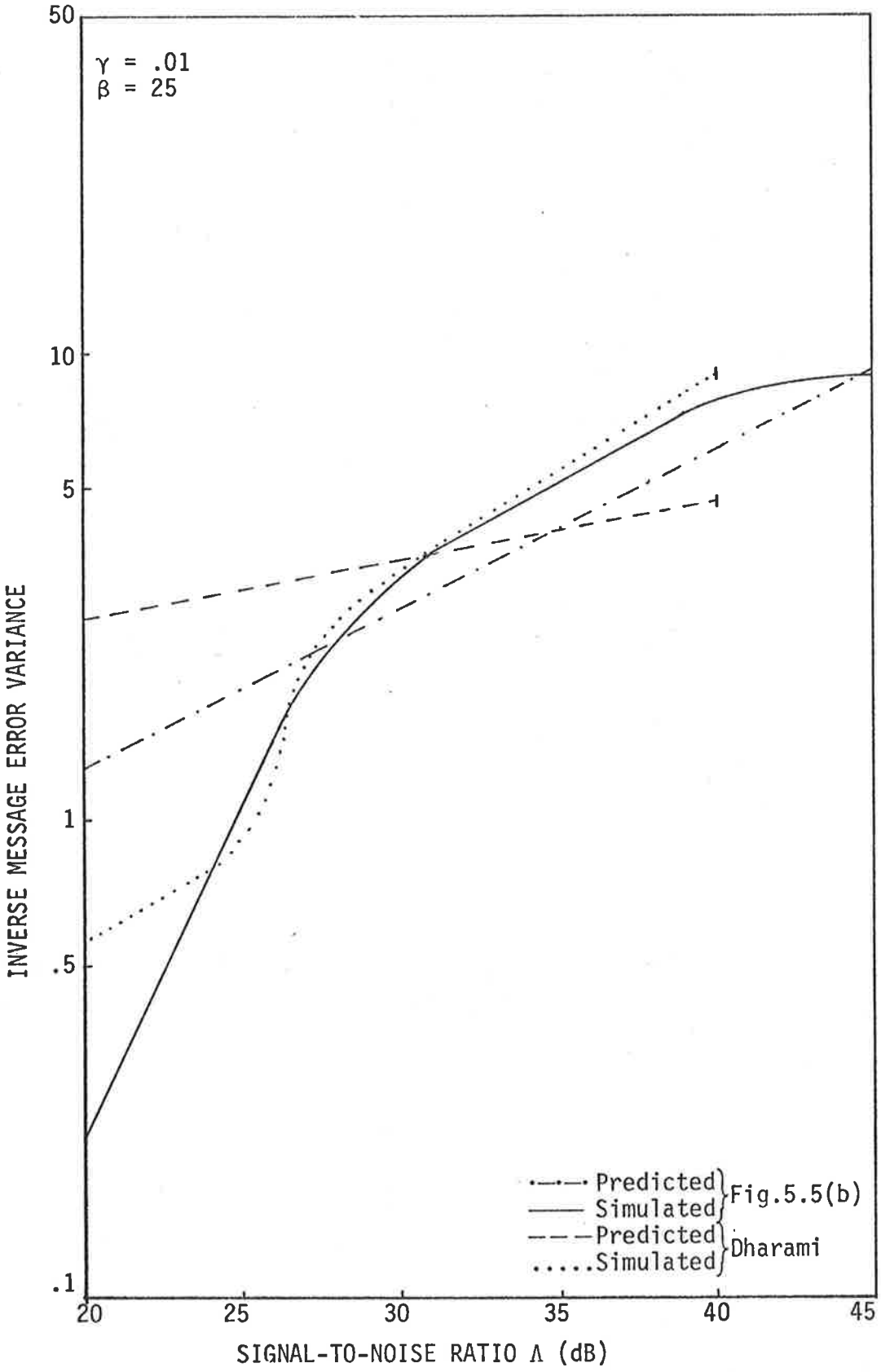

Fig. 5.7: Comparison with Dharami's results.

5.2 Quasi-stationary analysis: slow fading

In the early stage of this work, due to the limited access to the computer for running long simulation programs, effort was made in simplifying the receiver structures and therefore reducing the execution time. This was done for slowly varying channels ($\gamma \leq .01$) by using a "quasi-stationary" analysis proposed by Van Trees (1971, p. 253) which requires the following assumptions to be made concerning the channel variations and consequent effects on the estimation algorithms:

(i) The channel measurement error is small.

(ii) The cross-coupling term may be neglected.

(iii) A quasi-stationary solution to the variance equation is valid.

5.2.1 Quasi-stationary receivers

The error variance matrix is now assumed to be approximated by

$$\underset{\sim}{V}_{\underset{\sim}{X}}(k) = \begin{pmatrix} V_{\tilde{x}_1}(k) & V_{\tilde{x}_1\tilde{x}_2}(k) & 0 & 0 \\ V_{\tilde{x}_1\tilde{x}_2}(k) & V_{\tilde{x}_2}(k) & 0 & 0 \\ 0 & 0 & V_{\tilde{x}_3}(k) & 0 \\ 0 & 0 & 0 & V_{\tilde{x}_4}(k) \end{pmatrix} \qquad (5.7)$$

and the baseband EKF algorithms in Table VI are modified to result in a simpler set of algorithms shown in Table VII. The corresponding flowchart is shown in Figure 5.8.

A block diagram of the receiver structure to be called the quasi-stationary receiver is shown in Figure 5.9(a) where the output from the function generator block is given by

$$H_1 = \hat{x}_3(k|k-1)\cos\hat{\Omega}(k|k-1) - \hat{x}_4(k|k-1)\sin\hat{\Omega}(k|k-1) \qquad \text{(See Eq. VII.8)}$$

TABLE VII.

QUASI-STATIONARY BASEBAND FORM OF THE DISCRETE EKF FILTERING ALGORITHMS FOR FM SYSTEM WITH SLOW RAYLEIGH FADING

Error variance algorithm

For phase and message

$$V_{\tilde{x}_1}(k) = V_{\tilde{x}_1}(k|k-1)\,[1-D_1 V_{\tilde{x}_1}(k|k-1)] \tag{1a}$$

$$V_{\tilde{x}_1\tilde{x}_2}(k) = V_{\tilde{x}_1\tilde{x}_2}(k|k-1)\,[1-D_1 V_{\tilde{x}_1}(k|k-1)] \tag{1b}$$

$$V_{\tilde{x}_2}(k) = V_{\tilde{x}_2}(k|k-1) - D_1 V_{\tilde{x}_1\tilde{x}_2}(k|k-1) \tag{1c}$$

For channel estimation

$$V_{\tilde{x}_3}(k|k-1) = V_{\tilde{x}_3}(k|k-1)\,[1-D_2 V_{\tilde{x}_3}(k|k-1)] \tag{2a}$$

$$V_{\tilde{x}_4}(k|k-1) = V_{\tilde{x}_4}(k|k-1)\,[1-D_3 V_{\tilde{x}_4}(k|k-1)] \tag{2b}$$

Filtering algorithm

Phase and message

$$\begin{pmatrix}\hat{x}_1(k)\\ \hat{x}_2(k)\end{pmatrix} = \begin{pmatrix}\hat{x}_1(k|k-1)\\ \hat{x}_2(k|k-1)\end{pmatrix} + \frac{H_1}{(r/T)} \begin{pmatrix}V_{\tilde{x}_1}(k)\\ v_{\tilde{x}_1\tilde{x}_2}(k)\end{pmatrix} z(k) \tag{3}$$

Channel estimator

$$\begin{pmatrix}\hat{x}_3(k)\\ \hat{x}_4(k)\end{pmatrix} = \begin{pmatrix}\hat{x}_3(k|k-1)\\ \hat{x}_4(k|k-1)\end{pmatrix} - \frac{P_t}{(r/T)} \begin{pmatrix}\hat{x}_3(k|k-1)\ V_{\tilde{x}_3}(k)\\ \hat{x}_4(k|k-1)\ V_{\tilde{x}_4}(k)\end{pmatrix} + \frac{1}{(r/T)} \begin{pmatrix}H_2\ V_{\tilde{x}_3}(k)\\ H_3\ V_{\tilde{x}_4}(k)\end{pmatrix} \tag{4}$$

Definitions

$$\begin{pmatrix} D_1 \\ D_2 \\ D_3 \end{pmatrix} = \Delta P_t \begin{pmatrix} \hat{x}_3^2(k|k-1) + \hat{x}_4^2(k|k-1) \\ 1 \\ 1 \end{pmatrix} + \frac{m_s(1-m_o\Delta)}{m_s^2 + m_c^2} P_t \begin{pmatrix} -2\hat{x}_3(k|k-1)\hat{x}_4(k|k-1) \\ 0 \\ 0 \end{pmatrix}$$

$$+ \frac{m_c(1-m_o\Delta)}{m_s^2 + m_c^2} P_t \begin{pmatrix} \hat{x}_3^2(k|k-1) - \hat{x}_4^2(k|k-1) \\ -1 \\ 1 \end{pmatrix} \tag{5}$$

$$\left.\begin{aligned} m_o &= \left(\frac{r}{T}\right) + P_t\left\{\left(\hat{x}_3^2(k|k-1) + \hat{x}_4^2(k|k-1)\right) V_{\tilde{x}_1}(k|k-1) + V_{\tilde{x}_3}(k|k-1) + V_{\tilde{x}_4}(k|k-1)\right\} \\ m_s &= 2P_t\{-\hat{x}_3(k|k-1)\hat{x}_4(k|k-1) V_{\tilde{x}_1}(k|k-1)\} \\ m_c &= P_t\left\{\left(\hat{x}_3^2(k|k-1) - \hat{x}_4^2(k|k-1)\right) V_{\tilde{x}_1}(k|k-1) - V_{\tilde{x}_3}(k|k-1) + V_{\tilde{x}_4}(k|k-1)\right\} \end{aligned}\right\} \tag{6}$$

$$\Delta = \frac{1}{\sqrt{m_o^2 - m_s^2 - m_c^2}} \tag{7}$$

$$\begin{pmatrix} H_1 \\ H_2 \\ H_3 \end{pmatrix} = \sqrt{2P_t} \begin{pmatrix} \hat{x}_3(k|k-1)\cos\hat{\Omega}(k|k-1) - \hat{x}_4(k|k-1)\sin\hat{\Omega}(k|k-1) \\ \sin\hat{\Omega}(k|k-1) \\ \cos\hat{\Omega}(k|k-1) \end{pmatrix} \tag{8}$$

$$\hat{\Omega}(k|k-1) = \omega_c t_k + \hat{x}_1(k|k-1) \tag{9}$$

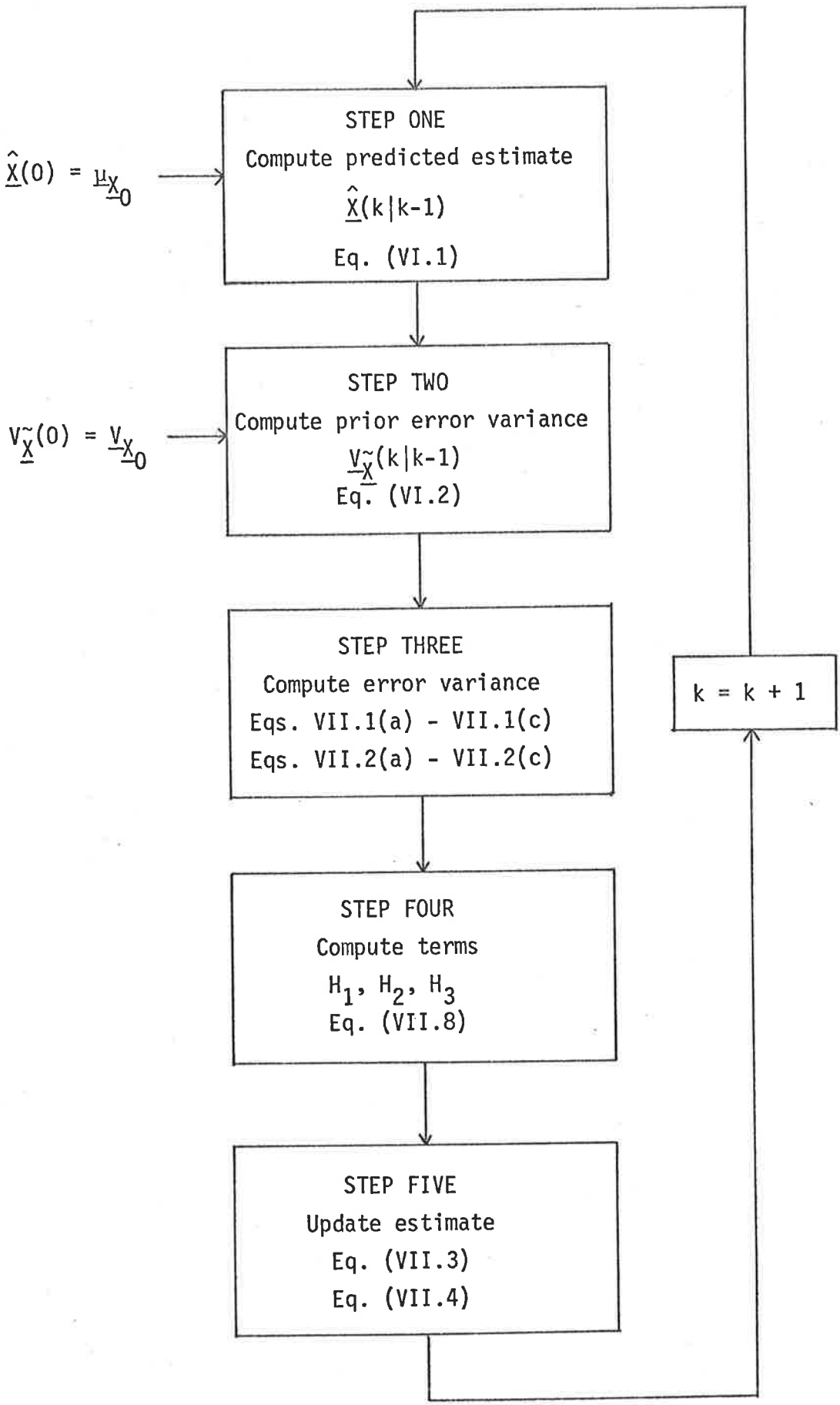

Figure 5.8: Flow chart of Quasi - stationary EKF Receivers (Table VII). (See also Table VI).

and the quantities $V_{\tilde{x}_1}(k)$, $V_{\tilde{x}_1\tilde{x}_2}(k)$, $V_{\tilde{x}_3}(k)$, $V_{\tilde{x}_4}(k)$ are solutions of the error variance algorithm in Table VII.

From the diagram, the receiver is seen to consist of two parts: the upper part is to estimate the phase and message, while the lower part is to estimate the channel processes. To facilitate discussion, the upper part will be called the message estimator (as the message estimate is the desired one in a practical solution) and the lower part will be termed the channel estimator. Each estimator is recognised as a feedback structure similar to those of a phase-locked loop and consists of various multiplexers, gains, loop filters and is driven by the same incoming observed signal z(k) plus a feedback path from the phase modulator common to both. By redrawing Figure 5.9(a) in another form (Figure 5.9(b)), the receiver can be readily recognised as an adaptive version of the digital phase-locked loops (Gupta, 1975).

The basic operation can be recognised as the maximal-ratio combining of the in-phase and quadrature components of the carrier signal: the outputs from the voltage controlled oscillators (VCO) of the phase-locked loops are used to cross-correlate with the input signal to produce a measure of the in-phase and quadrature components of the fading process (characterising the Rayleigh fading channel) and the output from the channel estimator is used to update the variance processor for the message process, trying to keep the carrier level constant so as to allow for normal demodulation of an FM signal.

5.2.2. Performance

The parameter set is the same as in Section 5.1.4 and the simulation results are discussed below.

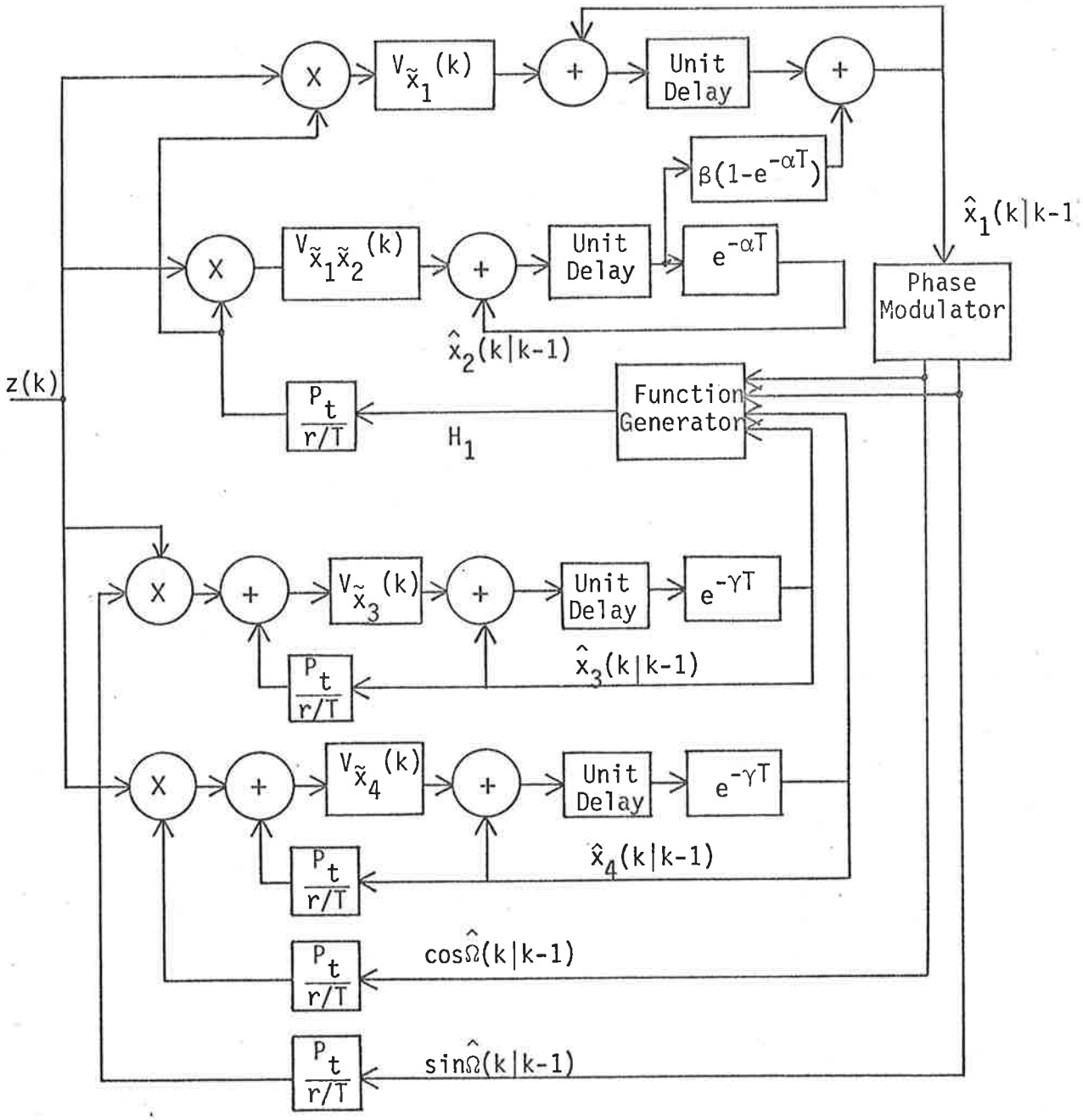

Figure 5.9(a): Quasi-stationary Receivers For Slow Fading Channels

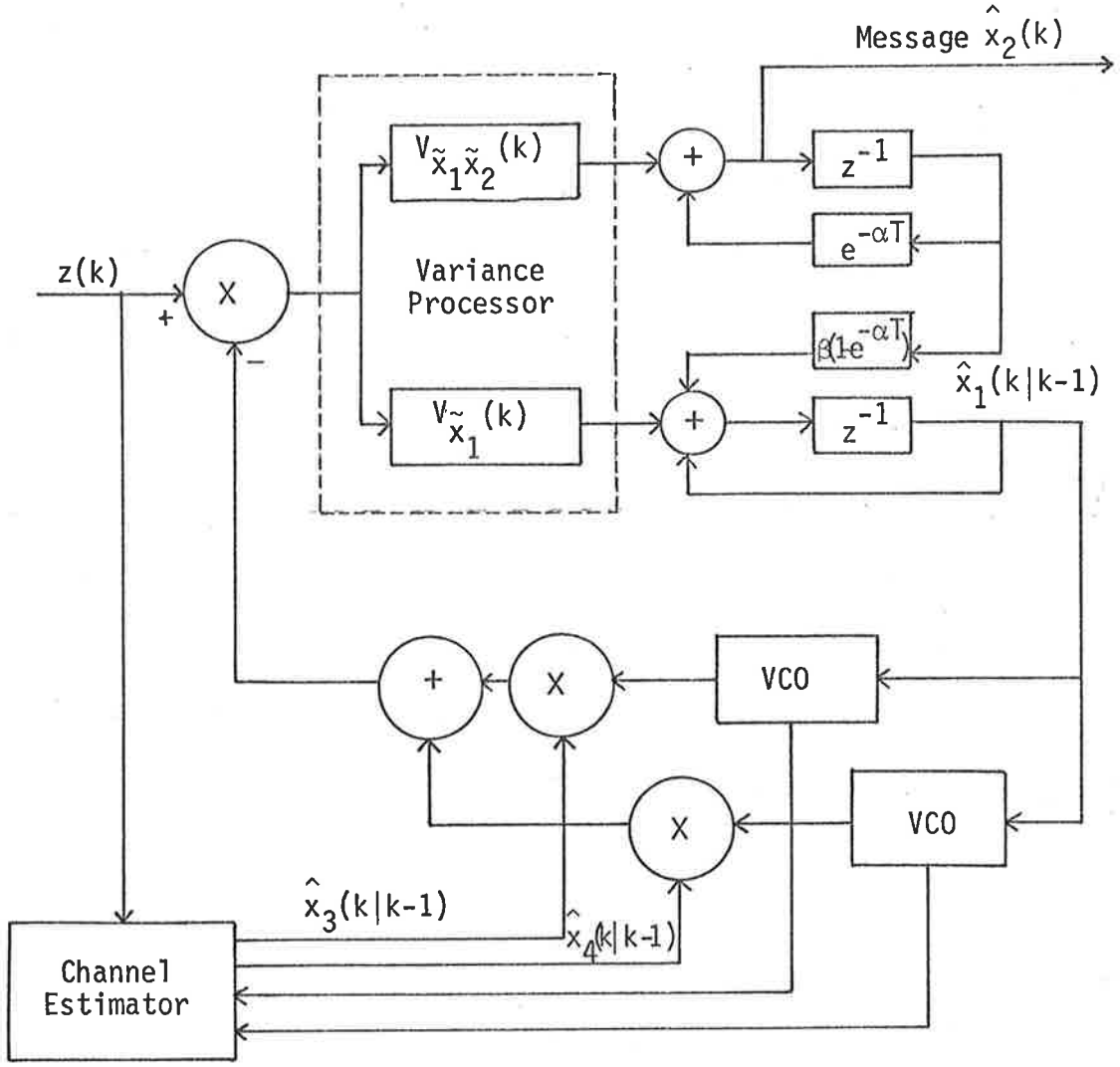

Figure 5.9(b): Quasi-stationary EKF Receiver.

Figure 5.10(b): Curves B show the simulated inverse error variances (with $\beta = 25$, $\gamma = .01$) for the quasi-stationary receiver using EKF algorithms and when compared with the results (curves A) for the baseband EKF receivers (from Figures 5.5(a) and 5.5(b)), it can be seen that the quasi-stationary receivers do not perform as well. This is rather disappointing at first. However, when considering the results for $\beta = 25$ and $\gamma = .001$ (very slow fading) shown in

Figure 5.11(a) and 5.11(b): It can be seen that the performances of the quasi-stationary receivers (curves B) are almost the same as those obtained for the baseband receivers (from Figures 5.6(a) and 5.6(b)). The assumptions regarding the validity of a quasi-stationary analysis discussed at the beginning of this section are thus valid for very slow fading channels only.

Curves C on Figures 5.10(a) through 5.11(b) are for the performance of the MAP receivers to be discussed in the following section.

5.3 Discrete MAP Receivers

5.3.1. Algorithm

The discrete MAP algorithm in Chapter 3 (Table III) is applied to the FM communication system in Table IV. The resulting algorithms are similar to those obtained in Table V for the EKF algorithm except for the error variance equation which requires some further discussion.

In Table III, the error variance equation takes two alternative forms. The first form (Eq. III.6) is commonly found in the literature (e.g. Sage and Melsa, 1971, Table 9.3-1, p. 452) and requires

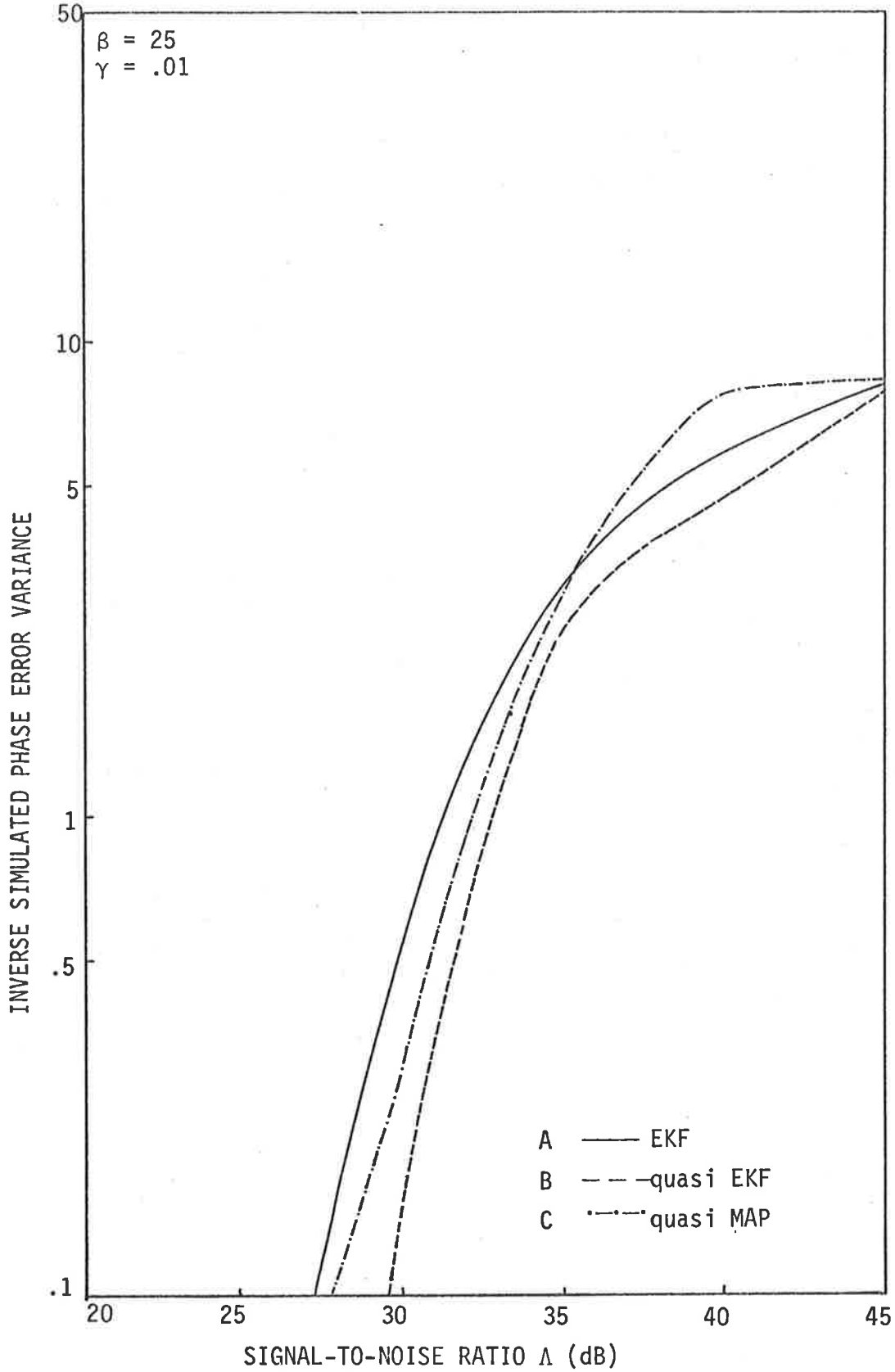

Fig. 5.10(a): Receiver performance (phase) for slow fading channels using quasi-stationary analysis.

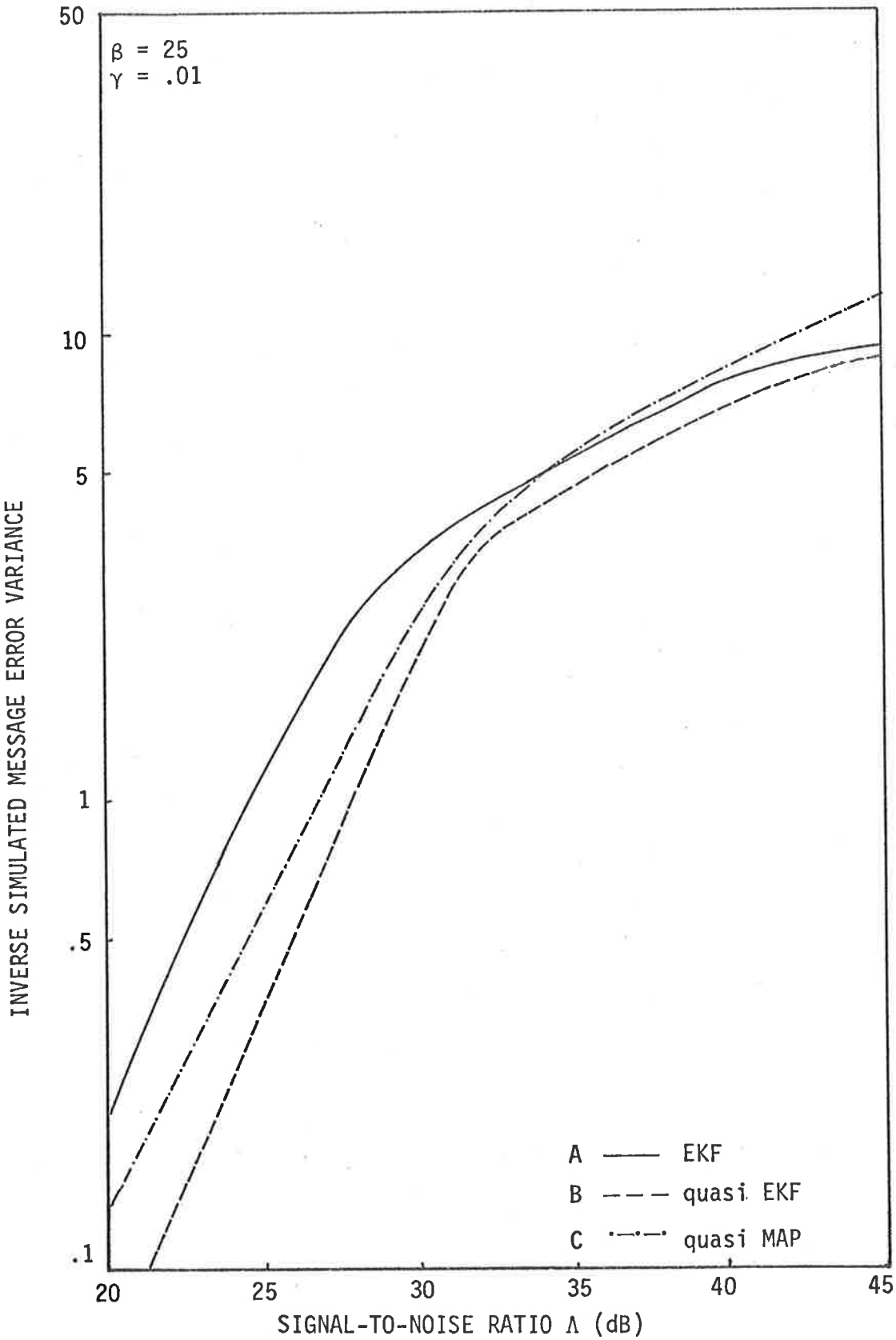

Fig. 5.10(b): Receiver performance (message) for slow fading channels using quasi-stationary analysis

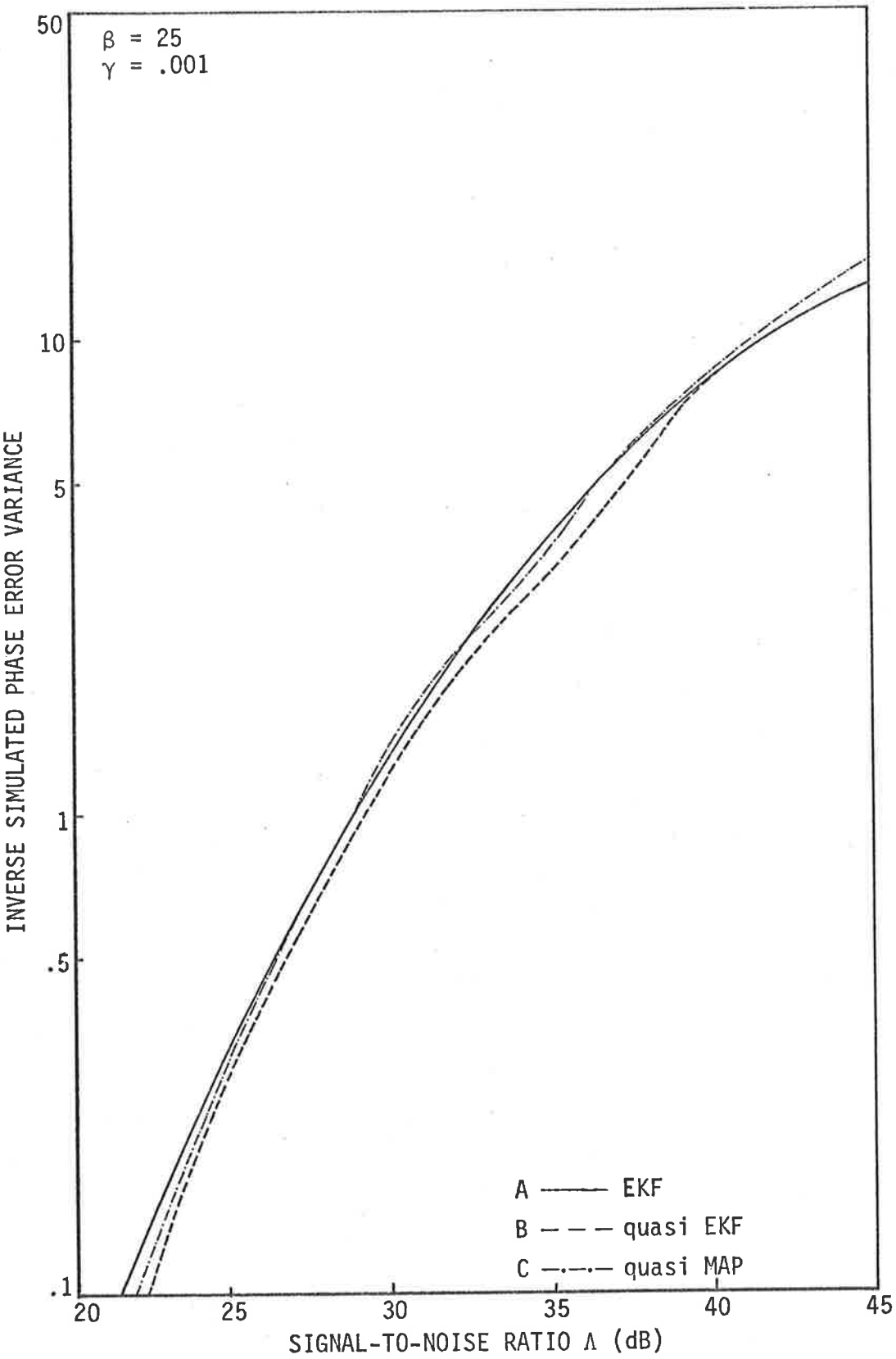

Fig. 5.11(a): Receiver performance (phase) for very slow fading channels using quasi-stationary analysis.

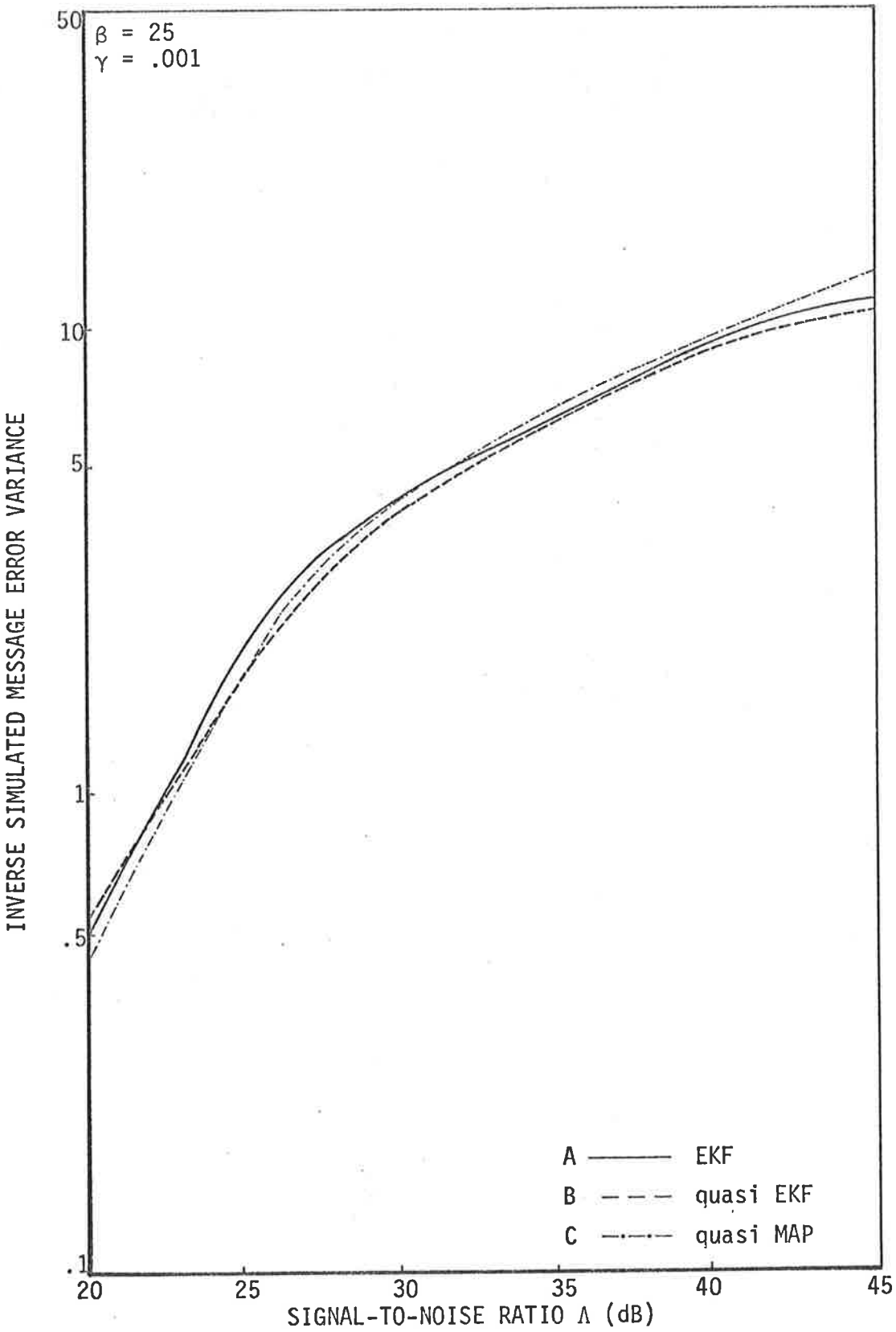

Fig. 5.11(b): Receiver performance (message) for very slow fading channels using quasi-stationary analysis.

the factorisation of the Hessian matrix (of dimension 4 x 4)

$$\underline{M}[\hat{\underline{X}}(k|k-1),k] = \frac{-\partial}{\partial\hat{\underline{X}}(k|k-1)}\left[\frac{\partial \underline{h}^T[\hat{\underline{X}}(k|k-1)]}{\partial\hat{\underline{X}}(k\ k-1)}\ \underline{R}^{-1}(k)\ \underline{\nu}(k)\right] \qquad (5.8)$$

$$= \underline{L}^T \begin{bmatrix} m_{11} & m_{12} & m_{13} \\ m_{12} & m_{22} & m_{23} \\ m_{13} & m_{23} & m_{33} \end{bmatrix} \underline{L} \qquad \text{(Eq. VIII.2)}$$

with m_{ij}'s given by Eqs. VIII.2(a) through VIII.2(f).

The (2, 2) minor of $\underline{M}[\hat{\underline{X}}(k|k-1),k]$ is calculated to be

$$|M_{22}| = \begin{vmatrix} m_{11} & m_{12} & m_{13} \\ m_{12} & m_{22} & m_{23} \\ m_{13} & m_{23} & m_{33} \end{vmatrix}$$

$$= -2\nu^2(k)$$

and $\underline{M}[\hat{\underline{X}}(k|k-1),k]$ is not positive definite and cannot be factorised as $\underline{J}(k)\underline{R}^{-1}(k)\underline{J}(k)$ (Eq. III.6(a)) (Bellman, 1960.)

The alternative form (Eq. III.7) is used and is summarised in Table VIII. The flowchart for the MAP algorithm is shown in Figure 5.12.

TABLE VIII.

DISCRETE MAP FILTERING ALGORITHM FOR FM COMMUNICATION SYSTEM WITH RAYLEIGH FADING (UNIFORM SAMPLING)

Error variance algorithm

$$\underline{V}_{\tilde{\underline{X}}}(k) = \left(I + \underline{V}_{\tilde{\underline{X}}}(k|k-1)\underline{M}[\underline{X}(k|k-1),k]\right)^{-1} \underline{V}_{\tilde{\underline{X}}}(k|k-1) \tag{1}$$

where

$$\underline{M}[\hat{\underline{X}}(k|k-1),k] = \underline{L}^T \begin{pmatrix} m_{11} & m_{12} & m_{13} \\ m_{12} & m_{22} & m_{23} \\ m_{13} & m_{23} & m_{33} \end{pmatrix} \underline{L} \tag{2}$$

$$m_{11} = \frac{\sqrt{2P_t}}{(r/T)} z(k)[\hat{x}_3(k|k-1)\sin\hat{\Omega}(k|k-1)+\hat{x}_4(k|k-1)\cos\hat{\Omega}(k|k-1)]$$

$$+\frac{2P_t}{(r/T)}\Big[[\hat{x}_3^2(k|k-1)-\hat{x}_4^2(k|k-1)]\cos 2\hat{\Omega}(k|k-1)$$

$$-2\hat{x}_3(k|k-1)\hat{x}_4(k|k-1)\sin 2\hat{\Omega}(k|k-1)\Big] \tag{2a}$$

$$m_{22} = \frac{2P_t}{(r/T)}\sin^2\hat{\Omega}(k|k-1) \tag{2b}$$

$$m_{33} = \frac{2P_t}{(r/T)}\cos^2\hat{\Omega}(k|k-1) \tag{2c}$$

$$m_{12} = -\frac{\sqrt{2P_t}}{(r/T)} z(k)\cos\hat{\Omega}(k|k-1)$$

$$+\frac{2P_t}{(r/T)}[\hat{x}_3(k|k-1)\sin 2\hat{\Omega}(k|k-1)+\hat{x}_4(k|k-1)\cos 2\hat{\Omega}(k|k-1)] \tag{2d}$$

$$m_{13} = \frac{\sqrt{2P_t}}{(r/T)} z(k)\sin\hat{\Omega}(k|k-1)$$

$$+\frac{2P_t}{(r/T)}[\hat{x}_3(k|k-1)\cos 2\hat{\Omega}(k|k-1)-\hat{x}_4(k|k-1)\sin 2\hat{\Omega}(k|k-1)] \tag{2e}$$

$$m_{23} = \frac{2P_t}{(r/T)}\sin\hat{\Omega}(k|k-1)\cos\hat{\Omega}(k|k-1) \tag{2f}$$

$$\hat{\Omega}(k|k-1) \triangleq \omega_c t_k + \hat{x}_1(k|k-1) \tag{3}$$

$$\underline{L} = \begin{pmatrix} 1 & 0 & 0 & 0 \\ 0 & 0 & 1 & 0 \\ 0 & 0 & 0 & 1 \end{pmatrix} \tag{4}$$

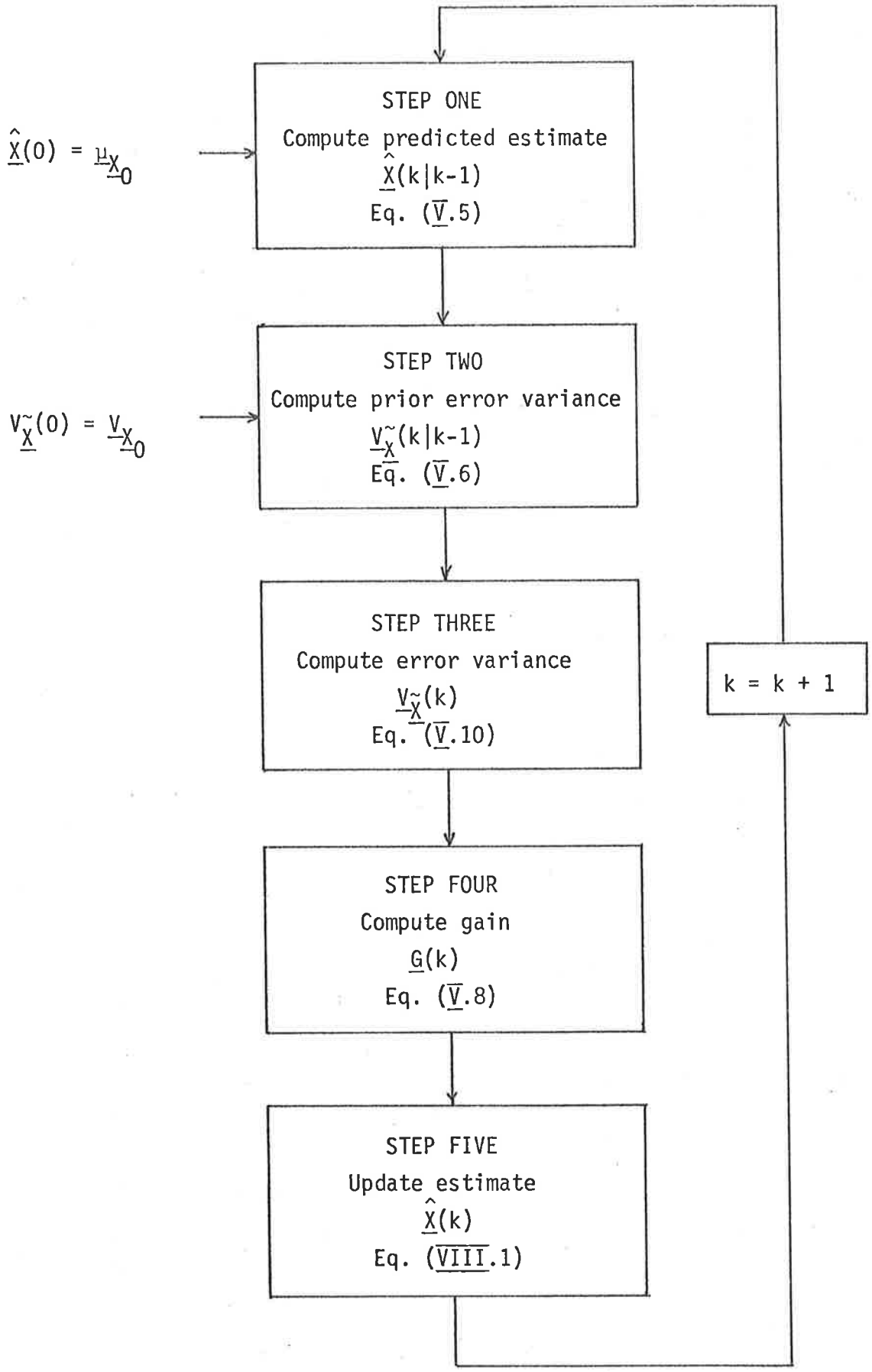

Figure 5.12. Flow chart for MAP algorithm (Table VIII; see also Table V)

5.3.2. Receiver Performance

Attempts to derive the baseband form for the MAP algorithm as was done for the EKF was not successful due to the complexity of the matrix $\underline{M}[\hat{\underline{X}}(k|k-1),k]$. To overcome this problem, two solutions are proposed:

(i) Employ quadrature sampling techniques to derive a set of algorithms that lend themselves to direct simulation as will be done in Chapter 6.

(ii) To make further assumptions allowing some simplifications of the MAP error variance algorithm and require

  (a) high SNR to uncouple the observation z(k) from the equations for m_{ij}'s, and

  (b) very slow fading and use the quasi-stationary form of the error variance matrix as given in Equation 5.7.

The actual amount of computation required is found to be comparable to the time required for the baseband EKF receivers.

The performance is shown in Figure 5.10(a) through 5.11(b) (Curve C) and is seen to be better than the EKF baseband and quasi-receivers at high SNR but is worse than the baseband EKF receivers at low SNR. Also noted is the seemingly better performance of the quasi-MAP receivers when compared with the quasi-EKF receivers at low SNR but this is not meaningful as these receivers are designed to operate at high SNR only.

5.4 Summary

The results shown in this chapter have demonstrated the feasibility of applying modern estimation to derive receiver structures which are "quasi-optimum" and dependent on the validity of various assumptions regarding the signal-to-noise ratio (relative to the additive

noise) and the rate of fading. For very slowly fluctuating channels, it has been shown that a quasi-stationary approach has allowed the receivers to be simplified and recognised as an adaptive version of the digital phase-locked loops. When the fading is relatively slow (say $\gamma = .01$) the performance of the receiver is still far below that achieved in a nonfading situation and other techniques will be employed in the later chapters to improve the performance.

The theoretical performance of these receivers cannot be calculated analytically except in the case of very slow fading and Van Trees (1971) gave an approximate performance bound for the inverse message error variance of the unrealisable continuous MAP demodulator that he derived. This is used to compare with the results obtained in Figure 5.11(b) ($\beta = 25$, $\gamma = .001$) and is shown in Figure 5.13. Note that the signal-to-noise ratio is defined as the "effective" SNR in the message bandwidth as given in Equation 4.17.

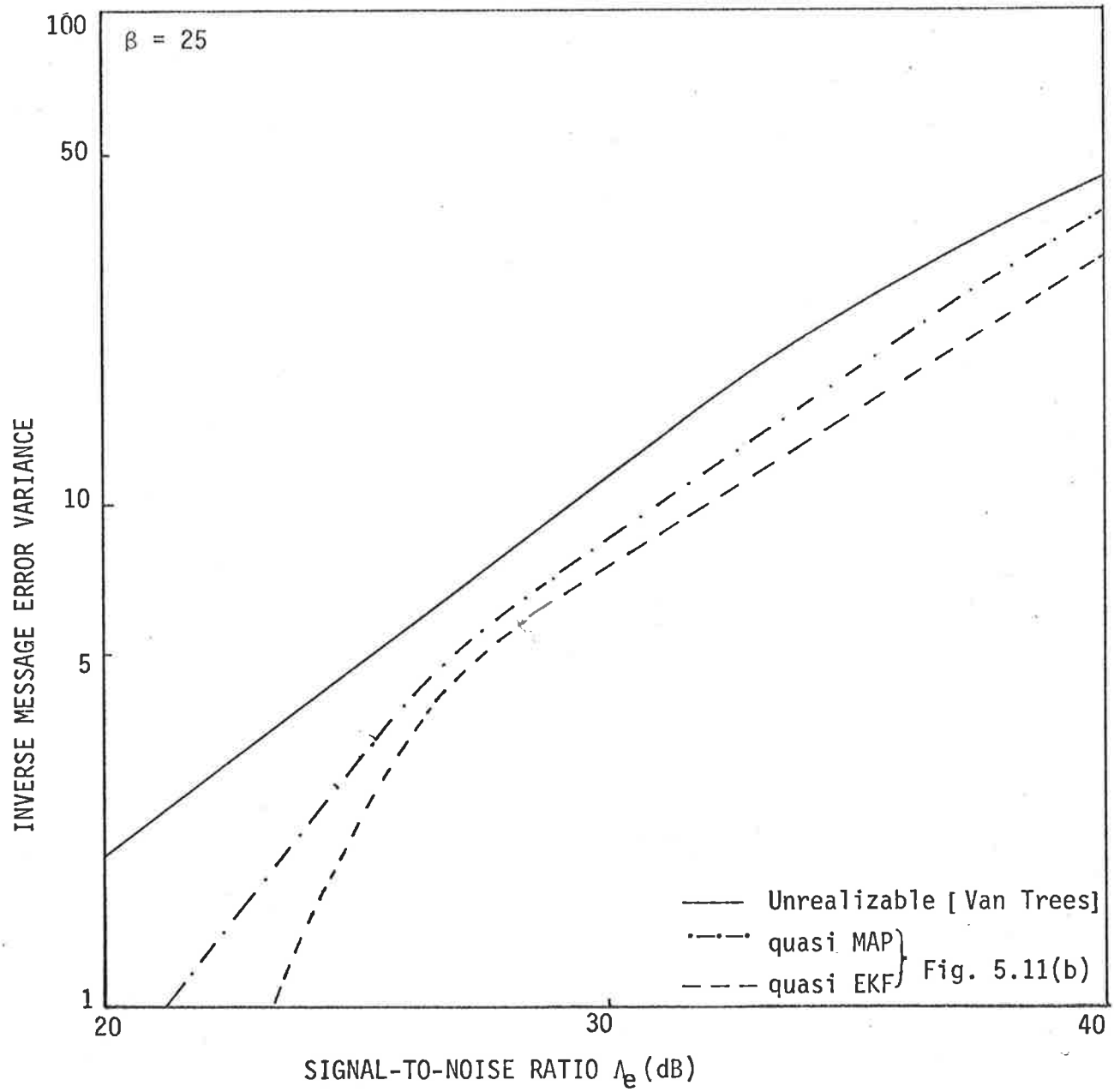

Fig. 5.13: Performance of very slow fading channels: quasi-stationary analysis

6. RECEIVERS USING QUADRATURE SAMPLING

It was mentioned in Section 2.3 that the use of quadrature sampling techniques has resulted in better performance for FM demodulators with no fading. This chapter will investigate the performance of receivers using quadrature sampling for Rayleigh fading channels. In Section 6.1, the receiver structures using the EKF algorithm will be derived and their performances are studied using computer simulation. Section 6.2 will apply the MAP algorithm to obtain quadrature receivers whose performance are found to be better than those using the EKF algorithms and are chosen for studying the effect of varying the bandwidth expansion ratio and the fading rate. Section 6.3 will consider the effects of varying the sampling rate for the quadrature receivers as well as for those obtained in the previous chapter. The performance of receivers in a Rayleigh fading environment is compared with the non-fading case in the last section and the need for more complex receivers is also discussed.

6.1 Discrete EKF receivers using quadrature sampling

As was done in Section 5.1, the general discrete EKF algorithm (Table II) is applied to the example in Table IV using quadrature sampling to obtain the set of algorithms summarised in Table IX, and the corresponding flowchart is shown in Figure 6.1.

In deriving the filtering algorithm (Equation IX.7) and the error variance algorithm (Equation IX.10), the following shorthand notations have been defined

TABLE IX.

DISCRETE EKF FILTERING ALGORITHM FOR FM COMMUNICATION SYSTEM WITH RAYLEIGH FADING (SINGLE CHANNEL, QUADRATURE SAMPLING)

System model: $\underline{X}(k) = \Phi(k,k-1)\underline{X}(k-1)+\underline{W}(k)$

$$\begin{pmatrix} x_1(k) \\ x_2(k) \\ x_3(k) \\ x_4(k) \end{pmatrix} = \begin{pmatrix} 1 & \beta(1-e^{-\alpha T}) & 0 & 0 \\ 0 & e^{-\alpha T} & 0 & 0 \\ 0 & 0 & e^{-\gamma T} & 0 \\ 0 & 0 & 0 & e^{-\gamma T} \end{pmatrix} \begin{pmatrix} x_1(k-1) \\ x_2(k-1) \\ x_3(k-1) \\ x_4(k-1) \end{pmatrix} + \begin{pmatrix} w_1(k) \\ w_2(k) \\ w_3(k) \\ w_4(k) \end{pmatrix} \quad (1)$$

Observation model (quadrature sampling): $\underline{Z}(k) = \underline{h}[\underline{X}(k)]+\underline{V}(k)$

$$\begin{pmatrix} z_1(k) \\ z_2(k) \end{pmatrix} = \sqrt{2P_t} \begin{pmatrix} x_3(k) & x_4(k) \\ -x_4(k) & x_3(k) \end{pmatrix} \begin{pmatrix} \sin x_1(k) \\ \cos x_1(k) \end{pmatrix} + \begin{pmatrix} v_1(k) \\ v_2(k) \end{pmatrix} \quad (2)$$

Statistical parameters

$$E[\underline{W}(k)\underline{W}^T(j)] = \underline{Q}(k)\delta_{kj} \quad (3)$$

$$E[\underline{V}(k)\underline{V}^T(j)] = \underline{R}(k)\delta_{kj} \quad (4)$$

See Table IV.

One stage prediction algorithm

$$\hat{\underline{X}}(k|k-1) = \underline{\Phi}(k,k-1)\hat{\underline{X}}(k-1) \quad (5)$$

$$\hat{\underline{X}}(0) = \underline{\mu}_{\underline{X}_0} \quad (5a)$$

Prior error variance algorithm

$$\underline{V}_{\tilde{\underline{X}}}(k|k-1) = \Phi(k,k-1)\underline{V}_{\tilde{\underline{X}}}(k-1)\Phi^T(k,k-1)+\underline{Q}(k) \quad (6)$$

$$\underline{V}_{\tilde{\underline{X}}}(0) = \underline{V}_{\underline{X}_0} \quad (6a)$$

Filtering algorithm

$$\hat{\underline{X}}(k) = \hat{\underline{X}}(k|k-1)+\underline{V}_{\tilde{\underline{X}}}(k)\underline{L}^T\underline{D}(k) \quad (7)$$

Error variance algorithm

$$\underline{V}_{\tilde{\underline{X}}}(k) = \underline{V}_{\tilde{\underline{X}}}(k|k-1) - \underline{V}_{\tilde{\underline{X}}}(k|k-1)\underline{L}^T\{\underline{H}^T(k)\underline{M}^{-1}(k)\underline{H}(k)\}\underline{L}\underline{V}_{\tilde{\underline{X}}}(k|k-1) \tag{10}$$

Definitions

$$\underline{L} \triangleq \begin{pmatrix} 1 & 0 & 0 & 0 \\ 0 & 0 & 1 & 0 \\ 0 & 0 & 0 & 1 \end{pmatrix} \tag{11}$$

$$\underline{D}(k) \triangleq \frac{\sqrt{2P_t}}{(r/T)} \begin{pmatrix} \hat{x}_3(k|k-1)Z_{C2}(k) - \hat{x}_4(k|k-1)Z_{C1}(k) \\ Z_{C1}(k) - \sqrt{2P_t}\hat{x}_3(k|k-1) \\ Z_{C2}(k) - \sqrt{2P_t}\hat{x}_4(k|k-1) \end{pmatrix} \tag{12}$$

$$\underline{H}(k) = \sqrt{2P_t} \begin{pmatrix} -\hat{x}_4(k|k-1) & 1 & 0 \\ -x_3(k|k-1) & 0 & -1 \end{pmatrix} \sin \hat{x}_1(k|k-1)$$

$$+ \sqrt{2P_t} \begin{pmatrix} \hat{x}_3(k|k-1) & 0 & 1 \\ -\hat{x}_4(k|k-1) & 1 & 0 \end{pmatrix} \cos \hat{x}_1(k|k-1) \tag{13}$$

$$\underline{M}(k) = \underline{H}(k)\{\underline{L}\underline{V}_{\tilde{\underline{X}}}\underline{L}^T\}\underline{H}^T(k) + \underline{R}(k) \tag{14}$$

$$\begin{pmatrix} Z_{C1}(k) \\ Z_{C2}(k) \end{pmatrix} \triangleq \begin{pmatrix} z_1(k) & z_2(k) \\ -z_2(k) & z_1(k) \end{pmatrix} \begin{pmatrix} \sin \hat{x}_1(k|k-1) \\ \cos \hat{x}_1(k|k-1) \end{pmatrix} \tag{15}$$

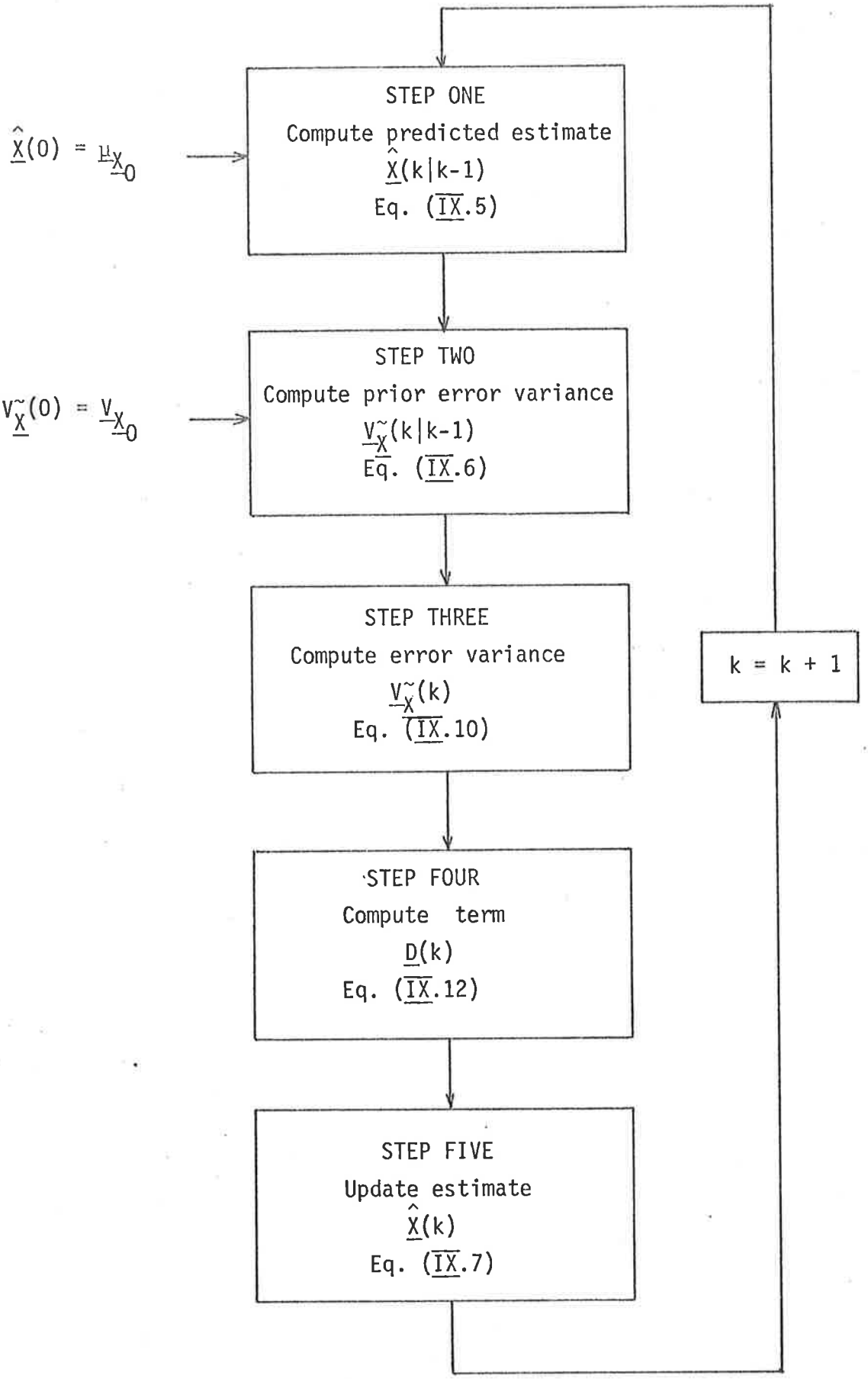

Figure 6.1 Flow chart for EKF algorithm using quadrature sampling (Table IX.)

$$\underline{L} \triangleq \begin{pmatrix} 1 & 0 & 0 & 0 \\ 0 & 0 & 1 & 0 \\ 0 & 0 & 0 & 1 \end{pmatrix} \qquad \text{(Eq. IX.11)}$$

$$\frac{\partial \underline{h}[\underline{X}(k|k-1)]}{\partial \hat{\underline{X}}(k|k-1)} \triangleq \underline{H}(k)\underline{L} \qquad (6.1)$$

$$\underline{D}(k) \triangleq \underline{H}^T(k)\underline{R}^{-1}(k)\underline{\nu}(k) \qquad (6.2)$$

$$\begin{pmatrix} Z_{C1}(k) \\ Z_{C2}(k) \end{pmatrix} \triangleq \begin{pmatrix} z_1(k) & z_2(k) \\ -z_2(k) & z_1(k) \end{pmatrix} \begin{pmatrix} \sin \hat{x}_1(k|k-1) \\ \cos \hat{x}_1(k|k-1) \end{pmatrix} \qquad \text{(Eq. IX.15)}$$

Figure 6.2 is a block diagram of the receiver as depicted by the algorithms in Table IX.

Using the parameter set chosen in Chapter 4, the receiver performance is shown in Figures 6.3(a) and 6.3(b) for $\beta = 25$ and $\gamma = .01$. When compared with the results for scalar sampling, the improvement is in the order of 1dB at high signal-to-noise ratio. The below threshold behaviour does not seem to be conclusive from the results obtained although the threshold is marginally lower for the quadrature receivers. For no fading case, Tam and Moore (1975) obtained results that indicated overall better performance by the use of quadrature sampling.

The total computational effort using quadrature sampling is comparable to the scalar sampling due to the lower sampling frequency required.

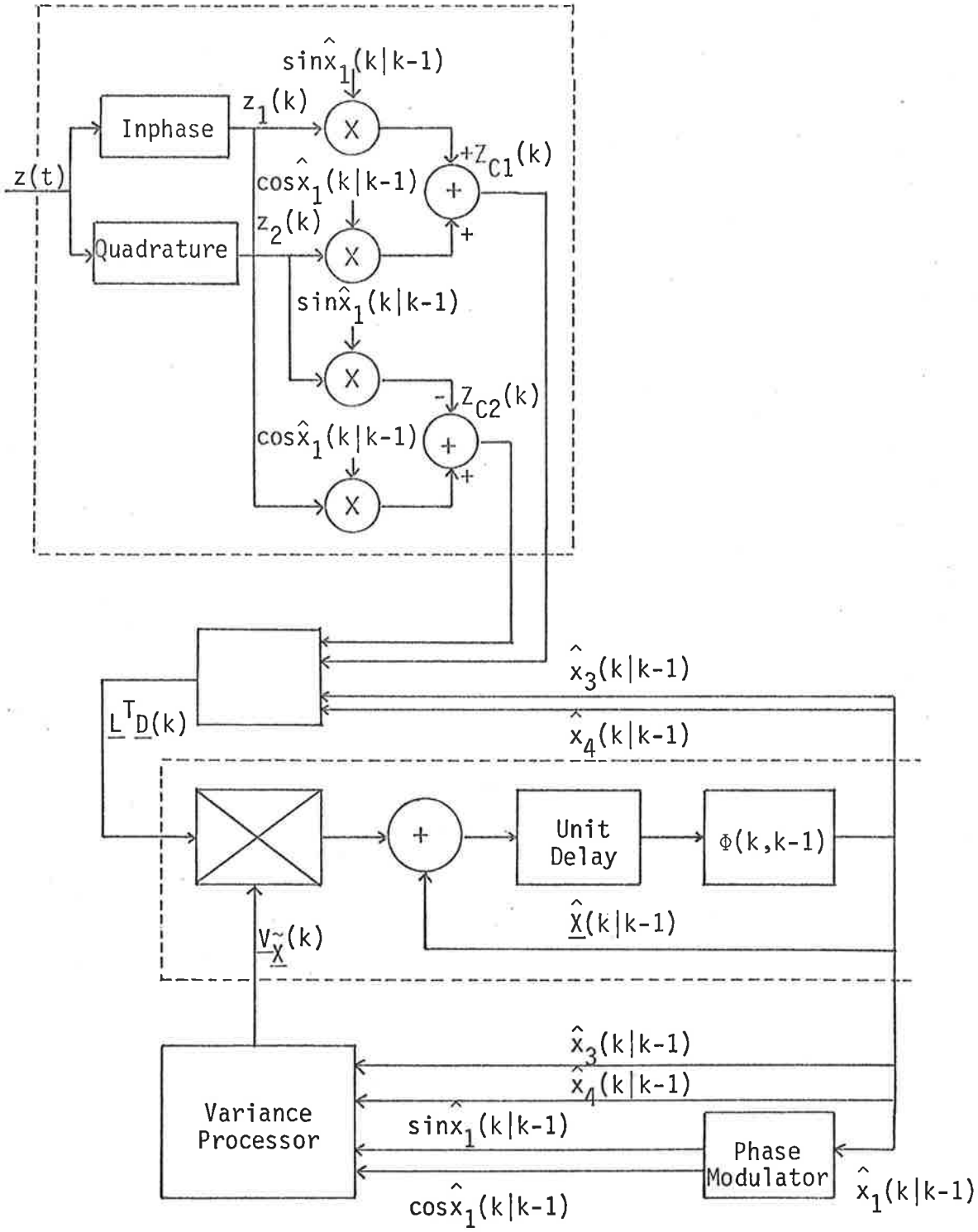

Figure 6.2: EKF Receiver Using Quadrature Sampling.

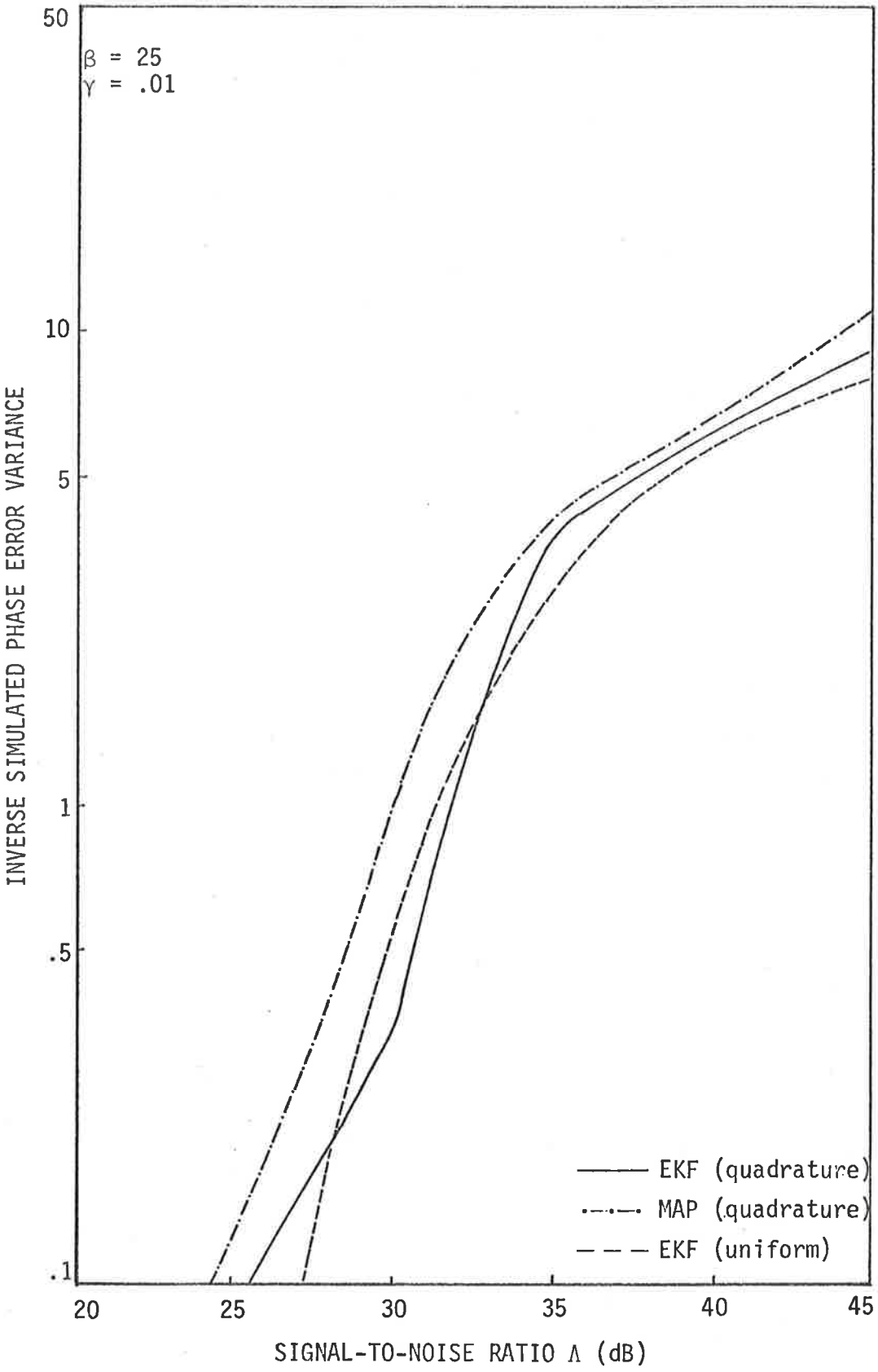

Fig. 6.3(a): Receiver performance (phase) using quadrature sampling.

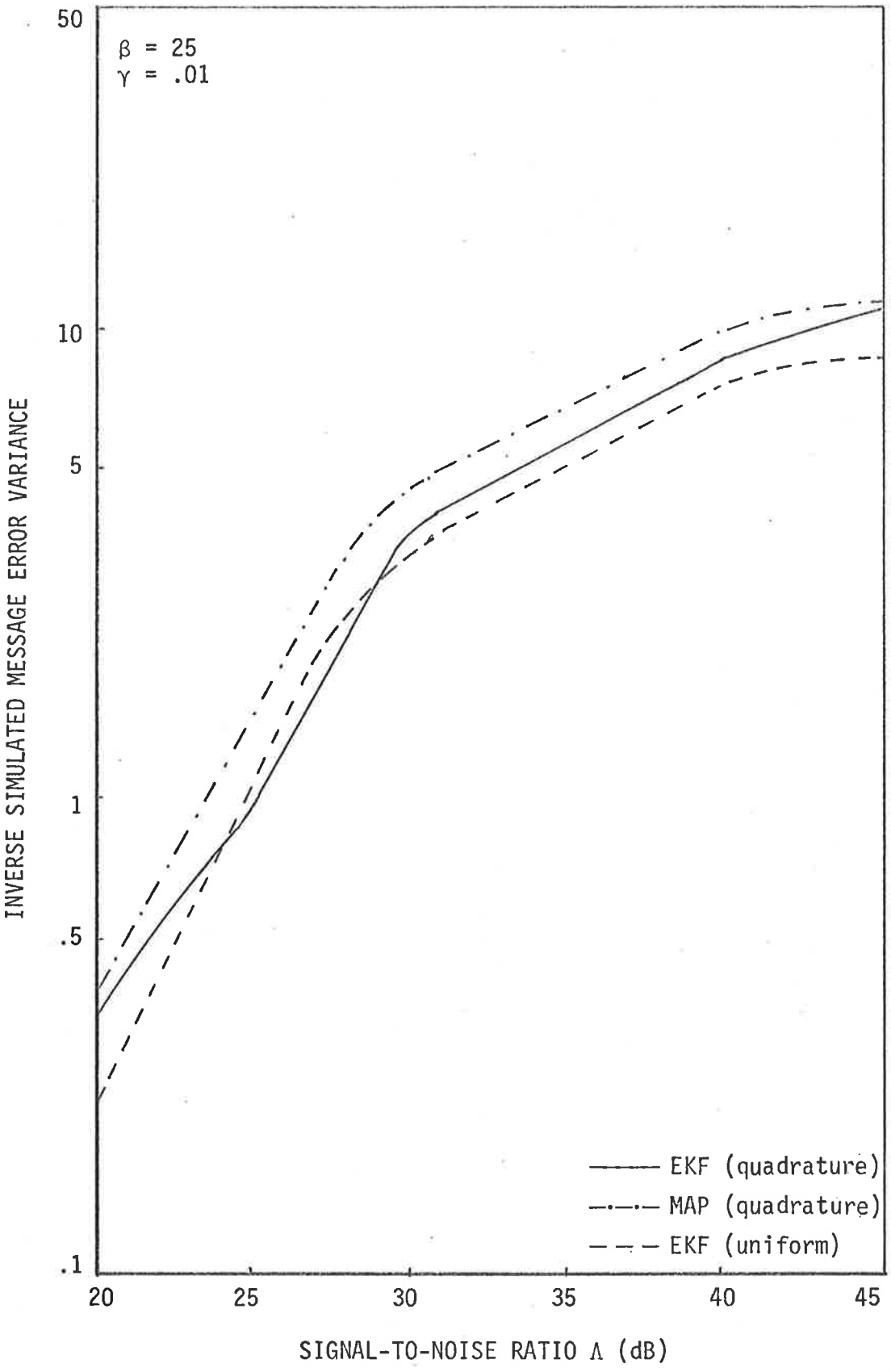

Fig. 6.3(b): Receiver performance (message) using quadrature sampling.

6.2 Discrete MAP Receivers Using Quadrature Sampling

Using quadrature sampling, the MAP algorithm for the FM communication model in Section 4.1 is obtained and is different from the EKF algorithm of Table IX in the error variance algorithm. Equations (1) and (10) in Table X show two alternative forms of the error variance algorithms that can be used. The first equation

$$\underline{V}_{\underline{X}}^{\sim}(k) = \left(\underline{I}+\underline{V}_{\underline{X}}^{\sim}(k|k-1)\underline{M}[\hat{\underline{X}}(k|k-1),k]\right)^{-1} \underline{V}_{\underline{X}}^{\sim}(k|k-1) \tag{6.3}$$

was used in Chapter 5 but found to be unstable when used in this immediate study.

The alternative form

$$\underline{V}_{\underline{X}}^{\sim}(k) = \underline{V}_{\underline{X}}^{\sim}(k|k-1)-\underline{V}_{\underline{X}}^{\sim}(k|k-1)\underline{M}[\hat{\underline{X}}(k|k-1),k]$$

$$\cdot\left(I+\underline{V}_{\underline{X}}^{\sim}(k|k-1)\underline{M}[\hat{\underline{X}}(k|k-1),k]\right)^{-1} \underline{V}_{\underline{X}}^{\sim}(k|k-1) \tag{6.4}$$

is used instead and was found to be more stable. This can be understood by considering, for simplicity, the evaluation of

$$(1+ab)^{-1}\ a = \left(\frac{1}{a}+b\right)^{-1} \tag{6.5a}$$

$$= a - ab\ (1+ab)^{-1}\ a \tag{6.5b}$$

Assuming a = 1 and b = .001

Then $\left(\frac{1}{a}+b\right)^{-1} = 0.9901.$

Assuming however a .05% numerical error involved in evaluating the inverse $\left(\frac{1}{a}+b\right)^{-1}$, the calculated results could then be (say)

$$.999 + .0005 = .9995$$

TABLE X

DISCRETE MAP FILTERING ALGORITHMS FOR FM COMMUNICATION SYSTEM WITH RAYLEIGH FADING (SINGLE CHANNEL, QUADRATURE SAMPLING)

Error variance algorithm

$$\underline{V}_{\tilde{\underline{X}}}(k) = \left[\underline{I}+\underline{V}_{\tilde{\underline{X}}}(k|k-1)\underline{M}[\hat{\underline{X}}(k|k-1),k]\right]^{-1}\underline{V}_{\tilde{\underline{X}}}(k|k-1) \qquad (1)$$

or alternatively,

$$\underline{V}_{\tilde{\underline{X}}}(k) = \underline{V}_{\tilde{\underline{X}}}(k|k-1)-\underline{V}_{\tilde{\underline{X}}}(k|k-1)\underline{M}[\hat{\underline{X}}(k|k-1),k]$$

$$\cdot\left[\underline{I}+\underline{V}_{\tilde{\underline{X}}}(k|k-1)\underline{M}[\hat{\underline{X}}(k|k-1),k]\right]^{-1}\underline{V}_{\tilde{\underline{X}}}(k|k-1) \qquad (1a)$$

where

$$\underline{M}[\hat{\underline{X}}(k|k-1),k] \triangleq \frac{\sqrt{2P_t}}{(r/T)}\,\underline{L}^T \begin{bmatrix} \hat{x}_3(k|k-1)Z_{C1}(k) & -Z_{C2}(k) & Z_{C1}(k) \\ +\hat{x}_4(k|k-1)Z_{C2}(k) & & \\ -Z_{C2}(k) & \sqrt{2P_t} & 0 \\ Z_{C1}(k) & 0 & \sqrt{2P_t} \end{bmatrix} \underline{L} \qquad (2)$$

Definitions

See Table IX for definitions of $\underline{L}$, $Z_{C1}(k)$ and $Z_{C2}(k)$.

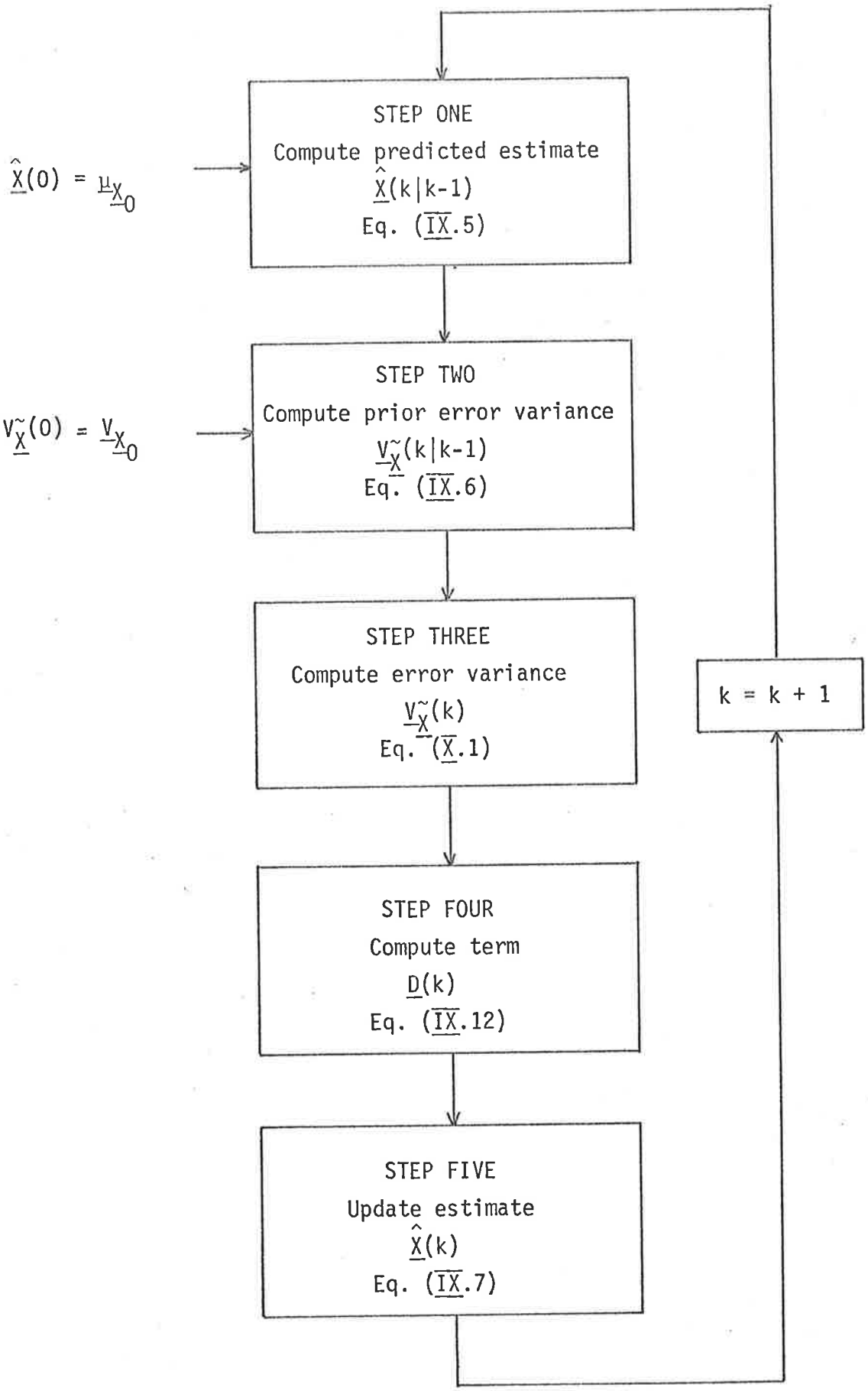

Figure 6.4 Flow chart for MAP algorithm using quadrature sampling (Table X. See also Table IX).

If the alternative form (Equation 6.5(b)) is used instead, then the calculated result is

$$1 - 0.001(.9995) = .999$$

which is closer to the actual result. Figure 6.4 shows the flowchart of the MAP algorithm and Figure 6.5 is a block diagram of the receiver. The MAP quadrature receiver is seen to be different from the EKF quadrature receiver in the additional coupling terms driving the error variance processor.

The performance of the MAP receiver for $\beta = 25$ and $\gamma = .01$ is shown in Figure 6.3(a) and 6.3(b) presented previously. The overall performance is in the order of 1-2 dB when compared with the EKF receivers. The extra complexity involved in the solution of the error variance algorithm is to be taken into account. As the main purpose of this investigation is to determine how much the performance of receivers for fading channels can be improved, the MAP algorithm will be preferred to the EKF algorithm for further investigations.

When varying the bandwidth expansion ratio β (with $\gamma = .01$) the performance of the MAP quadrature receivers is shown in Figures 6.6(a) and 6.6(b). Also shown on the same graph are the results for no fading obtained by Polk (1973) and McBride (1973). The expected improvement is even more pronounced when compared with similar results obtained in Chapter 5.

Effects of the fading rate are also studied and are shown in Figure 6.7(a) and 6.7(b) for $\beta = 25$. These results confirm the conclusions already discussed in Chapter 5, namely the very poor performance for "fast" fading ($\gamma = .1$) and the very much better performance for very slow fading ($\gamma = .001$).

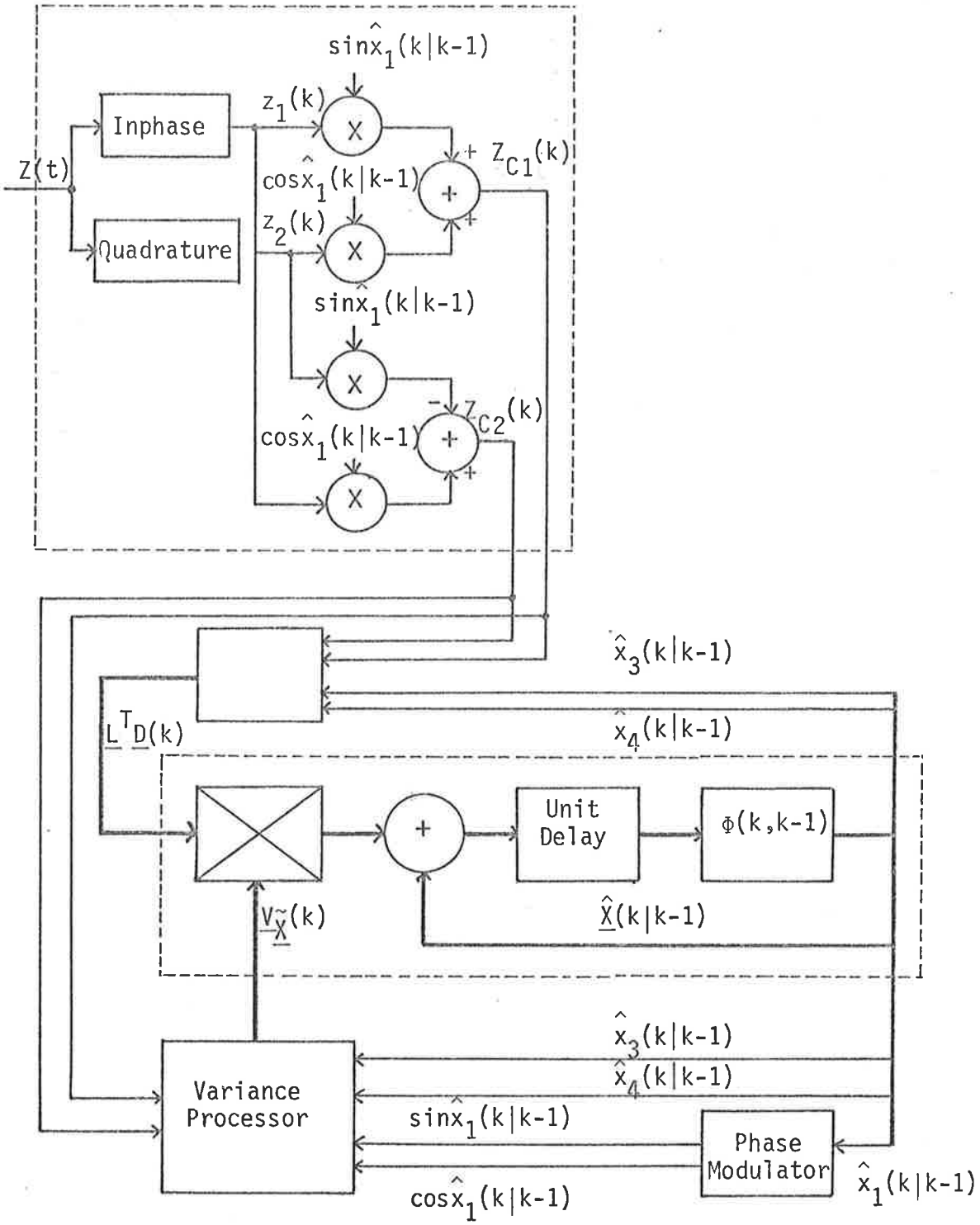

Figure 6.5: MAP Receiver Using Quadrature Sampling.

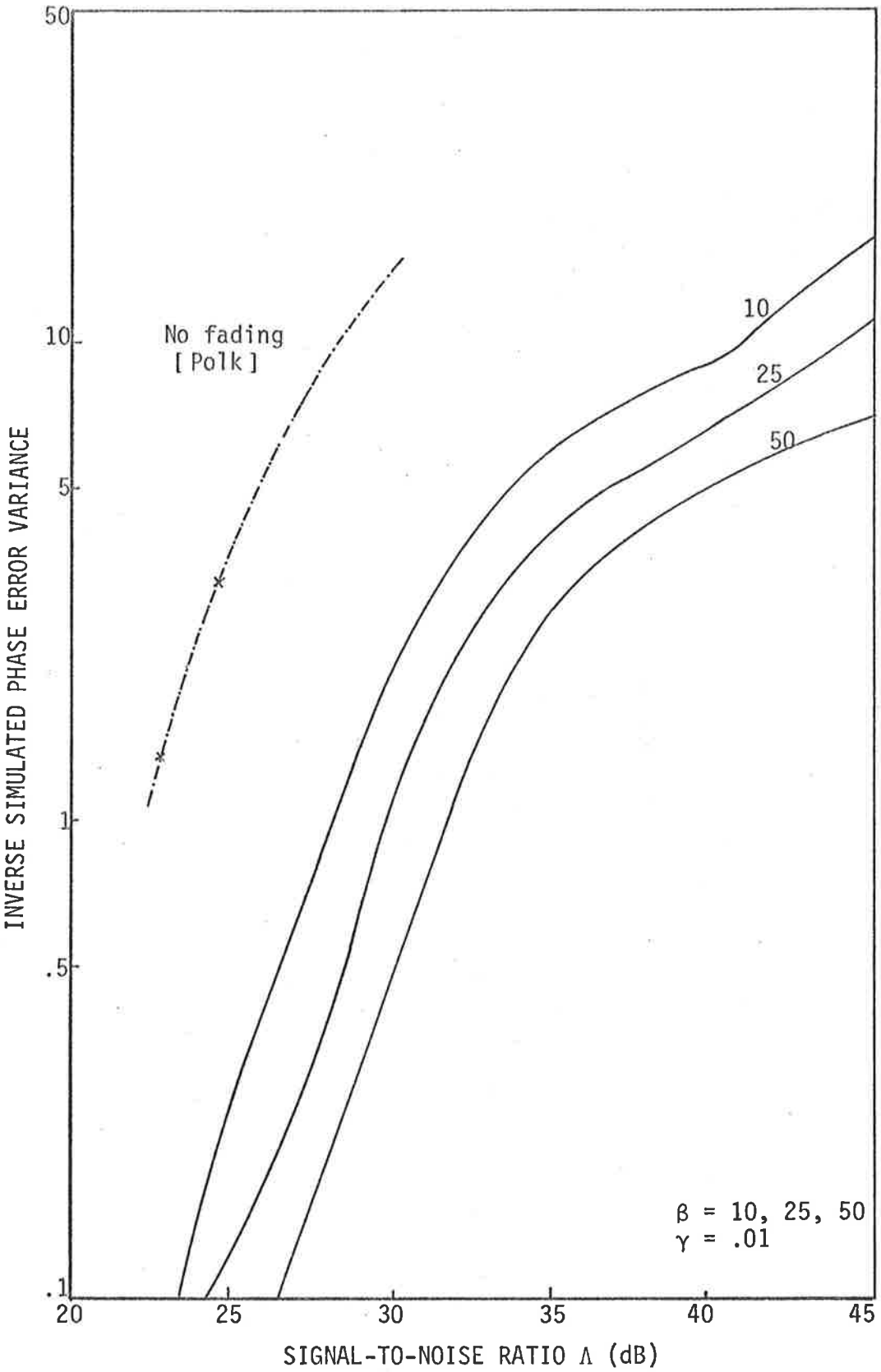

Fig. 6.6(a): Simulated inverse phase error variance (MAP, Quadrature, β varying)

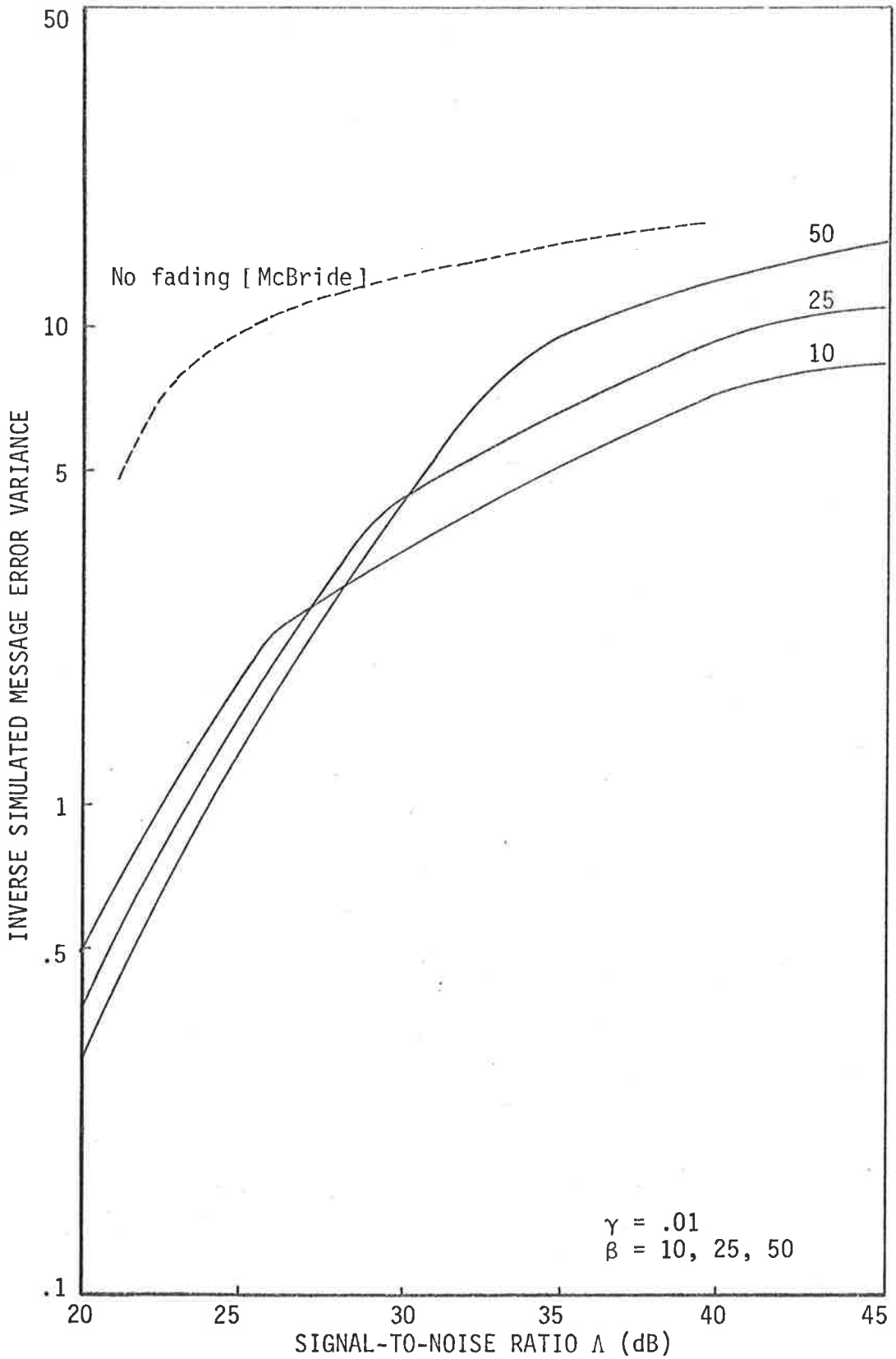

Fig. 6.6(b): Simulated inverse message error variance (MAP, quadrature, β varying)

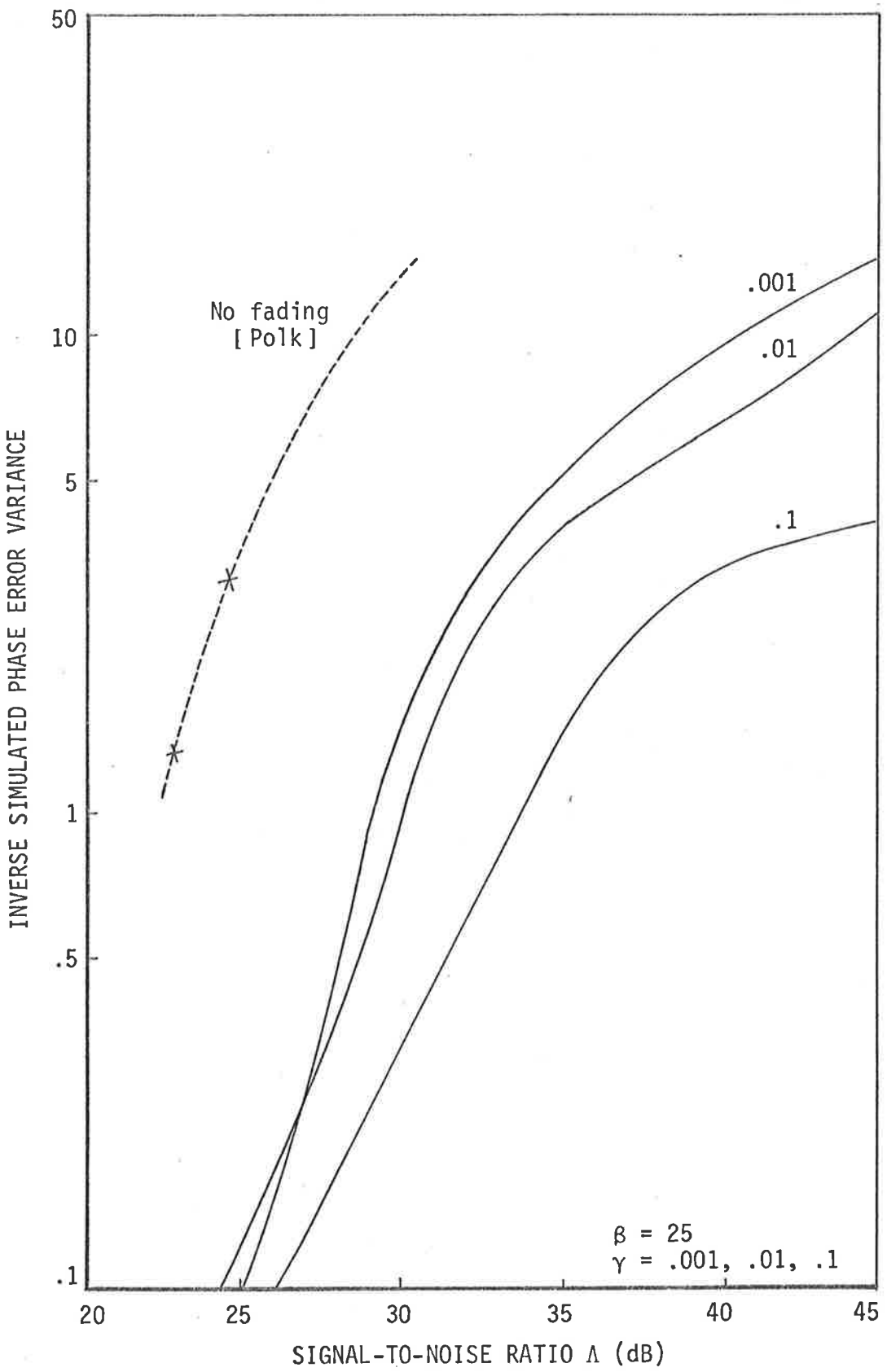

Fig. 6.7(a): Simulated inverse phase error variance (MAP, quadrature, γ varying)

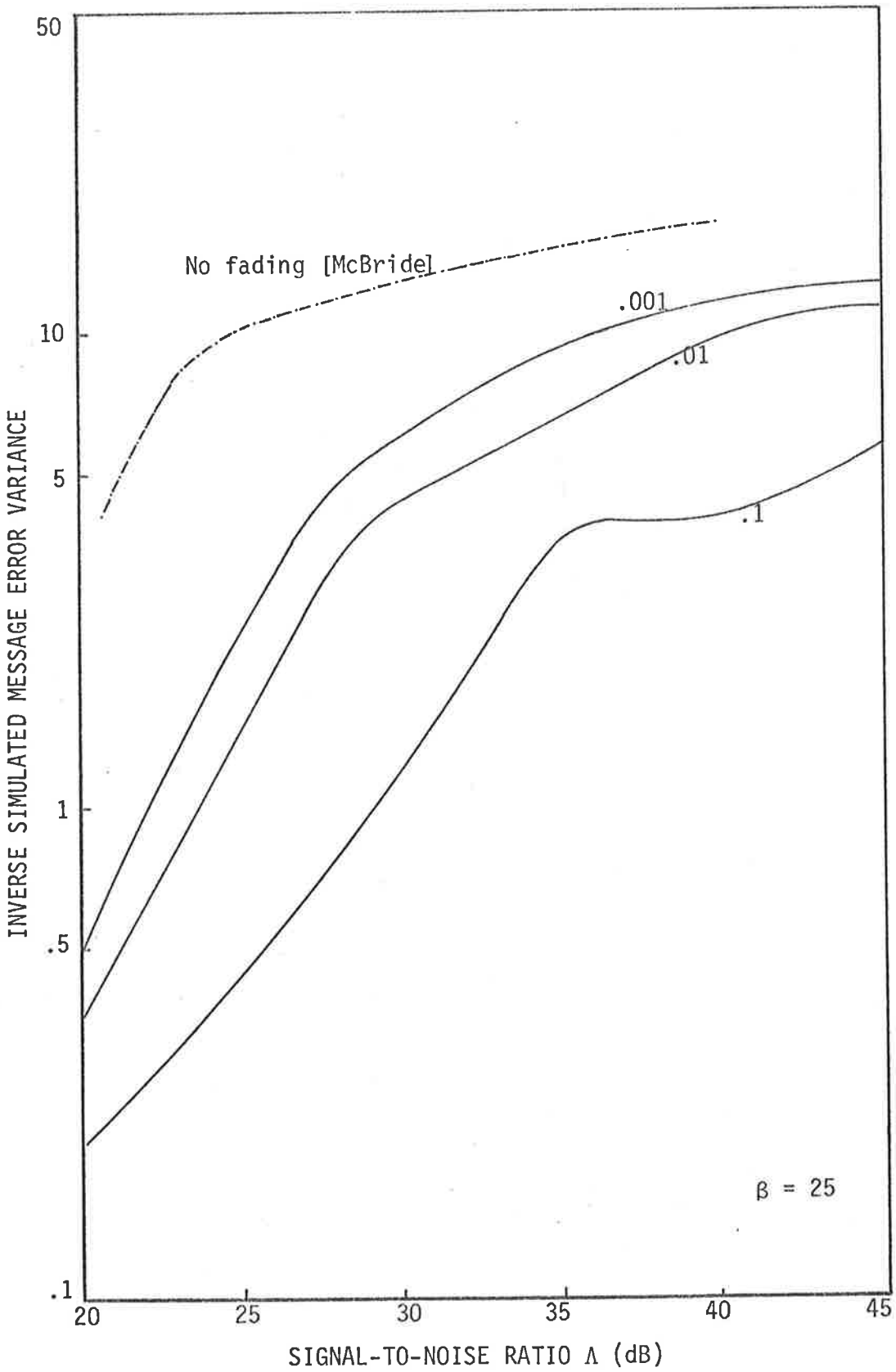

Fig. 6.7(b): Simulated inverse message error variance (MAP, quadrature, γ varying)

6.3 Effects of Sampling Rate

By varying the sampling rates and adjust the sample sizes accordingly to maintain the same confidence in the simulation results, the effects of varying sampling rate are shown in Figure 6.8 for all three types of receivers. The inverse simulated message error variances (for Λ = 30dB) are plotted against the sampling frequency normalised with respect to the sampling frequency chosen in Chapter 4. The effect of under-sampling is very distinct and results in rapid increase in the message error variance. Over-sampling, however, does not improve the performance.

6.4 Comparison of Results

Figure 6.9 summarises the results for Rayleigh fading channels when compared with those obtained for no fading (for β = 25, γ = .01). The difference is in the order of 5-7dBs in terms of output signal-to-noise ratio. This is accounted for by the deep fade problem made more severe by the assumption of slow fading. If the Rayleigh fading envelope goes down below a certain threshold level, it is likely to remain below threshold for a longer period. Two solutions are proposed to attempt to improve the overall performance of the receivers:

(i) Fixed-lag Smoothing (Chapter 7); and

(ii) Diversity Systems (Chapter 8).

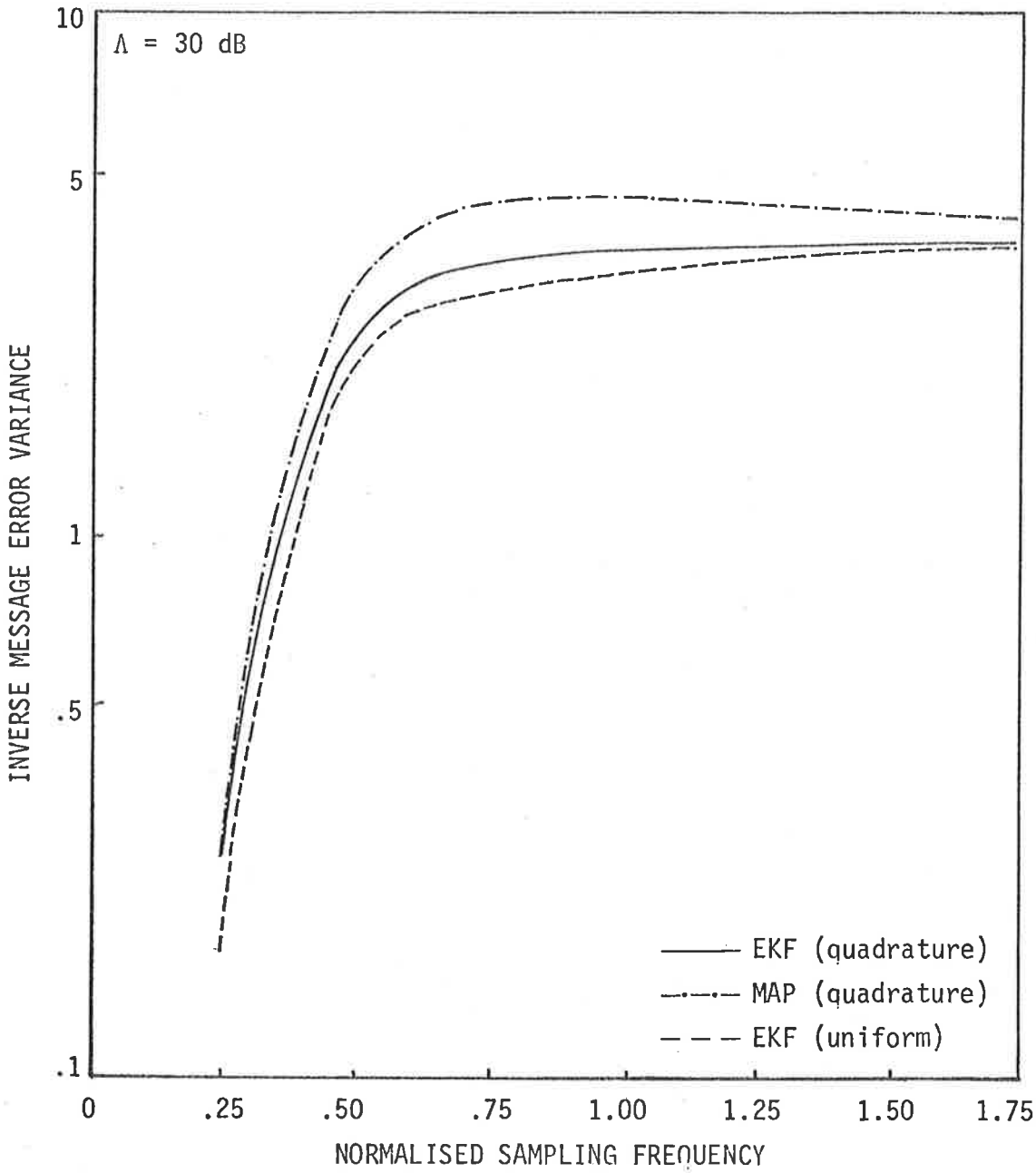

Fig. 6.8: Effects of sampling rate

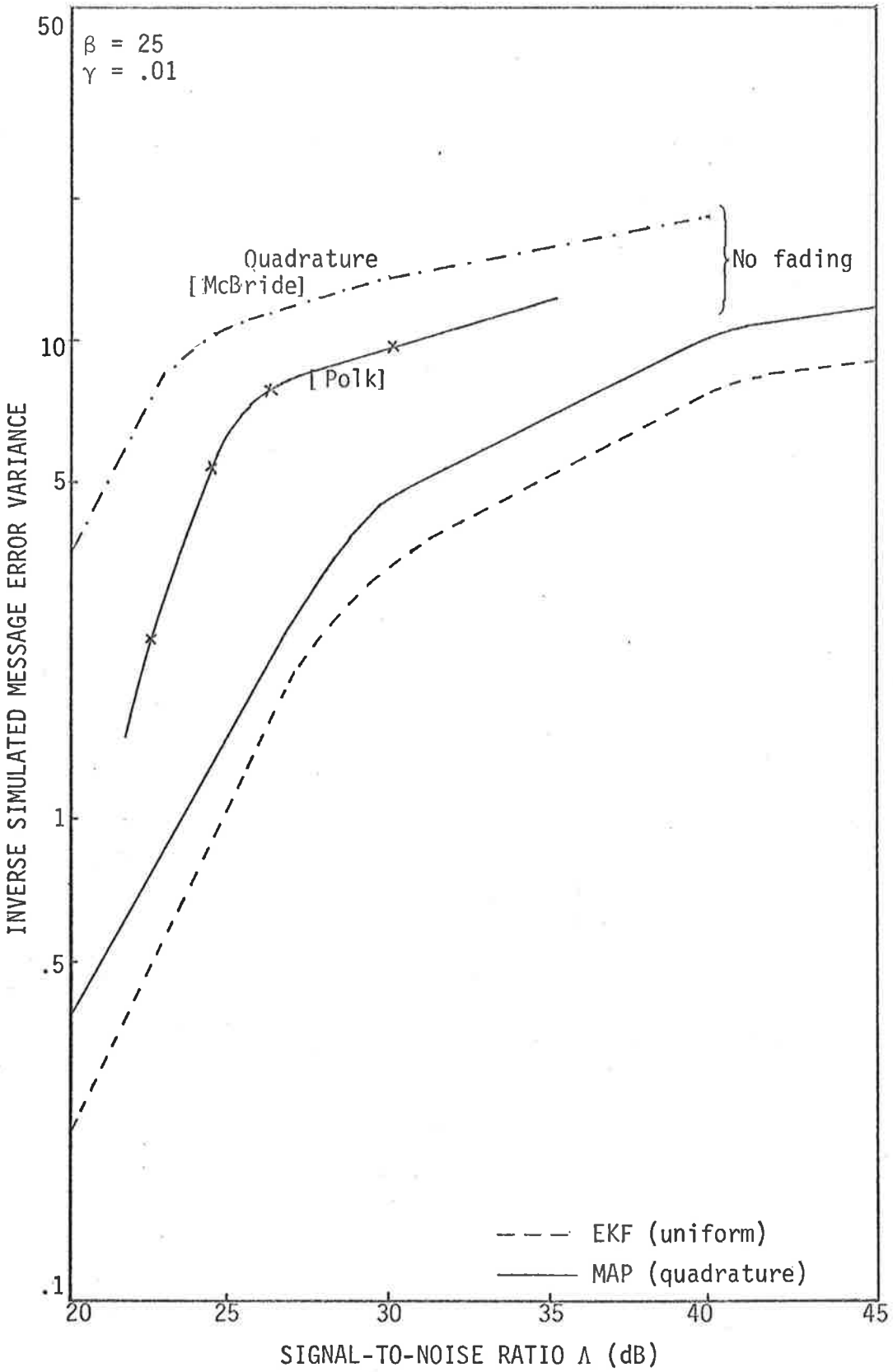

Fig. 6.9: Comparison with results for no fading

7. RECEIVERS USING FIXED-LAG SMOOTHING

It is well known that by allowing a fixed amount of lags in the receivers, significant improvement is achieved. For the non-fading case, Tam and Moore (1973) employ uniform sampling and present good results for high SNR. They further extended it (Tam and Moore, 1975) to employ quadrature sampling and found that the improvement in high noise situations (low SNR) is not as good as could be expected from the results for the linear cases (Moore and Hetrakul, 1973; Prasad and Mahalanabis, 1975). For the fading case, Prasad and Mahalanabis, (1974) obtained some simulation results for the PM case which also show some improvements at high SNR. This chapter will consider the use of fixed-lag smoothing for the FM communication model used in this investigation. The fixed-lag smoothing algorithm is formulated in Section 7.1 and the performance of the fixed-lag receivers will be discussed in Section 7.2.

7.1 Fixed-lag smoothing algorithms

Data smoothing is a more difficult subject to deal with due to the instability problem associated with the delay implicit in any smoothing scheme. Meditch (1973, see also Kailath, 1975) gives a very good survey of the subject. The algorithms used in this chapter are drawn, however, from two complementary papers, one by Moore (1973) for linear system and the other by Moore and Tam (1973) for non-linear systems. The development of these algorithms are outlined below.

Consider the discrete system and observation models

$$\underline{X}(k) = \Phi(k,k-1)\underline{X}(k)+\underline{W}(k) \tag{7.1}$$

$$\underline{Z}(k) = \underline{h}[\underline{X}(k)]+\underline{V}(k) \tag{7.2}$$

By allowing a fixed amount of L lags with each lag corresponds to one sampling interval and define

$$\underline{X}_L(k) \triangleq \underline{X}(k-L) \tag{7.3}$$

as the state delayed by L lags.

The minimum variance filtered estimates $\hat{\underline{X}}(k|k)$ and the fixed-lag smoothed estimates $\hat{\underline{X}}(k-L|k)$ are defined as

$$\hat{\underline{X}}(k|k) = E[\underline{X}(k)|\underline{Z}^k] \tag{7.4}$$

$$\begin{aligned}\hat{\underline{X}}(k-L|k) &= E[\underline{X}(k-L)|\underline{Z}^k] \\ &= E[\underline{X}_L(k)|\underline{Z}^k] \\ &= \hat{\underline{X}}_L(k|k)\end{aligned} \tag{7.5}$$

In other words, the optimal fixed-lag smoothed estimate of the state $\hat{\underline{X}}(k-L|k)$ is simply the optimal filtered estimate of the state delayed by the fixed-lag $\hat{\underline{X}}_L(k|k)$. This means that by an appropriate augmentation of the system model to include the states $\underline{X}_L(k)$, filtering algorithms as those in Chapter 3 can be applied to the augmented model to achieve an optimal filter which has as its output $\hat{\underline{X}}_L(k)$.

The augmented state vector is defined as

$$\begin{pmatrix} \underline{X}_0(k) \\ \underline{X}_1(k) \\ \vdots \\ \underline{X}_i(k) \\ \vdots \\ \underline{X}_L(k) \end{pmatrix}$$

where

$$\underline{X}_i(k) \triangleq \underline{X}_0(k-i), \qquad i = 1, 2, \ldots, L \tag{7.6}$$

and L is the number of lags.

The system state equation for the augmented state vector is now given by

$$\begin{pmatrix} \underline{X}_0(k) \\ \underline{X}_1(k) \\ \vdots \\ \underline{X}_i(k) \\ \vdots \\ \underline{X}_L(k) \end{pmatrix} = \begin{pmatrix} \Phi(k,k-1) & \underline{\phi} & \cdots & \underline{\phi} & \underline{\phi} \\ & & & & \underline{\phi} \\ & & & & \vdots \\ & \underline{I} & & & \underline{\phi} \\ & & & & \vdots \\ & & & & \underline{\phi} \end{pmatrix} \begin{pmatrix} \underline{X}_0(k-1) \\ \underline{X}_1(k-1) \\ \vdots \\ \underline{X}_i(k-1) \\ \vdots \\ \underline{X}_L(k-1) \end{pmatrix} + \begin{pmatrix} \underline{W}(k) \\ \underline{\phi} \\ \vdots \\ \underline{\phi} \\ \vdots \\ \underline{\phi} \end{pmatrix} \tag{7.7}$$

and the observation model is now given by

$$\underline{Z}(k) = \underline{h}(\underline{X}_0(k)) + \underline{V}(k) \tag{7.8}$$

where $\underline{X}_0(k), \Phi(k,k-1), \underline{W}(k), \underline{Z}(k), \underline{h}(\underline{X}_0(k))$, and $\underline{V}(k)$ correspond to the filtering case (i.e. no lag, see Equations 7.1 and 7.2 above), and for the FM communication model in Section 4.1 with quadrature sampling they are given in Table IV.

Define the error covariance matrix as

$$\begin{pmatrix} \underline{V}_{00}(k) & \underline{V}_{01}(k) & \cdots & \underline{V}_{0i}(k) & \cdots & \underline{V}_{0L}(k) \\ \underline{V}_{10}(k) & \underline{V}_{11}(k) & \cdots & \underline{V}_{1i}(k) & \cdots & \underline{V}_{1L}(k) \\ \vdots & \vdots & \ddots & \vdots & \ddots & \vdots \\ \underline{V}_{i0}(k) & \underline{V}_{i1}(k) & \cdots & \underline{V}_{ii}(k) & \cdots & \underline{V}_{iL}(k) \\ \vdots & \vdots & \ddots & \vdots & \ddots & \vdots \\ \underline{V}_{L0}(k) & \underline{V}_{L1}(k) & \cdots & \underline{V}_{Li}(k) & \cdots & \underline{V}_{LL}(k) \end{pmatrix}$$

where

$$\underline{V}_{ij}(k) \triangleq E[\underline{X}_i(k)\underline{X}_j^T(k)] \tag{7.9}$$

is the error covariance matrix between the system vectors associated with various amount of lags and note that

$$\underline{V}_{ij}(k) = \underline{V}_{ji}^T(k) \tag{7.10}$$

the algorithms of Chapter 3 can be applied to obtain the MAP algorithms as shown in Table XI, from where it can be seen that

Equations (3a)
Equations (4a)
Equations (5a)
} correspond to the filtering case

TABLE XI.

DISCRETE MAP FIXED-LAG SMOOTHING ALGORITHMS FOR FM COMMUNICATION SYSTEMS WITH RAYLEIGH FADING

System model:

$$\begin{pmatrix} \underline{X}_0(k) \\ \underline{X}_1(k) \\ \vdots \\ \underline{X}_i(k) \\ \vdots \\ \underline{X}_L(k) \end{pmatrix} = \left(\begin{array}{c|ccc|c} \Phi(k,k-1) & \underline{\phi} & \cdots & \underline{\phi} & \underline{\phi} \\ \hline & & & & \underline{\phi} \\ & & & & \vdots \\ & & \underline{I} & & \underline{\phi} \\ & & & & \vdots \\ & & & & \underline{\phi} \end{array}\right) \begin{pmatrix} \underline{X}_0(k-1) \\ \underline{X}_1(k-1) \\ \vdots \\ \underline{X}_i(k-1) \\ \vdots \\ \underline{X}_L(k-1) \end{pmatrix} + \begin{pmatrix} \underline{W}(k) \\ \underline{\phi} \\ \vdots \\ \underline{\phi} \\ \vdots \\ \underline{\phi} \end{pmatrix} \qquad (1)$$

Observation model

$$\underline{Z}(k) = \underline{g}(\underline{X}(k)) + \underline{V}(k)$$
$$= \underline{h}(\underline{X}_0(k)) + \underline{V}(k) \qquad (2)$$

where

$\underline{X}_0(k), \Phi(k,k-1), \underline{W}(k), \underline{Z}(k), \underline{h}(\underline{X}_0(k))$, and $\underline{V}(k)$ correspond to the filtering case (see Table IV.)

L is the number of lags: $\underline{X}_i(k) \triangleq \underline{X}(k-i)$, $\quad i = 1, 2, \ldots, L$

$\underline{I}$ and $\underline{\phi}$ are the identity and null matrices respectively.

One-stage prediction algorithm

$$\hat{\underline{X}}_0(k|k-1) = \Phi(k,k-1)\hat{\underline{X}}_0(k-1) \qquad (3a)$$
$$\hat{\underline{X}}_i(k|k-1) = \hat{\underline{X}}_{i-1}(k-1), \qquad i = 1, 2, \ldots, L \qquad (3b)$$

Prior error variance algorithm

$$\underline{V}_{00}(k|k-1) = \Phi(k,k-1)\underline{V}_{00}(k-1)\Phi^T(k,k-1) + \underline{Q}(k) \qquad (4a)$$
$$\left.\begin{aligned} \underline{V}_{0i}(k|k-1) &= \Phi(k,k-1)\underline{V}_{0,i-1}(k-1) \qquad (4b) \\ \underline{V}_{ii}(k|k-1) &= \underline{V}_{i-1,i-1}(k-1) \qquad (4c) \end{aligned}\right\} \quad i = 1, 2, \ldots, L$$

Error variance algorithm

$$\underline{V}_{00}(k) = [I+\underline{V}_{00}(k|k-1)\underline{M}_0]^{-1}\,\underline{V}_{00}(k|k-1)$$

$$= \underline{V}_{00}(k|k-1)-\underline{V}_{00}(k|k-1)\underline{M}_0[I+\underline{V}_{00}(k|k-1)\underline{M}_0]^{-1}\,\underline{V}_{00}(k|k-1) \qquad (5a)$$

$$\underline{V}_{0i}(k) = [I+\underline{V}_{00}(k|k-1)\underline{M}_0]^{-1}\,\underline{V}_{0i}(k|k-1)$$

$$= \underline{V}_{0i}(k|k-1)-\underline{V}_{00}(k|k-1)\underline{M}_0[I+\underline{V}_{00}(k|k-1)\underline{M}_0]^{-1}\,\underline{V}_{0i}(k|k-1) \qquad (5b)$$

$$\underline{V}_{ii}(k) = \underline{V}_{ii}(k|k-1)-\underline{V}_{0i}{}^{T}\underline{M}_0[I+\underline{V}_{00}(k|k-1)\underline{M}_0]^{-1}\,\underline{V}_{0i}(k|k-1) \qquad (5c)$$

$$i = 1, 2, \ldots, L$$

Filtering algorithm

$$\hat{\underline{X}}_i(k) = \hat{\underline{X}}_i(k|k-1)+\underline{V}_{i0}(k)\underline{L}^{T}\underline{D}(k), \qquad i = 0, 1, 2, \ldots, L \qquad (6)$$

Definitions

$$\underline{M}_0 \triangleq \frac{\sqrt{2P_t}}{(r/T)}\;\underline{L}^{T}\left[\begin{array}{c|c|c} \hat{x}_3(k|k-1)Z_{C1}(k) & -Z_{C2}(k) & Z_{C1}(k) \\ +\hat{x}_4(k|k-1)Z_{C2}(k) & & \\ \hline -Z_{C2}(k) & \sqrt{2P_t} & 0 \\ \hline Z_{C1}(k) & 0 & \sqrt{2P_t} \end{array}\right]\underline{L} \qquad (7)$$

$$\begin{bmatrix} Z_{C1}(k) \\ Z_{C2}(k) \end{bmatrix} \triangleq \begin{bmatrix} z_1(k) & z_2(k) \\ -z_2(k) & z_1(k) \end{bmatrix} \begin{bmatrix} \sin \hat{x}_1(k|k-1) \\ \cos \hat{x}_1(k|k-1) \end{bmatrix} \qquad (8)$$

Equation (3b) gives the fixed-lag estimate for various amount of lags up to L.

Equation (4b) and (5c) are only required to calculate the steady-state error variance of the fixed-lag smoothed estimate.

It is appropriate to comment at this point that when using the EKF algorithm, the corresponding equation giving $\underline{V}_{ii}(k)$ is

$$\underline{V}_{ii}(k) = \underline{V}_{ii}(k-1) \qquad i = 1, 2, \ldots, L$$

which implies that no improvement is expected by using fixed-lag smoothing. This is not surprising as the error variance equation in the EKF algorithm is not coupled to the innovation process and consequently is not expected to allow new data to improve past (and consequently fixed-lag) estimates.

Figure 7.1 is a flowchart of the algorithms in Table XI and Figure 7.2 is a block diagram of the MAP fixed-lag receivers.

The receiver is seen to be made up of the same basic structure as the MAP quadrature receiver in Chapter 6 plus additional smoothing stages to give fixed-lag estimates for various amount of lags. Up to 4 lags are allowed due to the increased complexity and computations required.

7.2 Performance

The performance of the fixed-lag receivers are shown in Figures 7.3(a) and 7.3(b) and prove to be rather disappointing. The rather marginal improvement definitely does not warrant the extra complexity of the receivers. This is due to the deep fade problem already discussed in Chapter 6 and would require the use of diversity technique as will be done in the next chapter.

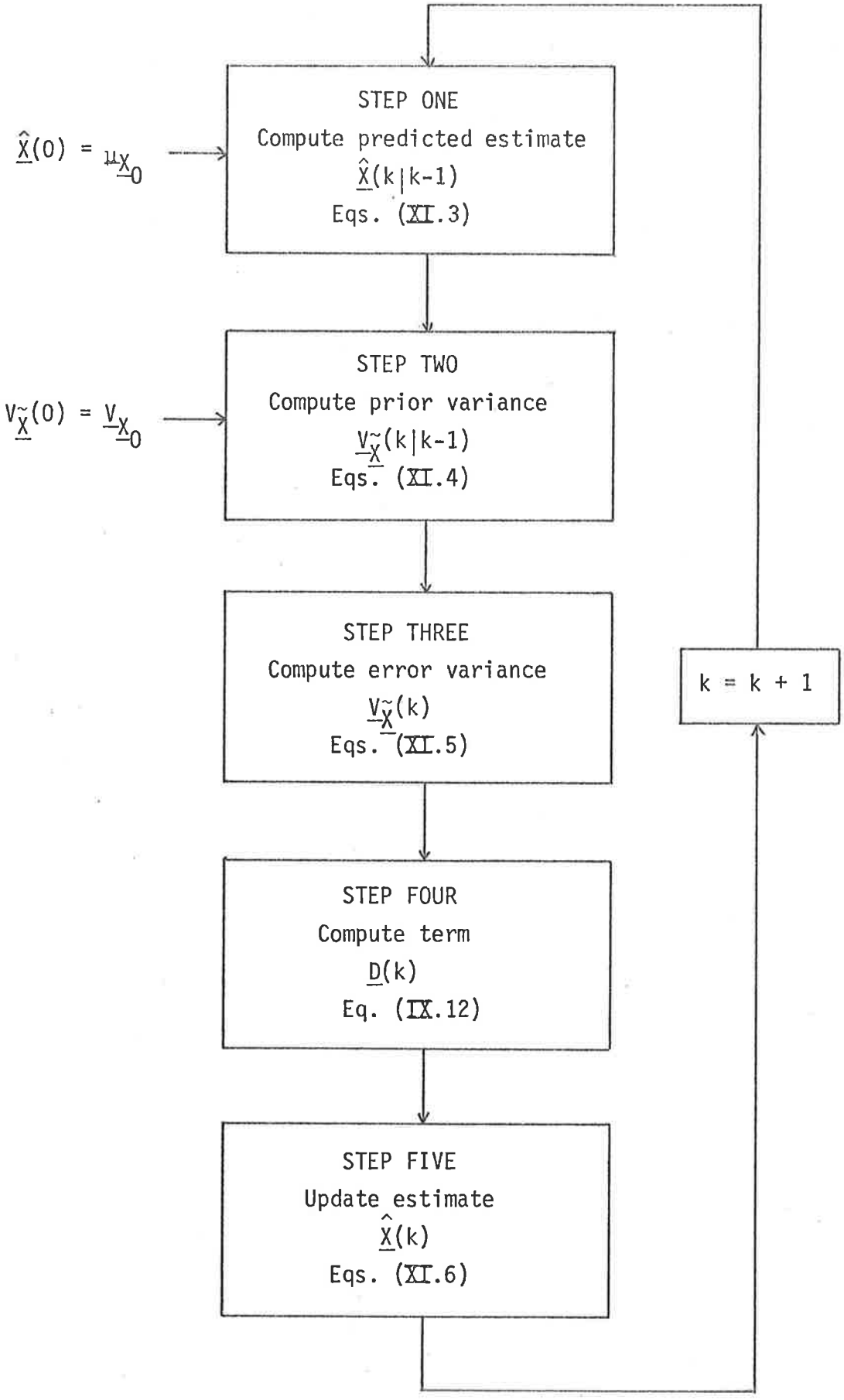

Figure 7.1 . Flowchart of MAP Fixed-lag Smoothing Algorithm (Table XI).

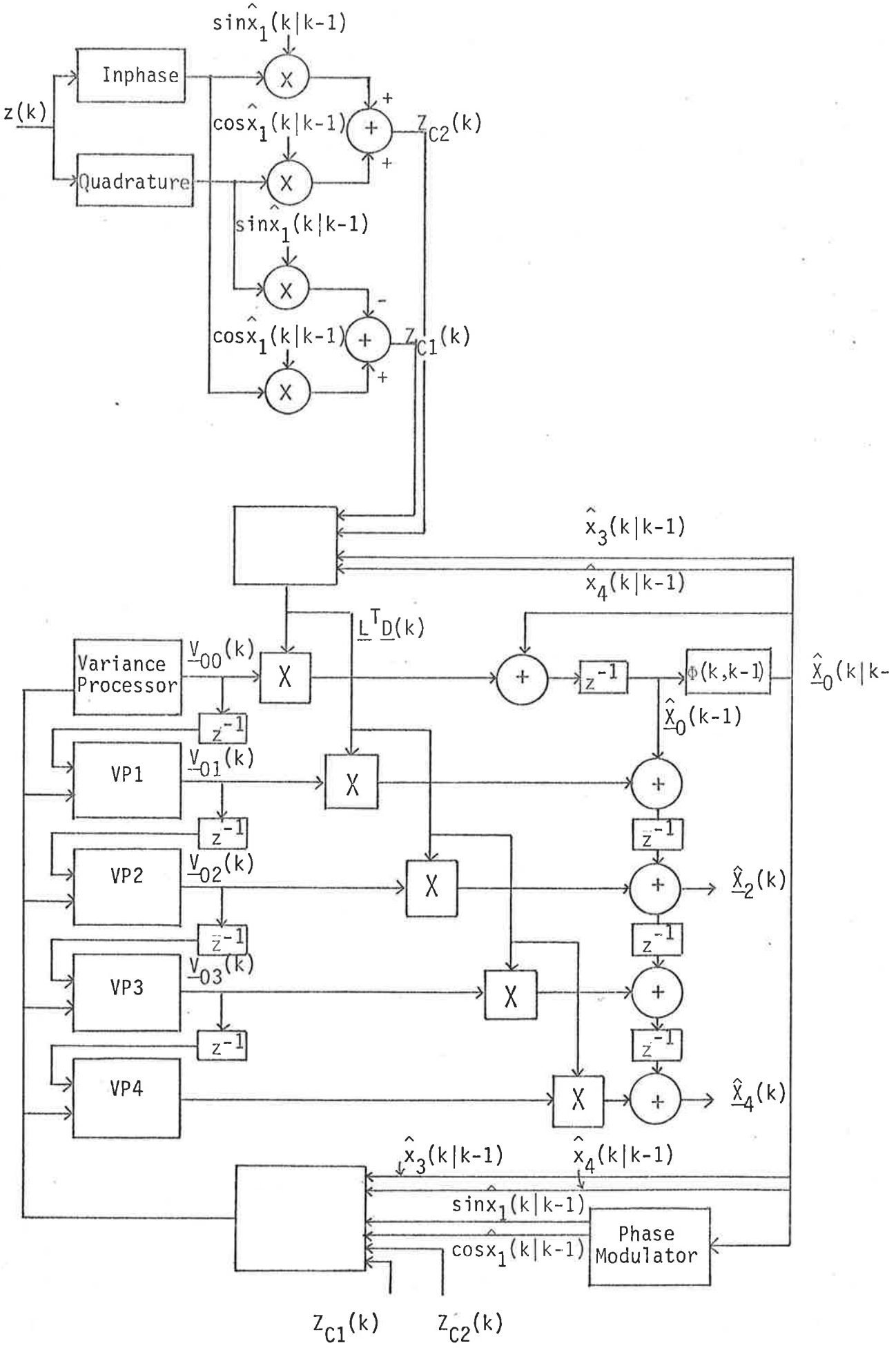

Figure 7.2: Fixed-Lag Receivers (for L = 4).

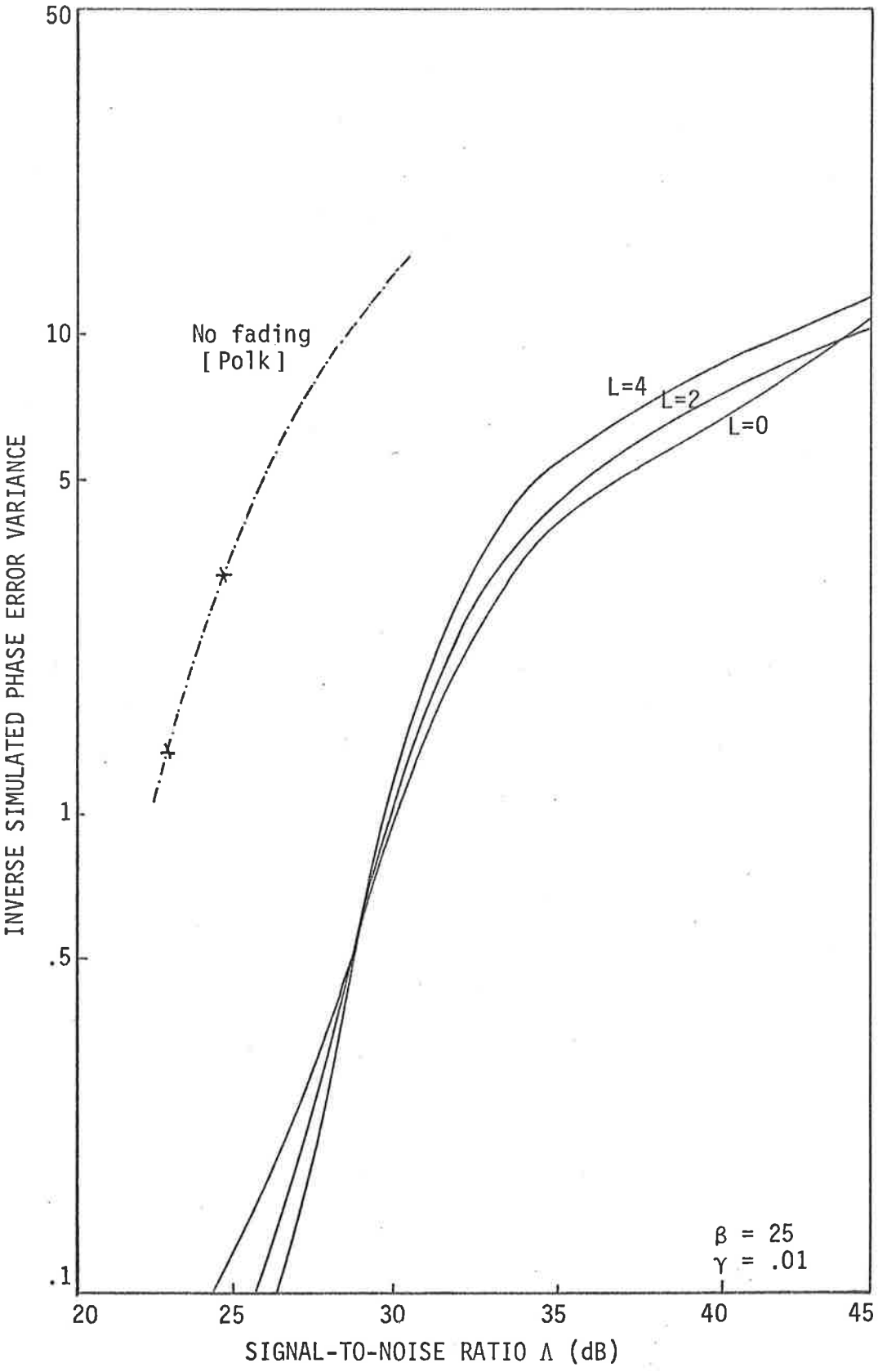

Fig. 7.3(a): Simulated inverse phase error variance (MAP, Quadrature, Fixed-lag)

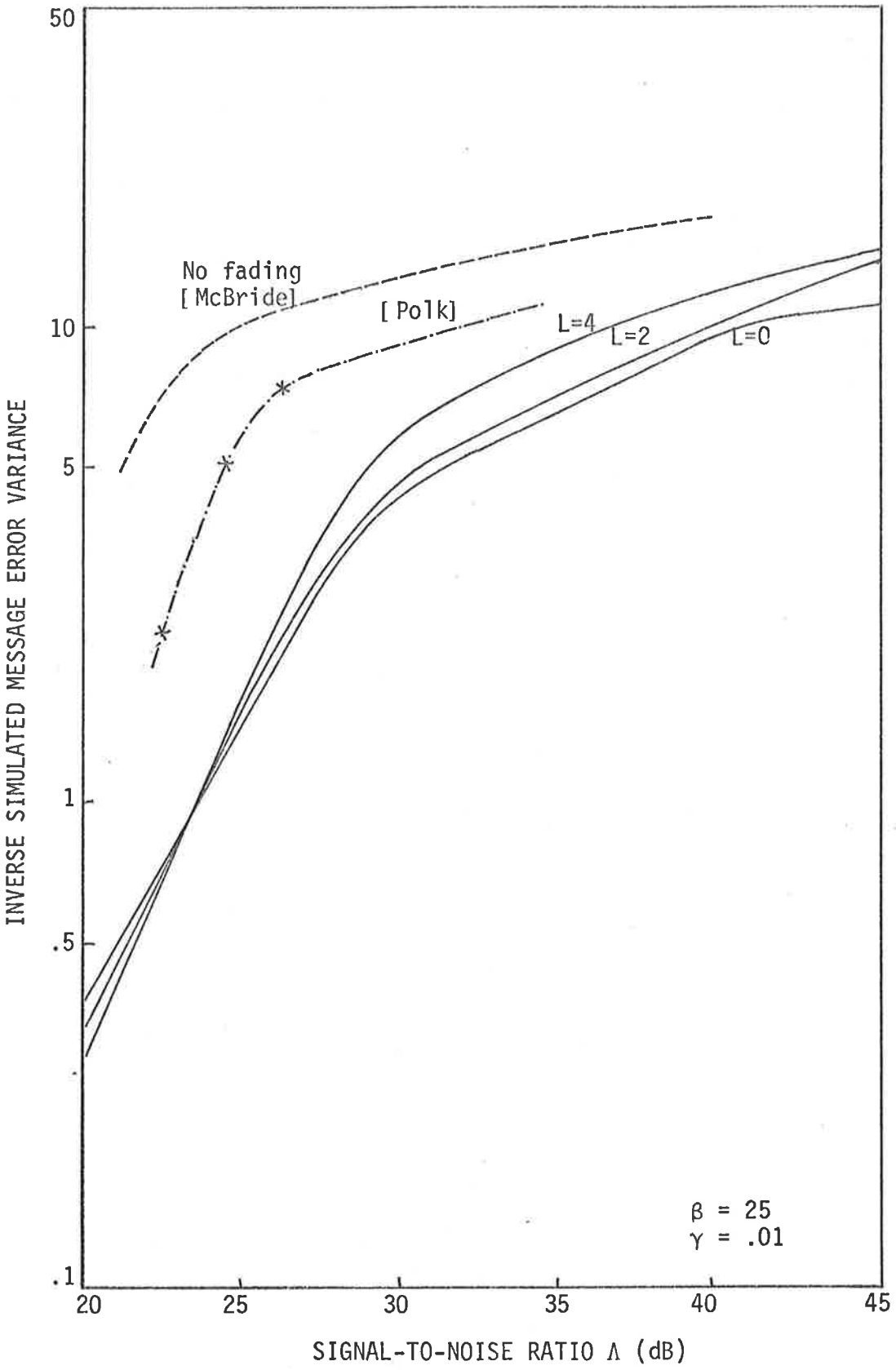

Fig. 7.3(b): Simulated Inverse Message Error Variance (MAP, Quadrature, Fixed-lag)

8. DIVERSITY RECEIVERS

To combat deep fades and to improve the overall performance of receivers in a fading environment, diversity techniques are investigated in this chapter using the framework of optimum design based on estimation theory as was done in the previous chapters for a single channel situation. Section 8.1 introduces the use of diversity techniques and Section 8.2 will formulate the two common techniques, frequency and space diversity, as an estimation model. Section 8.3 developes the resulting MAP algorithms. The receiver performance is to be investigated in Section 8.4.

8.1 Diversity Reception

Various types of diversity reception are used widely on point-to-point HF systems, on transhorizon microwaves (troposcatter channel), and to an increasing extent on radio links (Freeman, 1975).

Diversity reception is based on the fact that radio signals arriving at a point of reception over "separate" paths may have non-correlated signal levels. More simply, at one instant of time a signal on one path may be in a condition of fade while the identical signal on another path may not.

The separation may be in

(i) frequency, and

(ii) space, and

result in the two most common forms of diversity.

A frequency diversity system utilizes the phenomenon that the period of fading differs for carrier frequencies separated by 2-5%. Such a system normally employs two transmitters and two receivers, with each pair tuned to a different frequency (usually

2-3% separation since the frequency band allocations are limited). If the fading period at one frequency extends for a period of time, the same signal on the other frequency will be received at a higher level, with the resultant improvement in propagation reliability.

In a space diversity system, if two or more antennas are spaced many wavelengths apart (in the vertical plane), it has been observed that multipath fading will not occur simultaneously at both antennas. Sufficient output is almost always available from one of the antennas to provide useful signal to the receiver diversity system. The use of the two antennas at different heights provides a means of compensating, to a certain degree, for change in electrical path differences between direct and reflected rays by favouring the stronger signal in the diversity combiner.

A diversity combiner combines signals from two or more diversity paths (also called branches or channels). Most of the existing combiners in use are broken down into two major categories.

(i) Predetection;

(ii) Post-detection

depending on where in the receiver the combining takes place. They are further divided into three types:

(i) Selection combiner.

(ii) Equal gain combiner.

(iii) Maximal ratio combiner.

The selection combiner uses one receiver at a time. The output signal-to-noise ratio is equal to the input signal-to-noise ratio from the receiver selected for use at the time.

The equal gain combiner simply adds the diversity receiver outputs and the output signal-to-noise ratio of the combiner is

$$(SNR)_0 = \frac{1}{m\sigma_n^2} \sum_{i=1}^{m} S_i \qquad (8.1)$$

where

S_i is the input signal level in the i^{th} branch

σ_n^2 is the receiver noise

m is the order of diversity i.e. the number of independent diversity paths.

The maximal ratio combiner uses a relative gain change between the output signal in use. For example, assume that the stronger signal has unity output and the weaker signal has an output proportional to gain G; it then can be shown that (Brennan, 1958)

$$G = \frac{S_1}{S_2} \qquad (8.2)$$

such that the signal gain is adjusted to be proportional to the ratio of the input signals. The output signal-to-noise ratio is then given by

$$(SNR)_0 = \left(\frac{S_1}{\sigma_n^2}\right)^2 + \left(\frac{S_2}{\sigma_n^2}\right)^2 \qquad (8.3)$$

The efficiency of diversity depends on the correlation of fading of the diversity paths (Schwartz etal, 1966). In the following section, when modelling the diversity systems using state-variable approach, the correlation is assumed negligible to allow the assumption of independent diversity paths.

8.2 State-Variable Modelling of Diversity Systems

8.2.1 Frequency FM Diversity Systems

Consider an m-branch, frequency diversity system as shown in Figure 8.1(a). The signal transmitted over the i^{th} branch is

$$s_i(t) = \sqrt{2P_i}\sin(\omega_i t + d_f \int_0^t a(\tau)d\tau) \tag{8.4}$$

where

P_i's is the average transmitter power in i^{th} branch and is normally assumed to be the same for every branch.

d_f is the frequency deviation assumed to be the same in every branch.

Each branch (or path) is assumed to exhibit Rayleigh fading and the output from each branch can be written as

$$z_i(t) = \sqrt{2P_i}\Big[b_1^i(t)\sin(\omega_i t+\theta(t)) + b_2^i(t)\cos(\omega_i(t)+\theta(t))\Big]+v_i(t), \quad i = 1, 2, \ldots, m \tag{8.}$$

where

$$\theta(t) \triangleq d_f \int_0^t a(\tau)d\tau \tag{8.6}$$

and $b_1^i(t)$ and $b_2^i(t)$, to be called fading processes, are statistically independent gaussian processes each having zero mean and variance P_f^i, also. Normally assumed to be the same for each branch.

In addition, the carrier frequencies are assumed to be separated enough so that the fading on each branch are statistically independent.

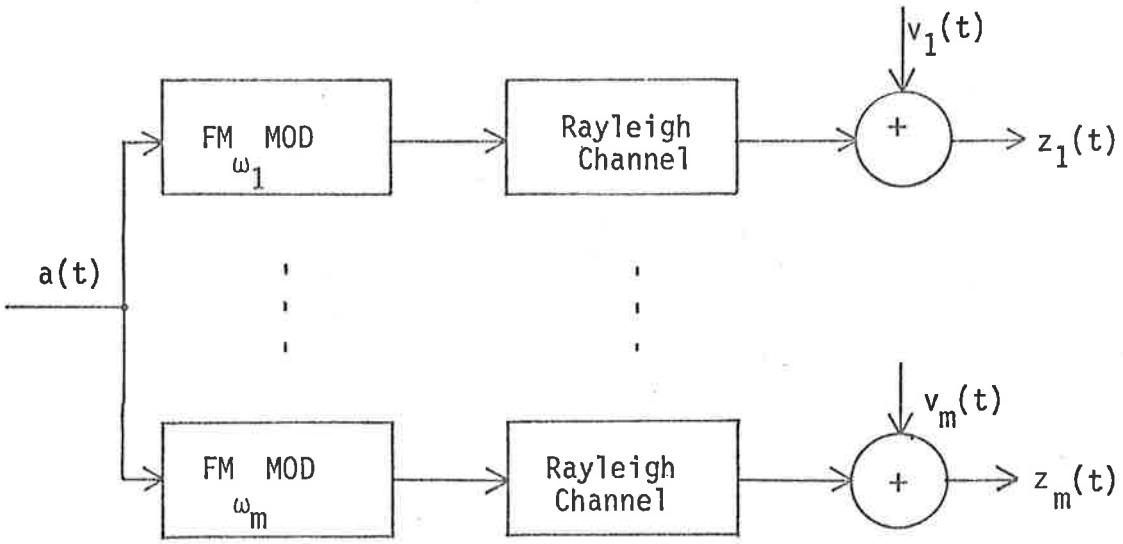

(a) Frequency FM diversity system (m carrier frequencies)

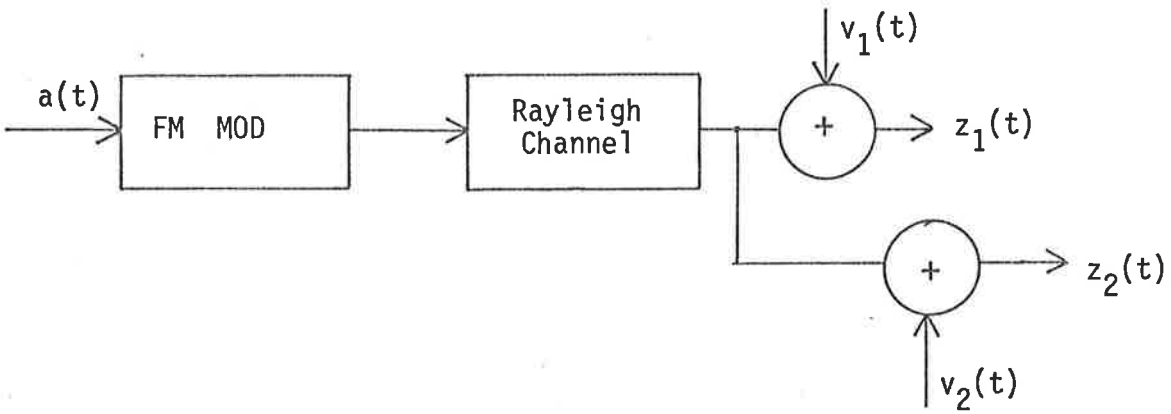

(b) Space FM diversity systems (2 antennas)

Figure 8.1 FM DIVERSITY SYSTEMS

The additive noise is normally assumed to be gaussian and have a spectrum broad enough to be considered as white noise.

For simplicity, the message process and the fading processes of each branch are modelled as first-order Markov process having first-order Butterworth spectrum as was done in Section 4.1.

$$\dot{a}(t) = -\alpha a(t)+\sqrt{2\alpha P_a}\, u_a(t) \tag{8.7}$$

$$\left.\begin{aligned} \dot{b}_1^i(t) &= -\gamma_i b_1^i(t)+\sqrt{2\gamma_i P_f^i}\, u_{b_1}^i(t) \qquad (8.8)\\ \dot{b}_2^i(t) &= -\gamma_i b_2^i(t)+\sqrt{2\gamma_i P_f^i}\, u_{b_2}^i(t) \qquad (8.9)\end{aligned}\right\} \quad i = 1, \ldots m$$

where the meanings of α, P_a, γ_i, P_f^i are the same as those given in Section 4.1.

Define the augmented state vector $\underline{X}(t)$ of dimension (2m+2) as

$$\underline{X}(t) \triangleq \begin{pmatrix} \theta(t) \\ a(t) \\ b_1^1(t) \\ b_2^1(t) \\ \vdots \\ b_1^i(t) \\ b_2^i(t) \\ \vdots \\ b_1^m(t) \\ b_2^m(t) \end{pmatrix} \begin{matrix} \leftarrow \text{ phase} \\ \leftarrow \text{ message} \\ \left.\begin{matrix} \\ \\ \end{matrix}\right\} 1^{st} \text{ branch} \\ \\ \\ \left.\begin{matrix} \\ \\ \end{matrix}\right\} i^{th} \text{ branch} \\ \\ \\ \left.\begin{matrix} \\ \\ \end{matrix}\right\} m^{th} \text{ branch} \end{matrix} \tag{8.10}$$

The state equation for $\underline{X}(t)$ is then given by

$$\dot{\underline{X}}(t) = \underline{F}\,\underline{X}(t) + \underline{G}\,\underline{U}(t) \tag{8.11}$$

where $\underline{F}$ is an $(2m+2) \times (2m+2)$ matrix.

$$\underline{F} = \begin{pmatrix} 0 & d_f & 0 & 0 & \cdots & 0 & 0 \\ 0 & -\alpha & 0 & 0 & \cdots & 0 & 0 \\ 0 & 0 & -\gamma_1 & 0 & \cdots & 0 & 0 \\ 0 & 0 & 0 & -\gamma_1 & \cdots & 0 & 0 \\ \vdots & \vdots & \vdots & \vdots & & \vdots & \vdots \\ 0 & 0 & 0 & 0 & \cdots & -\gamma_m & 0 \\ 0 & 0 & 0 & 0 & \cdots & 0 & -\gamma_m \end{pmatrix} \tag{8.12}$$

$\underline{G}$ is a $(2m+2) \times (2m+1)$ matrix

$$\underline{G} = \begin{pmatrix} 0 & 0 & 0 & \cdots & 0 & 0 \\ \sqrt{2\alpha P_a} & 0 & 0 & \cdots & 0 & 0 \\ 0 & \sqrt{2\gamma_1 P_f^1} & 0 & \cdots & 0 & 0 \\ 0 & 0 & \sqrt{2\gamma_1 P_f^1} & \cdots & 0 & 0 \\ \vdots & \vdots & \vdots & & \vdots & \vdots \\ 0 & 0 & 0 & \cdots & \sqrt{2\gamma_m P_f^m} & 0 \\ 0 & 0 & 0 & \cdots & 0 & \sqrt{2\gamma_m P_f^m} \end{pmatrix} \tag{8.13}$$

and $\underline{U}(t)$ is a $(2m+1)$ column vector

$$\underline{U}(t) = \left(u_a(t)\ u_{b_1}^1(t)\ u_{b_2}^1(t) \cdots u_{b_1}^m(t)\ u_{b_2}^m(t) \right)^T \tag{8.14}$$

The discrete system model corresponding to the analog model given by Equation 8.11 is shown in Equation (1) of Table XII.

The variance of $\underline{W}(k)$ is defined as

$$\underline{Q}(k) = \begin{pmatrix} Q_{11} & Q_{12} & 0 & 0 & \cdots & 0 & 0 \\ Q_{12} & Q_{22} & 0 & 0 & \cdots & 0 & 0 \\ 0 & 0 & Q_{33} & 0 & \cdots & 0 & 0 \\ 0 & 0 & 0 & Q_{44} & \cdots & 0 & 0 \\ \vdots & \vdots & \vdots & \vdots & & \vdots & \vdots \\ 0 & 0 & 0 & 0 & \cdots & Q_{mm} & 0 \\ 0 & 0 & 0 & 0 & \cdots & 0 & Q_{mm} \end{pmatrix} \tag{8.15}$$

and the non-zero elements are given in Equations 3(a) through 3(d) in Table XII.

Using quadrature sampling, the received signal in each branch is given by

$$\begin{pmatrix} z_{i1}(k) \\ z_{i2}(k) \end{pmatrix} = \sqrt{2P_i} \begin{pmatrix} x_{2i+1}(k) & x_{2i+2}(k) \\ -x_{2i+2}(k) & x_{2i+1}(k) \end{pmatrix} \begin{pmatrix} \sin x_1(k) \\ \cos x_1(k) \end{pmatrix} + \begin{pmatrix} v_{i1}(k) \\ v_{i2}(k) \end{pmatrix} \quad i = 1,2,\ldots,r \tag{8.16}$$

where the sampled noise

$$\underline{V}_i(k) \triangleq \begin{pmatrix} v_{i1}(k) \\ v_{i2}(k) \end{pmatrix} \tag{8.17}$$

are gaussian white sequences having zero mean and variance

$$E\left(\underline{V}_i(k)\underline{V}_i^T(j)\right) = \begin{pmatrix} \frac{r_i}{T} & 0 \\ 0 & \frac{r_i}{T} \end{pmatrix} \delta_{kj} \qquad (8.18)$$

with r_i being the two-sided spectral height of the continuous additive gaussian noise in each branch.

The formulation of the frequency FM diversity system as a discrete state-variable model is thus complete and is summarised in Equation (1) through (4) in Table XII.

8.2.2. Space FM Diversity System

In the space diversity system, a single FM modulated carrier is transmitted over the Rayleigh fading channel and at the receiver, there are m antennas separated by several wavelengths in the vertical plane and the reflected rays from the multipath fading medium received by the various antennas are assumed to exhibit Rayleigh fading independently. Assuming identical fading statistics and equal average received power, the signal received by each antenna can be written as

$$z_i(t) = \sqrt{2P_t}\left[b_1^i(t)\sin\left(\omega_c t+\theta(t)\right) + b_2^i(t)\cos\left(\omega_c t+\theta(t)\right)\right] + v_i(t), \quad i = 1,2,\ldots,m \qquad (8.19)$$

This is of the same form as the signal received in a frequency diversity system (Equation 8.5) and the formulation of an augmented state-variable model for the space diversity can be done in exactly the same way as was done in the previous section. Equations (1)

TABLE XII.

DISCRETE MAP FILTERING ALGORITHM FOR FM DIVERSITY SYSTEMS

System model $\underline{X}(k) = \Phi(k,k-1)\underline{X}(k-1)+\underline{W}(k)$

$$\begin{pmatrix} x_1(k) \\ x_2(k) \\ x_3(k) \\ x_4(k) \\ \vdots \\ x_{2m+1}(k) \\ x_{2m+2}(k) \end{pmatrix} = \left(\begin{array}{cc:cc:c:cc} 1 & \beta(1-e^{-\alpha T}) & 0 & 0 & \cdots & 0 & 0 \\ 0 & e^{-\alpha T} & 0 & 0 & \cdots & 0 & 0 \\ \hdashline 0 & 0 & e^{-\gamma_1 T} & 0 & \cdots & 0 & 0 \\ 0 & 0 & 0 & e^{-\gamma_1 T} & \cdots & 0 & 0 \\ \hdashline \vdots & \vdots & \vdots & \vdots & \ddots & \vdots & \vdots \\ \hdashline 0 & 0 & 0 & 0 & \cdots & e^{-\gamma_m T} & 0 \\ 0 & 0 & 0 & 0 & \cdots & 0 & e^{-\gamma_m T} \end{array}\right) \begin{pmatrix} x_1(k-1) \\ x_2(k-1) \\ x_3(k-1) \\ x_4(k-1) \\ \vdots \\ x_{2m+1}(k-1) \\ x_{2m+2}(k-1) \end{pmatrix} + \begin{pmatrix} w_1(k) \\ w_2(k) \\ w_3(k) \\ w_4(k) \\ \vdots \\ w_{2m+1}(k) \\ w_{2m+2}(k) \end{pmatrix}$$

m is the number of diversity branches

Observation model $\underline{Z}(k) = \underline{h}[\underline{X}(k)]+\underline{V}(k)$

$$\underline{Z}(k) = \begin{pmatrix} \underline{h}_1(k) \\ \underline{h}_2(k) \\ \vdots \\ \underline{h}_i(k) \\ \vdots \\ \underline{h}_m(k) \end{pmatrix} + \begin{pmatrix} \underline{v}_1(k) \\ \underline{v}_2(k) \\ \vdots \\ \underline{v}_i(k) \\ \vdots \\ \underline{v}_m(k) \end{pmatrix} \begin{matrix} \leftarrow \text{branch 1} \\ \leftarrow \text{branch 2} \\ \\ \leftarrow \text{branch i} \\ \\ \leftarrow \text{branch m} \end{matrix} \qquad (2)$$

For each branch

$$\begin{pmatrix} z_{i1}(k) \\ z_{i2}(k) \end{pmatrix} = \sqrt{2P_i} \begin{pmatrix} x_{2i+1}(k) & x_{2i+2}(k) \\ -x_{2i+2}(k) & x_{2i+1}(k) \end{pmatrix} \begin{pmatrix} \sin x_1(k) \\ \cos x_1(k) \end{pmatrix} + \begin{pmatrix} v_{i1}(k) \\ v_{i2}(k) \end{pmatrix}, \quad i = 1, 2, \ldots, m \qquad (2a)$$

where P_i is the average transmitted power in each branch.

Statistical parameters

$$E[\underline{W}(k)\underline{W}^T(j)] = \underline{Q}(k)\delta_{kj} \tag{3}$$

the non-zero elements of $\underline{Q}(k)$ are

$$Q_{11} = P_a\beta^2(2\alpha T-3+4e^{-\alpha T}-e^{-2\alpha T}) \tag{3a}$$

$$Q_{12} = Q_{21} = P_a\beta(1-e^{-\alpha T})^2 \tag{3b}$$

$$Q_{22} = P_a(1-e^{-2\alpha T}) \tag{3c}$$

and other diagonal elements

$$Q_{2i+1} = Q_{2i+2} = P_f^i\ (1-e^{-2\gamma_i T}), \quad i = 1, 2, \ldots, m \tag{3d}$$

$$E[\underline{v}_i(k)\underline{v}_i^T(j)] = \underline{R}_i(k)\delta_{kj} = \begin{pmatrix} \frac{r_i}{T} & 0 \\ 0 & \frac{r_i}{T} \end{pmatrix}\delta_{kj}, \quad i = 1, 2, \ldots, m \tag{4}$$

where r_i is the two-sided spectral height of the continuous additive gaussian noise of each branch.

One stage prediction algorithm

$$\hat{\underline{X}}(k|k-1) = \Phi(k,k-1)\hat{\underline{X}}(k-1) \tag{5}$$

$$\hat{\underline{X}}(0) = \underline{\mu}_{X_0} \tag{5a}$$

Prior error variance algorithm

$$\underline{V}_{\tilde{X}}(k|k-1) = \Phi(k,k-1)\underline{V}_{\tilde{X}}(k-1)\Phi(k,k-1)+\underline{Q}(k) \tag{6}$$

$$\underline{V}_{\tilde{X}}(k) = \underline{V}_{X_0} \tag{6a}$$

Filtering algorithm

$$\hat{\underline{X}}(k) = \hat{\underline{X}}(k|k-1)+\underline{V}_{\tilde{X}}(k)\underline{D}(k) \tag{7}$$

where

$$\underline{D}(k) = \begin{pmatrix} \underline{D}_0(k) \\ \underline{D}_1(k) \\ \vdots \\ \underline{D}_i(k) \\ \vdots \\ \underline{D}_m(k) \end{pmatrix}$$

$$\underline{D}_0(k) \triangleq \sum_{i=1}^{m} \frac{\sqrt{2P_i}}{(r_i/T)} \begin{pmatrix} \hat{x}_{2i+1}(k|k-1)Z_{C2}^i(k)-\hat{x}_{2i+2}(k|k-1)Z_{C1}^i(k) \\ 0 \end{pmatrix}_{2x1} \tag{8a}$$

$$\underline{D}_i(k) \triangleq \frac{\sqrt{2P_i}}{(r_i/T)} \begin{pmatrix} Z_{C1}^i(k)-\sqrt{2P_i}\hat{x}_{2i+1}(k|k-1) \\ Z_{C2}^i(k)-\sqrt{2P_i}\hat{x}_{2i+2}(k|k-1) \end{pmatrix}_{2x1}, \quad i = 1,2,\ldots,m \tag{8b}$$

$$\begin{pmatrix} Z_{C1}^i(k) \\ Z_{C2}^i(k) \end{pmatrix} \triangleq \begin{pmatrix} z_{i1}(k) & z_{i2}(k) \\ -z_{i2}(k) & z_{i1}(k) \end{pmatrix} \begin{pmatrix} \sin \hat{x}_1(k|k-1) \\ \cos \hat{x}_1(k|k-1) \end{pmatrix}, \quad i = 1, 2, \ldots \tag{9}$$

Error variance algorithm

$$\underline{V}_{\tilde{\underline{X}}}(k) = \left[I+\underline{V}_{\tilde{\underline{X}}}(k|k-1)\underline{M}[\hat{\underline{X}}(k|k-1),k]\right]^{-1} \underline{V}_{\tilde{\underline{X}}}(k|k-1) \tag{10}$$

where

$$\underline{M}[\hat{\underline{X}}(k|k-1),k] \triangleq \frac{-\partial}{\partial \hat{\underline{X}}(k|k-1)}\left[\frac{\partial \underline{h}^T[\hat{\underline{X}}(k|k-1),k]}{\partial \hat{\underline{X}}(k|k-1)} \underline{R}^{-1}(k)\underline{\nu}(k)\right] \tag{11}$$

$$\triangleq \left[\begin{array}{cc|cc|ccc|cc} M_0 & 0 & M_{11} & M_{12} & \cdots & M_{m1} & M_{m2} \\ 0 & 0 & 0 & 0 & \cdots & 0 & 0 \\ \hline M_{11} & 0 & N_1 & 0 & \cdots & 0 & 0 \\ M_{12} & 0 & 0 & N_1 & \cdots & 0 & 0 \\ \hline \vdots & \vdots & \vdots & \vdots & \ddots & \vdots & \vdots \\ \hline M_{m1} & 0 & 0 & 0 & \cdots & N_m & 0 \\ M_{m2} & 0 & 0 & 0 & \cdots & 0 & N_m \end{array}\right] \tag{12}$$

$$M_0 \triangleq \sum_{i=1}^{m} \frac{\sqrt{2P_i}}{(r_i/T)}\left[\hat{x}_{2i+1}(k|k-1)Z^i_{C1}(k)+\hat{x}_{2i+2}(k|k-1)Z^i_{C2}(k)\right] \tag{12a}$$

$$M_{i1} \triangleq -\frac{\sqrt{2P_i}}{(r_i/T)} Z^i_{C2}(k) \tag{12b}$$

$$M_{i2} \triangleq \frac{\sqrt{2P_i}}{(r_i/T)} Z^i_{C1}(k) \qquad i = 1, 2, \ldots, m \tag{12c}$$

$$N_i \triangleq \frac{\sqrt{2P_i}}{(r_i/T)} \tag{12d}$$

through (4) in Table XII can thus represent either a frequency diversity system or a space diversity system.

8.3 MAP Algorithms for FM Diversity Systems

The MAP filtering algorithm in Table III is applied to the discrete FM diversity model as formulated in the preceding section and the resulting algorithms are shown in Equations (5) through (12) in Table XII. The derivation is tedious but straightforward and uses the following definitions

$$\underline{D}(k) \triangleq \frac{\partial \underline{h}^T[\hat{\underline{X}}(k|k-1)]}{\hat{\underline{X}}(k|k-1)} R^{-1}(k)\ \underline{\nu}(k) \tag{8.20}$$

$$\underline{M}[\hat{\underline{X}}(k|k-1),k] \triangleq \frac{-\partial}{\partial \hat{\underline{X}}(k|k-1)} \left(\frac{\partial \underline{h}^T\left[\hat{\underline{X}}(k|k-1),k\right]}{\partial \hat{\underline{X}}(k|k-1)} R^{-1}(k)\ \underline{\nu}(k) \right)$$

$$= \frac{-\partial \underline{D}(k)}{\partial \hat{\underline{X}}(k|k-1)} \tag{8.21}$$

The flowchart for the algorithms is shown in Figure 8.2 and a block diagram of the receiver is shown in Figure 8.3.

8.4 Performance

The performance of the diversity receivers is shown in Figure 8.4(a) and 8.4(b) (with $\beta = 25$ and $\gamma = 0.1$), for diversity a system of order 2 and order 4. On the same graph are plotted the results for single channel MAP quadrature receivers from Figures 6.3(a) and 6.3(b) and also the simulated results for no fading obtained by Polk (1973, using scalar sampling) and McBride (1973, using quadrature sampling). It can be seen that the use of

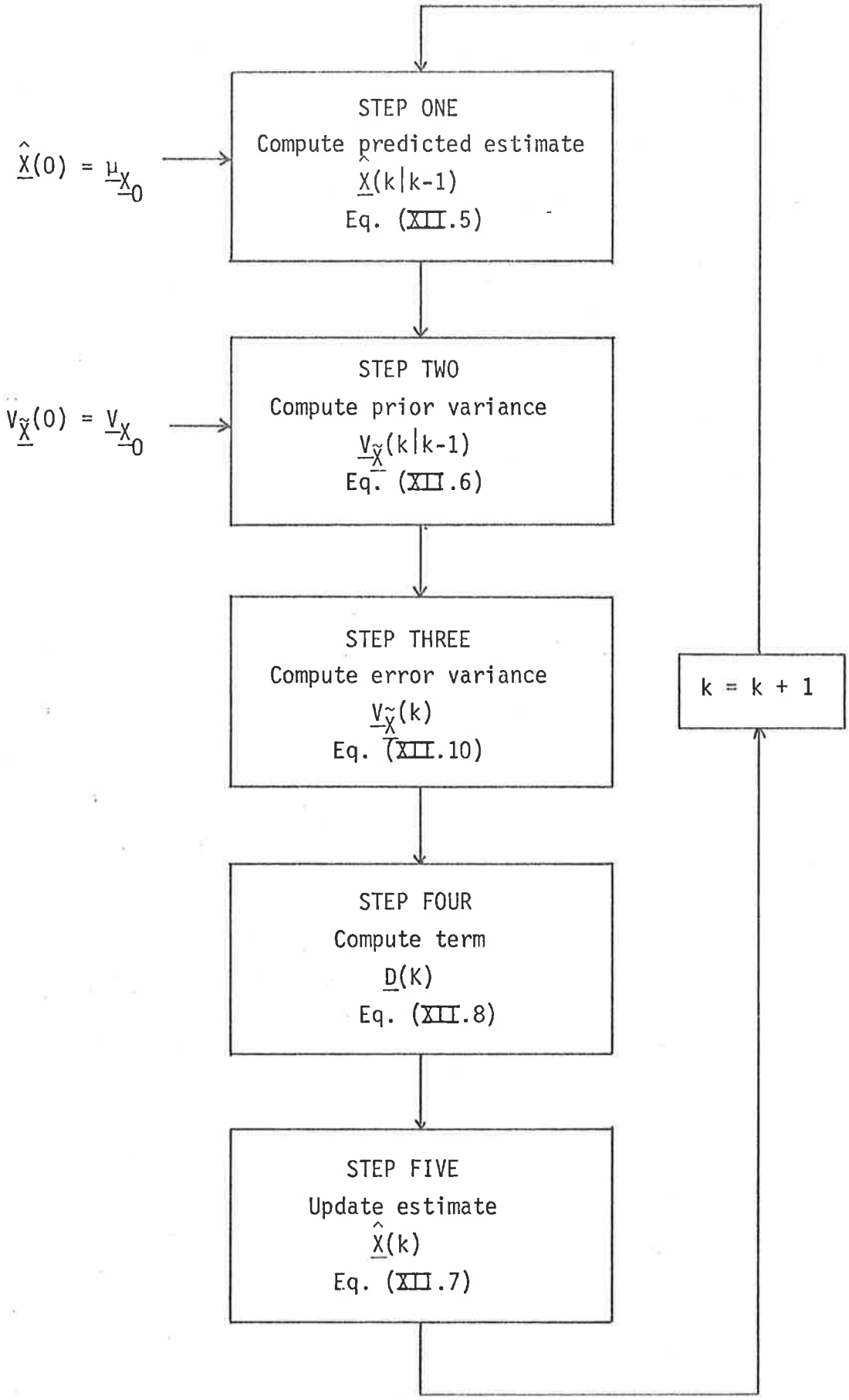

Figure 8.2 . Flowchart of MAP Algorithm For Diversity Systems (Table XII)

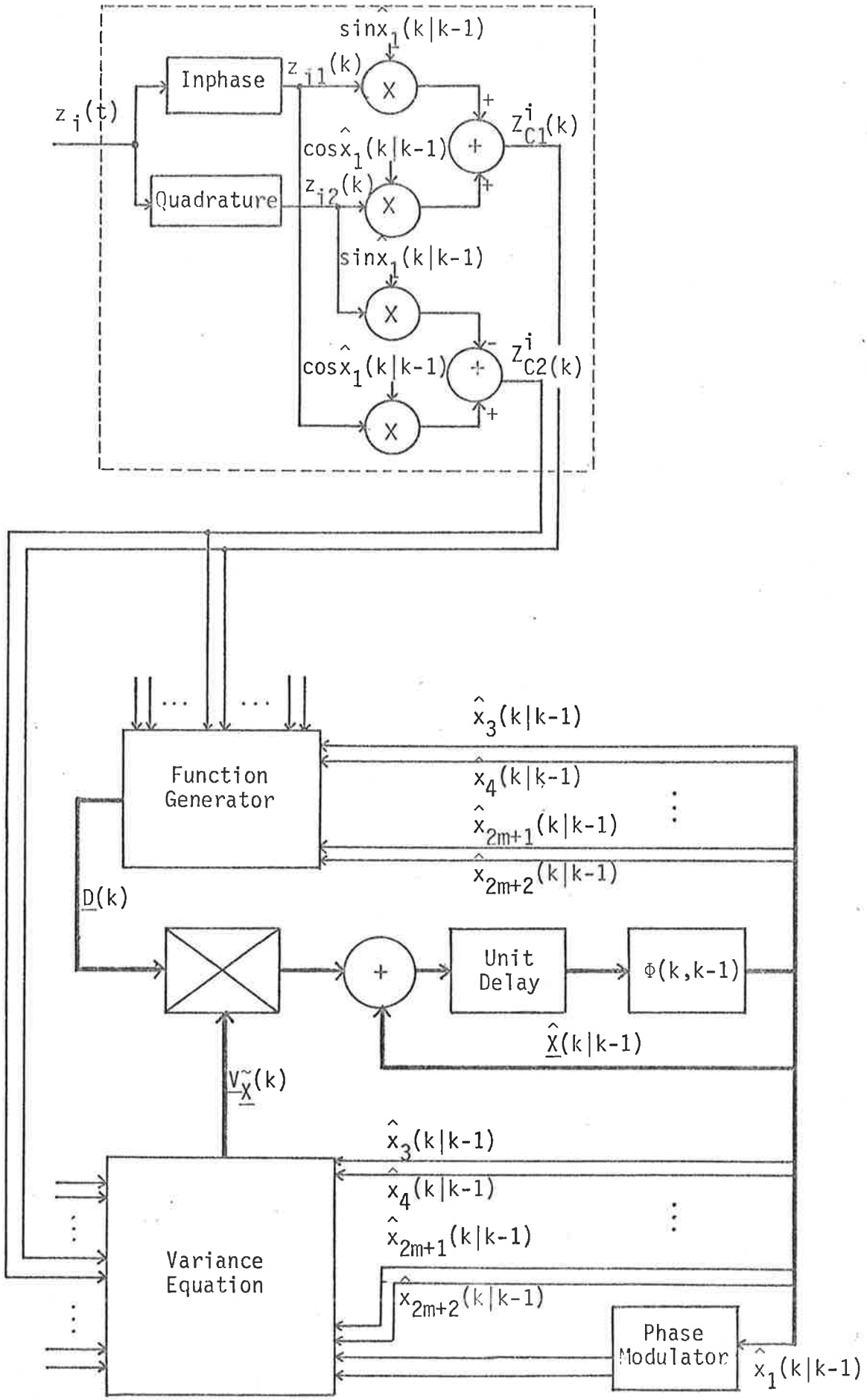

Figure 8.3: FM Diversity Receiver.

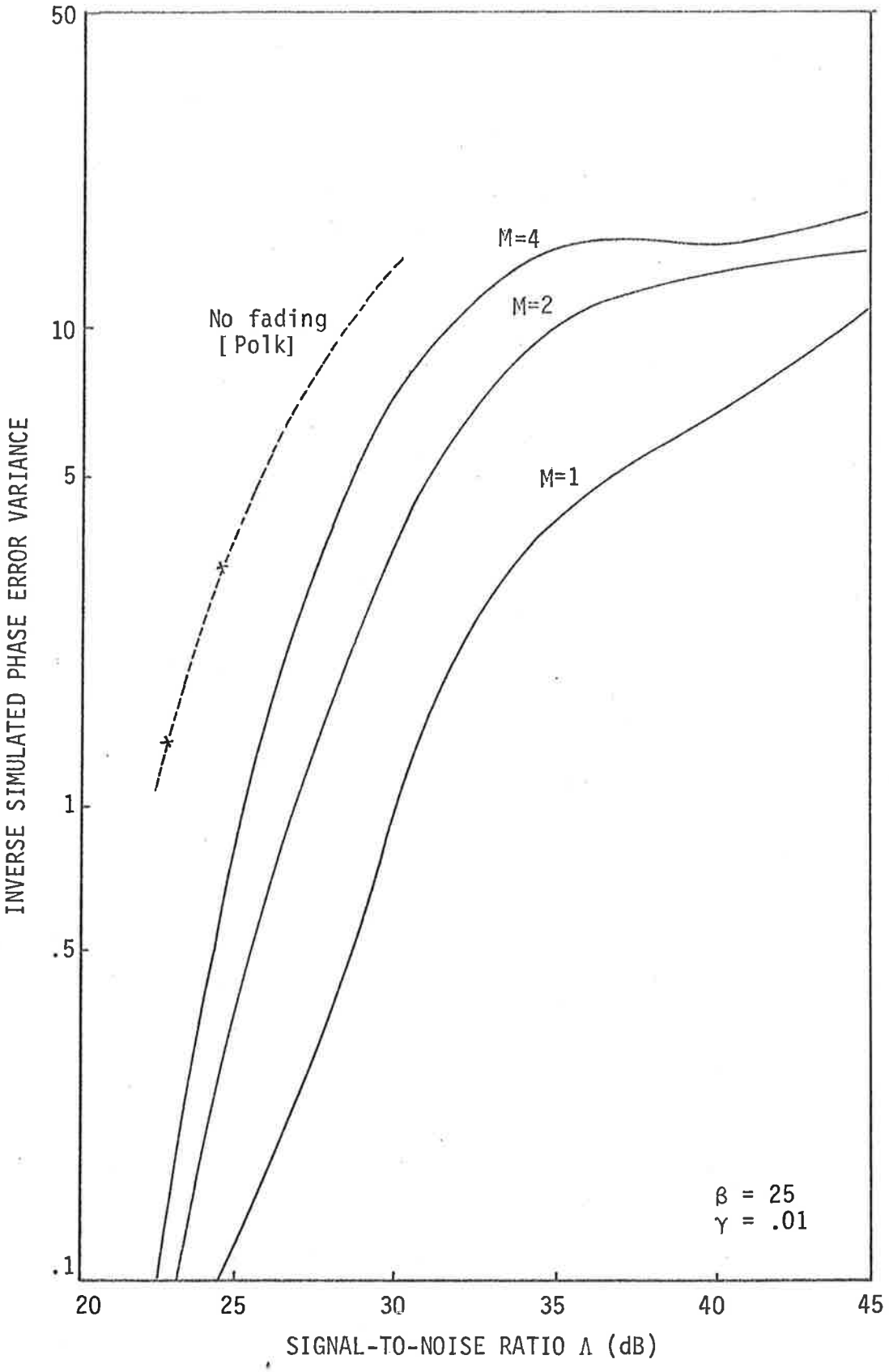

Fig. 8.4(a): Simulated Inverse Phase Error Variance
(MAP, Quadrature, Diversity)

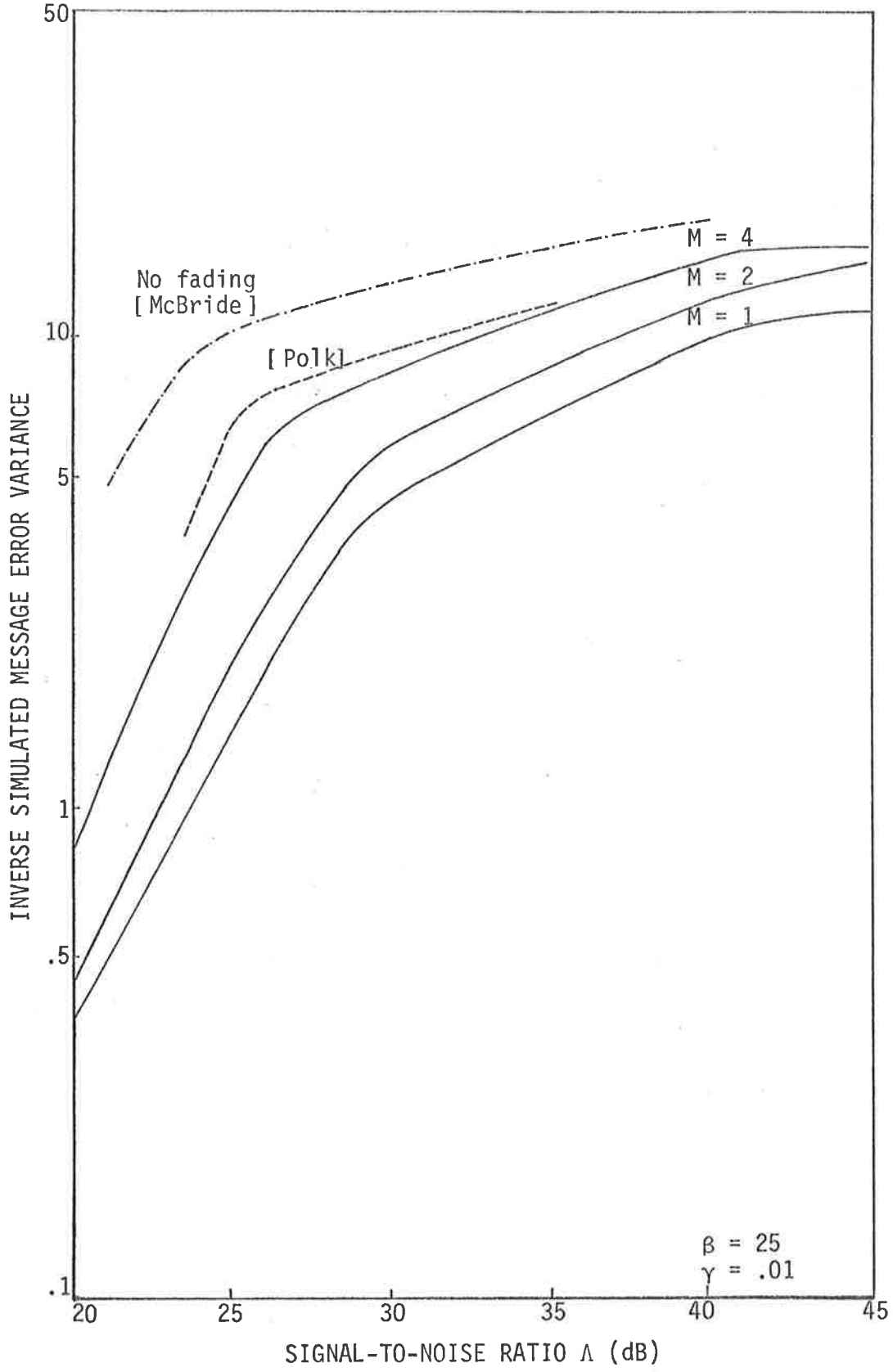

Fig. 8.4(b): Simulated inverse message error variance (MAP, Quadrature, Diversity)

diversity has improved the performance considerably in terms of threshold performance as well as output signal-to-noise ratio. In fact, the performance of the 4-branches diversity receiver is almost as good as those obtained by Polk (1974). The complexity of the receiver becomes rather formidable in terms of execution time while simulating them on the computer so higher order diversity systems are not investigated.

Figure 8.5 shows the performance of the diversity receivers in a "fast" fading situation (γ = .1) the solid lines are the simulated inverse message error variance for the quadrature MAP receivers for the single channel case (m = 1, from Figure 6.7(b)), and for the two-branch (m = 2) and four-branch cases. Curve A is the single channel performance of the quadrature MAP receiver for slow fading (γ = .01) whereas curve B shows the performance of the baseband EKF receiver (Figure 5.6(b)). It can be seen that when the fading is fast, the use of diversity technique improves the performance even more significantly but the performance achieved by a four-branch diversity system is still worse than that of a single channel under slower fading condition. The fast-fading problem is thus not solved by the use of diversity techniques. Fortunately, the assumption of slow fading has been found to agree well with many practical channels (Schwartz, 1966) where the most difficult problem is that of deep fade and the use of diversity technique is the best way of combatting this problem when transmitting analog information.

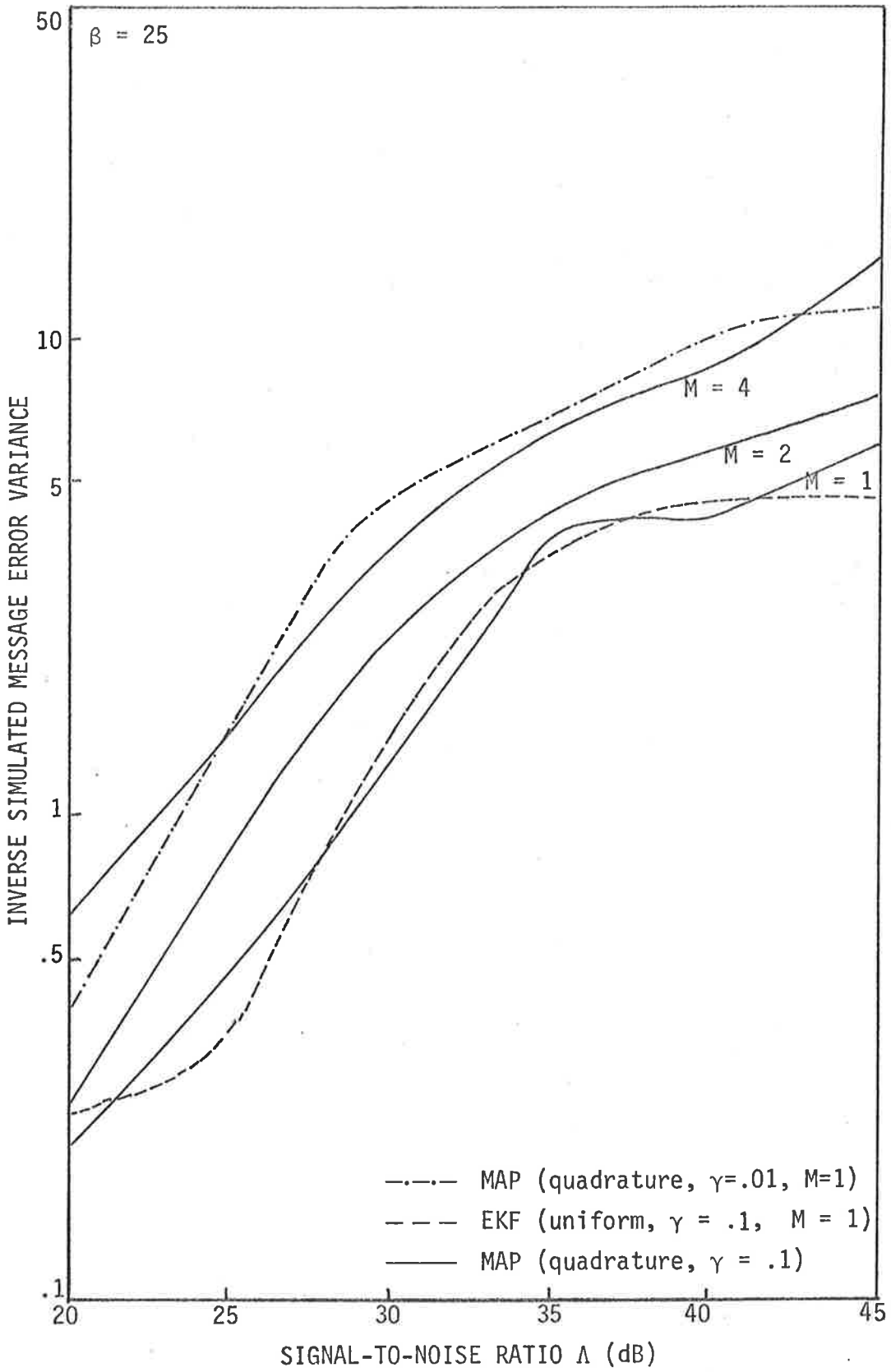

Fig. 8.5: Performance of diversity receivers for "fast" fading channels.

9. CONCLUSIONS

This thesis has been concerned with the problem of demodulating an analog FM signal transmitted over a Rayleigh fading channel. The approach taken has been to formulate the FM communication model as an estimation model and applied the nonlinear estimation algorithms to derive the receiver structures. No prior knowledge of the receiver structures was assumed.

In Chapter 2, an analog model was set up for the FM communication system using the state-variable formulation. The message, assumed to be sample function from a gaussian random process, is generated by a linear message model and was used to frequency-modulate a carrier signal before being transmitted over a fading channel. The fading was assumed to be slow and frequency nonselective and could be considered as multiplicative noise having a Rayleigh envelope distribution and a uniform phase distribution. The fading signal was thus represented as a sum of an in-phase and a quadrature component, each amplitude modulated by a gaussian low-pass process (called fading processes) generated by a linear model in the same way as was done for the message. An augmented state vector having for its components the message, the phase and the fading processes was formulated and allowed the output of the fading channel to be expressed as a nonlinear function of the system state vector. The fading signal was further contaminated by additive white gaussian noise and the received signal was sampled by two possible methods using either scalar sampling or quadrature sampling.

In order to apply results from discrete estimation theory, the analog model was also converted to an equivalent discrete model and was combined with the discrete observation model (as a result of

sampling) to form a complete estimation model as was presented in Table I (pp. 24-25).

Chapter 3 was an outline of the deviations of the extended Kalman filter algorithm and the maximum *a posterior* filtering algorithms to be applied to the estimation model already formulated in Chapter 2. These algorithms are the results of recent developments in nonlinear estimation theory and were summarized in Table II (pp. 40-41) and Table III (pp. 44-45). The validity of these algorithms, when applied to the FM communication system considered in this thesis, depended on the "instantaneous" signal-to-noise ratios which divided the operations of the receivers into an above and a below threshold regions. Furthermore, these algorithsm are only approximate and the receivers are therefore termed as being "quasi-optimum".

Chapter 4 considered the use of computer simulations in this study. Computer simulations were required as there are no analytical techniques that could be used to analyse the performance of the receivers to be proposed. For simplicity, an example of the FM communication system having an 4-dimensional state vector was derived and summarised in Table IV (pp. 53-54). This could be extended to higher order systems at the expense of longer computation time when simulated on the computer.

The theoretical considerations on various aspects of computer simulations were very important in ascertaining the validity of the results. It was found that to achieve a 5% accuracy with 98% confidence, the minimum required number of statistically independent simulation points was to be 4000 (Equation 4.36, p. 67) and this was used as a basis for determining the number of runs and the number of simulation points per run for the simulation program. The organization

of each simulation program was based on the following informations:

(i) The parameter set chosen in Section 4.3.2 (pp. 71-76).

(ii) The flowchart of the General Simulation Program (Figure 4.3, p. 68).

(iii) The flowchart associated with a particular algorithm and given immediately after the table showing the algorithm.

All the results obtained and plotted were interpreted as being correct to within 5% with a 98% degree of confidence. This is to be borne in mind when interpreting results represented by curves very close to each other.

The main development of the thesis was started in Chapter 5 when the algorithms derived in Chapter 3 were applied to the example of the FM communication model in Chapter 4 to obtain receiver structures under various situations. The receivers obtained were of a discrete type and would lend themselves to be implemented by the use of special purpose fast digital hardware consisting of an A/D converter, a digital demodulator and a D/A converter. The problem of on-line implementation using digital computers was not investigated but is quite conceivable with the coming of the new computer generations (Bucy et al., 1976).

The results obtained in Chapter 5 using scalar sampling strongly supports the feasibility of the approach taken in this thesis, namely, the application of estimation theory to rigorously derive the quasi-optimum receivers for analog FM signals transmitted over Rayleigh fading channel.

The results obtained in Chapter 5 also revealed that the performance of the receivers using scalar sampling for relatively slow fading (γ = .01) were still far below that achieved in a non-fading situation and require further improvement. For very slow fading channels however, the receivers can be simplified into

an adaptive version of the digital phase-locked loops. This is very satisfying as it could be intuitively conceived based on the development of the digital phase-locked loop as an optimum FM demodulator (See Section 1.2, pp. 1-5).

Chapter 6 was the parallel development of receivers using quadrature sampling. It turned out that the use of quadrature sampling allowed the receiver structures to be readily simulated without having to derive a baseband model as was done in Chapter 5. The receivers using quadrature sampling also showed better performance (see Figure 6.9, p. 137). The reason is not clear but the same observation was also made in the nonfading case. The improvement was not, however, sufficient to be comparable to the results obtained by the nonfading case. This was explained as being caused by the deep fade problems when the envelope of the received signal falls below a certain threshold level and is likely to remain there for a while due to the slow fading assumption. Two solutions were proposed. Fixed-lag smoothers were considered in Chapter 7, but the marginal improvement, however, did not warrant the extra complexity. This is in contrast to the results obtained for no fading case. Diversity techniques were employed in Chapter 8 and offered the best performance at the cost of extra complexity. This is indeed the case as has been found in many practical diversity systems already in operation and the results obtained were to rigorously demonstrate it.

Further research is needed, however, to study the actual mechanism of signal operation taking place in the rather complex receiver structure proposed in the thesis.

As a conclusion, the main results obtained in this thesis are related to the following areas:

(i) Derivation of the discrete receivers for demodulating an analog FM signal transmitted over Rayleigh fading channels using both scalar (Chapter 5) and quadrature (Chapter 6) sampling techniques and employing the EKF and MAP algorithms.

(ii) Simplification of the receiver into an adaptive phase-locked loop for very slow fading channels (Chapter 5).

(iii) Illustration of the better performance of the MAP algorithm over the EKF algorithm for the communication problem considered in this thesis (Chapter 6).

(iv) Showing that the use of fixed-lag smoothing does not improve the performance of the receivers to warrant the increased complexity (Chapter 7).

(v) Derivation of optimum diversity receiver structure based on estimation theory and demonstrate its superiority (Chapter 8).

APPENDIX A

DC COMPONENT OF A GENERAL RATIONAL FUNCTION OF SINE AND COSINE

To derive the baseband model of the estimation algorithms in Chapter 5, we need to evaluate the d.c. component of the function

$$f(x) = \frac{A + B\cos x + C\sin x}{a + b\cos x + c\sin x}$$

which is periodic having a period of 2π and can be represented by an exponential Fourier Series

$$f(x) = \sum_{n=-\infty}^{\infty} C_n e^{jnx}$$

where C_n, the general Fourier Series coefficient, is given by

$$C_n = \frac{1}{2\pi}\int_{-\pi}^{\pi} f(x)e^{-jnx}\,dx$$

In particular, the d.c. component C_o is given by the following definite integral

$$C_o = \frac{1}{2\pi}\int_{-\pi}^{\pi} f(x)\,dx = \frac{1}{2\pi}\int_{-\pi}^{\pi} \frac{A + B\cos x + C\sin x}{a + b\cos x + c\sin x}\,dx$$

From tables of integrals (Gradshteyn, 1965, p.149)

$$\int \frac{A + B\cos x + C\sin x}{a + b\cos x + c\sin x}\,dx = \frac{Bc - Cb}{b^2 + c^2}\ln(a + b\cos x + c\sin x)$$

$$+ \frac{Bb + Cc}{b^2 + c^2}x + \left(A - \frac{Bb + Cc}{b^2 + c^2}a\right)\int \frac{dx}{a + b\cos x + c\sin x}$$

where

$$\int \frac{dx}{a + b\cos x + c\sin x} = \frac{2}{\sqrt{a^2 - b^2 - c^2}}\arctan\left[\frac{(a - b)\tan\frac{x}{2} + c}{\sqrt{a^2 - b^2 - c^2}}\right]$$

if $a^2 - b^2 - c^2 > 0$ which is the case for the problem considered in Chapter 5.

Consequently

$$C_0 = \frac{1}{2\pi}\left(\frac{Bb + Cc}{b^2 + c^2}(2\pi) + \left(A - \frac{Bb + Cc}{b^2 + c^2}a\right)\frac{2(2k + 1)\pi}{\sqrt{a^2 - b^2 - c^2}}\right)$$

$$= \frac{(2k + 1)A}{\sqrt{a^2 - b^2 - c^2}} + \frac{Bb + Cc}{b^2 + c^2}\left(1 - \frac{(2k + 1)a}{\sqrt{a^2 - b^2 - c^2}}\right) \quad k = 0, \pm 1, \ldots$$

To determine a suitable value for k, consider

$$\lim_{\substack{b\to 0 \\ c\to 0}} C_0 = \frac{1}{2\pi}\int_{-\pi}^{\pi} \frac{A + B\cos x + C\sin x}{a}\,dx = \frac{A}{a}$$

and this would agree with C_0 if we choose k = 0

Therefore

$$C_0 = \frac{A1}{\sqrt{a^2 - b^2 - c^2}} + \frac{Bb + Cc}{b^2 + c^2}\left(1 - \frac{a}{\sqrt{a^2 - b^2 - c^2}}\right)$$

$$= A\Delta + \frac{Bb + Cc}{b^2 + c^2}(1 - a\Delta)$$

where $\Delta \triangleq \frac{1}{\sqrt{a^2 - b^2 - c^2}}$

APPENDIX B.

SIMPLIFICATION OF THE ERROR COVARIANCE EQUATION FOR THE MAP RECEIVER USING UNIFORM SAMPLING

In Chapter 5, Table VIII, the error covariance algorithm for the discrete MAP receiver for FM communication system with Rayleigh fading employing uniform sampling is given. Due to its complexity, the baseband model could not be derived and direct computation is formidable without making two further assumptions (i) low noise and (ii) very slow fading, to allow further simplification as follows:

B.1. Simplification of products involving z(k) (Equations 2a, 2d, 2e)

First, let define

$$\Omega(k) \triangleq \omega_c t_k + x_1(k), \hat{\Omega}(k|k-1) \triangleq \omega_c t_k + \hat{x}_1(k|k-1)$$

and consider the product

$$\begin{aligned} z(k)\hat{x}_3(k|k-1)\sin\hat{\Omega}(k|k-1) &= \sqrt{2P_t}\left(x_3(k)\sin\Omega(k)+x_4(k)\cos\Omega(k)+v(k)\right)\hat{x}_3(k|k-1)\sin\hat{\Omega}(k|k-1) \\ &= \sqrt{2P_t}\begin{bmatrix} x_3(k)\hat{x}_3(k|k-1)\sin\Omega(k)\sin\hat{\Omega}(k|k-1) \\ +x_4(k)\hat{x}_3(k|k-1)\cos\Omega(k)\sin\hat{\Omega}(k|k-1) \\ +v(k)\hat{x}_3(k|k-1)\sin\hat{\Omega}(k|k-1) \end{bmatrix} \end{aligned} \quad \text{(B.}$$

Using the trigonometric identities

$$\sin\alpha\sin\beta = \tfrac{1}{2}\cos(\alpha-\beta)-\tfrac{1}{2}\cos(\alpha+\beta)$$

$$\cos\alpha\sin\beta = \tfrac{1}{2}\sin(\alpha+\beta)-\tfrac{1}{2}\sin(\alpha-\beta)$$

and define

$$\tilde{\theta}_1 \triangleq x_1(k)-\hat{x}_1(k|k-1)$$

Under the assumption of slow fading and consequently availability of very good estimates of the channel fading components

$$\hat{x}_3(k|k-1) \approx x_3(k)$$

$$\hat{x}_4(k|k-1) \approx x_4(k)$$

coupled with the assumption of high SNR

$$\hat{x}_1(k|k-1) \approx x_1(k)$$

We then have for the first two terms of (B.1)

$$\tfrac{1}{2}x_3(k)\hat{x}_3(k|k-1)(\cos\tilde{\theta}_1(k)-\cos[2\hat{\Omega}(k|k-1)-\tilde{\theta}_1(k)])$$
$$+\tfrac{1}{2}x_4(k)\hat{x}_3(k|k-1)(\sin[2\hat{\Omega}(k|k-1)-\theta_1(k)]-\sin\tilde{\theta}_1(k))$$
$$\approx \tfrac{1}{2}\hat{x}_3^2(k|k-1)[1-\cos2\hat{\Omega}(k|k-1)]$$
$$+\tfrac{1}{2}\hat{x}_3(k|k-1)\hat{x}_4(k|k-1)\sin2\hat{\Omega}(k|k-1)$$

Furthermore, using similar arguments to that of Snyder (1969, p. 55), the random term of (B.1)

$$v(k)\hat{x}_3(k|k-1)\sin\hat{\Omega}(k|k-1)$$

can be neglected under high channel SNR conditions and therefore

$$z(k)\hat{x}_3(k|k-1)\sin\hat{\Omega}(k|k-1)$$
$$=\frac{\sqrt{2P_t}}{2}[\hat{x}_3^2(k|k-1)-\hat{x}_3^2(k|k-1)\cos2\hat{\Omega}(k|k-1)+\hat{x}_3(k|k-1)\hat{x}_4(k|k-1)\sin2\hat{\Omega}(k|k-1)] \quad (B.2)$$

Other products involving $z(k)$ can be simplified in a similar way

$$z(k)\hat{x}_4(k|k-1)\cos\hat{\Omega}(k|k-1)$$
$$=\frac{\sqrt{2P_t}}{2}[\hat{x}_4^2(k|k-1)+\hat{x}_4^2(k|k-1)\cos2\hat{\Omega}(k|k-1)+\hat{x}_3(k|k-1)\hat{x}_4(k|k-1)\sin2\hat{\Omega}(k|k-1)] \quad (B.3)$$

$$z(k)\cos\hat{\Omega}(k|k-1)$$
$$=\frac{\sqrt{2P_t}}{2}[\hat{x}_4(k|k-1)+\hat{x}_4(k|k-1)\cos2\hat{\Omega}(k|k-1)+\hat{x}_3(k|k-1)\sin2\hat{\Omega}(k|k-1)] \quad (B.4)$$

$$z(k)\sin\hat{\Omega}(k|k-1)$$
$$=\frac{\sqrt{2P_t}}{2}[\hat{x}_3(k|k-1)-\hat{x}_3(k|k-1)\cos2\hat{\Omega}(k|k-1)+\hat{x}_4(k|k-1)\sin2\hat{\Omega}(k|k-1)] \quad (B.5)$$

B.2. Evaluation of the inverse matrix

$$\underline{B} \triangleq (I+\underline{V}_{\underline{\tilde{X}}}(k|k-1)\underline{M}[\underline{\hat{X}}(k|k-1),k])^{-1} \quad (B.6)$$

By partitioning the square matrices $\underline{V}_{\underline{\tilde{X}}}(k|k-1)$ and $\underline{M}[\underline{\hat{X}}(k|k-1),k]$ as below

$$\underline{V}_{\underline{\tilde{X}}}(k|k-1)=\begin{bmatrix}\underline{P}_1 & \phi\\ \phi & \underline{P}_2\end{bmatrix} \quad \text{where} \quad \underline{P}_1 \triangleq \begin{bmatrix}V_{\tilde{x}_1}(k|k-1) & V_{\tilde{x}_1\tilde{x}_2}(k|k-1)\\ V_{\tilde{x}_1\tilde{x}_2}(k|k-1) & V_{\tilde{x}_2}(k|k-1)\end{bmatrix} \quad (B.7a)$$

$$\underline{P}_2 \triangleq \begin{bmatrix}V_{\tilde{x}_3}(k|k-1) & 0\\ 0 & V_{\tilde{x}_4}(k|k-1)\end{bmatrix} \quad (B.7b)$$

$$\underline{M}_{11} = \begin{pmatrix} m_{11} & 0 \\ 0 & 0 \end{pmatrix} \qquad (B.8a)$$

$$\underline{M}[\underline{X}(k\ k-1),k] = \left(\begin{array}{c|c} \underline{M}_{11} & \underline{M}_{12} \\ \hline \underline{M}_{21} & \underline{M}_{22} \end{array}\right) \text{ where } \underline{M}_{12} = \begin{pmatrix} m_{12} & m_{13} \\ 0 & 0 \end{pmatrix} = \underline{M}_{21}^{T} \qquad (B.8b)$$

$$\underline{M}_{22} = \begin{pmatrix} m_{22} & m_{23} \\ m_{23} & m_{33} \end{pmatrix} \qquad (B.8c)$$

where the elements of $\underline{M}$ are defined in Table VIII.

Now let

$$\underline{A} \triangleq \underline{B}^{-1} = I+V_{\underline{X}}(k|k-1)\underline{M}[\hat{\underline{X}}(k|k-1),k] = \left(\begin{array}{c|c} \underline{A}_{11} & \underline{A}_{12} \\ \hline \underline{A}_{21} & \underline{A}_{22} \end{array}\right)$$

where
$$\underline{A}_{11} = I+\underline{P}_1\underline{M}_{11} = \begin{pmatrix} 1+V_{\tilde{x}_1}(k|k-1)m_{11} & 0 \\ V_{\tilde{x}_1\tilde{x}_2}(k|k-1)m_{11} & 1 \end{pmatrix} \qquad (B.9a)$$

$$\underline{A}_{22} = I+\underline{P}_2\underline{M}_{22} = \begin{pmatrix} 1+V_{\tilde{x}_3}(k|k-1)m_{22} & V_{\tilde{x}_3}(k|k-1)m_{23} \\ V_{\tilde{x}_4}(k|k-1)m_{23} & 1+V_{\tilde{x}_4}(k|k-1)m_{33} \end{pmatrix} \qquad (B.9b)$$

$$\underline{A}_{12} = \underline{P}_1\ \underline{M}_{12} = \begin{pmatrix} V_{\tilde{x}_1}(k|k-1)m_{12} & V_{\tilde{x}_1}(k|k-1)m_{13} \\ V_{\tilde{x}_1\tilde{x}_2}(k|k-1)m_{12} & V_{\tilde{x}_1\tilde{x}_2}(k|k-1)m_{13} \end{pmatrix} \qquad (B.9c)$$

$$\underline{A}_{21} = \underline{P}_2\underline{M}_{21} = \begin{pmatrix} V_{\tilde{x}_3}(k|k-1)m_{12} & 0 \\ V_{\tilde{x}_4}(k|k-1)m_{13} & 0 \end{pmatrix} \qquad (B.9d)$$

Then
$$\underline{B} = \underline{A}^{-1} = \left(\begin{array}{c|c} \underline{B}_{11} & \underline{B}_{12} \\ \hline \underline{B}_{21} & \underline{B}_{22} \end{array}\right)$$

$$= \left(\begin{array}{c|c} \underline{A}_{11}^{-1}+\underline{A}_{11}^{-1}\underline{A}_{12}\underline{B}_{22}\underline{A}_{21}\underline{A}_{11}^{-1} & -\underline{A}_{11}^{-1}\underline{A}_{12}\underline{B}_{22} \\ \hline -\underline{B}_{22}\underline{A}_{21}\underline{A}_{11}^{-1} & \underline{B}_{22} \end{array}\right) \qquad (B.10)$$

with

$$\underline{A}_{11}^{-1} = \frac{1}{1+V_{\tilde{x}_1}(k|k-1)m_{11}} \begin{pmatrix} 1 & 0 \\ -V_{\tilde{x}_1\tilde{x}_2}(k|k-1)m_{11} & 1+V_{\tilde{x}_1}(k|k-1)m_{11} \end{pmatrix} \qquad (B.10$$

$$\underline{B}_{22}^{-1} = \underline{A}_{22}-\underline{A}_{21}\underline{A}_{11}^{-1}\underline{A}_{12} \qquad (B.10b)$$

APPENDIX C

SAMPLE VARIANCE OF MEAN SQUARE ERRORS

In Section 4.2.4, in determining the mimimum sample size, the statistic ξ_i computed as

$$\xi_i = \frac{1}{N_{eff}} \sum_{k=1}^{N_{eff}} \tilde{x}_i^2(k) \tag{C.1}$$

was shown to be asymtotically normal with the mean value and variance to be determined as follows:

The mean value of ξ_i is

$$E[\xi_i] = \frac{1}{N_{eff}} E\left[\sum_{k=1}^{N_{eff}} \tilde{x}_i^2(k)\right]$$

$$= \frac{1}{N_{eff}} \sum_{k=1}^{N_{eff}} E\left[\tilde{x}_i^2(k)\right]$$

$$= E\left[\tilde{x}_i^2(k)\right]$$

$$\triangleq \mu_2 \tag{C.2}$$

where μ_2 is the true mean square value which is not available.

The second moment of ξ_i^2 is

$$E\left(\xi_i^2\right) = \frac{1}{N_{eff}^2} E\left[\sum_{k=1}^{N_{eff}} \tilde{x}_i^2(k) \sum_{j=1}^{N_{eff}} \tilde{x}_i^2(j)\right]$$

$$= \frac{1}{N_{eff}^2} E\left[\sum_{k=1}^{N_{eff}} \tilde{x}_i^4(k) + \sum_{k=1}^{N_{eff}} \sum_{\substack{j=1 \\ k\neq j}}^{N_{eff}} \tilde{x}_i^2(k)\, x_i^2(j)\right]$$

$$= \frac{1}{N_{eff}^2} \left[N_{eff}\, E\left(\tilde{x}_i^4(k)\right) + (N_{eff}^2 - N_{eff})\, E\left(\tilde{x}_i^2(k)\tilde{x}_i^2(j)\right)\right]$$

and since $\tilde{x}_i(k)$ is assumed to be gaussian so (Papoulis, 1965, p. 147)

$$E\left(x_i^4(k)\right) = 3\mu_2^2$$

and it has also been assumed that the samples of size N_{eff} as given by Equation (4.31b) are statistically independent so

$$E\left(x_i^2(k)\, x_i^2(j)\right) = E\left(x_i^2(k)\right) E\left(x_i^2(j)\right)$$

$$= \mu_2^2$$

Therefore

$$E\left(\xi_i^2\right) = \frac{1}{N_{eff}^2} \left(3N_{eff}\, \mu_2^2 + (N_{eff}^2 - N_{eff})\, \mu_2^2\right)$$

$$= \frac{N_{eff} + 2}{N_{eff}} \mu_2^2 \qquad \text{(C.3)}$$

The variance of ξ_i^2 is thus

$$\sigma^2 = \frac{N_{eff} + 2}{N_{eff}} \mu_2^2 - \mu_2^2$$

$$= \frac{2}{N_{eff}} \mu_2^2 \qquad (C.4)$$

The probability density function of ξ_i is thus

$$p(\xi_i) = \frac{1}{\sqrt{2\pi}\ \sigma^2} e^{-(\xi_i - \mu_2)^2/2\sigma^2} \qquad (C.5)$$

and it is well known (Carlson, 1975, Table D) that

$$P(|\xi_i - \mu_2| \leq r\sigma) = 1 - 2Q(r) \qquad (C.6)$$

where

$$Q(r) \triangleq \frac{1}{\sqrt{2\pi}} \int_r^\infty e^{-\lambda^2/2}\, d\lambda$$

is called "the area under the gaussian tail" and is also called the "error probability" function.

From Equation C.2

$$\sigma = \sqrt{\frac{2}{N_{eff}}}\ \mu_2$$

by letting

$$s = r \sqrt{\frac{2}{N_{eff}}}$$

Equation C.6 becomes

$$P(|\xi_i - \mu_2| \leq s\mu_2) = 1 - 2Q\left(s\sqrt{\frac{N_{eff}}{2}}\right) \qquad (C.7)$$

REFERENCES

Abramowitz M., Stegun I.A., Handbook of Mathematical Functions, Dover, New York, Seventh Edition, 1970.

Anderson B.D.O., Moore J.B., "The Kalman-Bucy Filter as a true time-varying Wiener filter", IEEE Trans. Syst. Man & Cyber., Vol. SMC-1, 1971, pp.119-127.

Anderson T.W., Introduction to Multi-variate Statistical Analysis, Wiley, New York, 1958.

Bellman R., Introduction to Matrix Analysis, McGraw-Hill, New York, 1960.

Boorstyn R.R., Schwartz M.,"Performance of Analog Demodulators in a Fading Environment", IEEE Trans. Comm. Techno., Vol. COM-16, 1968, pp.45-51.

Brennan D.G., "Linear Diversity Combining Techniques", Proc. IRE, Vol. 46, March 1958, pp.555-570.

Bucy R.S., Hecht C., Senne K.D.,"New Methods for Nonlinear Filtering", Revue Francaise Informatique et Recherche Operationelle, No. J-1, 1973, pp.3-54.

Bucy R.S., Mallinckrodt A.J., "An Optimal Phase Demodulator", Stochastics, Vol. 1, Nc. 1, 1973, pp.3-23.

Bucy R.S., Senne K.D., Youssef H.M., "Pipeline, Parallel and Serial Realizing of Phase Demodulators", Institute of Computer Application in Science and Engineering, Report No. 76-31, Nov. 1976.

Carlson A.B., Communication Systems, McGraw-Hill, New York, 1975.

Cramer H., Mathematical Methods of Statistics, Princeton University Press, Princeton, N.J., 1946.

Dharamsi M.T., Gupta S.C., "Discrete-time Demodulation of Angle-modulated Analog Signals Transmitted Over Fading Channels", J. Information Sciences, Vol. 9, 1975a, pp.99-132.

Dharamsi M.T., Gupta S.C., "Performance of Quasi-optimum Digital Demodulators for Fading Channels", J. Computer and Elec. Eng., Vol. 2, 1975b, pp.175-193.

Fishman G.S., Concepts and Methods in Discrete Event Digital Simulation, Wiley, New York, 1973.

Freeman R.L., Telecommunication Transmission Handbook, Wiley, New York, 1975.

Gibson J.D., Melsa J.L., "Unified Development of Algorithms Used for Linear Predictive Coding of Speech Signals", J. Computer & Elec. Eng., Vol. 3, 1976, pp.75-91.

Gill G.C., Gupta S.C., "First-order Discrete Phase-Locked Loop with Applications to Demodulation of Angle-modulated Signals", IEEE Trans. Commun., June 1972, pp.454-462.

Grace O.D., "Two Finite Fourier Transforms for Bandpass Signals", IEEE Trans. Audio & Electroacoustics, Vol. AE-18, Dec. 1970, pp.501-502.

Grace O.D., Pitt S.P., "Quadrature Sampling of High-frequency Waveforms", J. Acoust. Society Amer., Vol. 44, 1968, pp.1453-1454.

Gradshteyn I.S., Ryzhik I.M., Table of Integrals, Series, and Products, Scripta Technica, Inc., Transl., Academic Press, New York, 1965.

Gupta S.C., "On Optimum Digital Phase Locked Loops", IEEE Trans. Commun. Systems, Vol. Com-16, 1968, pp.340-344.

Gupta S.C., "Phase-locked Loops", Proc. IEEE, Vol. 63, No.2, 1975, pp.251-306.

Hammersley J.M., Hanscombe D.C., Monto Carlo Methods, Menthuen, London, 1964.

Ho Y.C., Lee R.C.K., "A Bayesian Approach to Problems in Stochastic Estimation and Control", IEEE Trans. Automatic Control, Vol. AC-9, 1964, pp.333-339.

Jazwinski A.H., Stochastic Processes and Filtering Theory, Academic Press, New York, 1970.

Kailath T., "Supplement to 'Survey of Data Smoothing'", (Correspondence item), Automatica, Vol. 11, 1975, pp.109-111.

Kalman R.E., "A New Approach to Linear Filtering and Prediction Problems", J. Basic Eng., Ser. D, Vol. 82, March 1960, pp.35-45.

Kelly C., Gupta S.C., "The Digital Phase Locked Loop as a Near Optimum F.M. Demodulator", IEEE Trans. Commun., Vol. Com-20, 1972, pp.406-411.

Kennedy R.S., Fading Dispersive Communication Channels, Wiley, New York, 1969.

Klapper J., Frankle J.T., Phase-locked and Frequency-feedback Systems: Principle and Techniques, Academic Press, New York, 1972.

Knuth D.E., The Art of Computer Programming - Seminumerical Algorithm, Vol. 2, Addison-Wesley, Englewood Cliffs, N.J., 1969.

Kohlenberg A., "Exact Interpolation of Band-limited Functions", J. Appl. Phys., Vol. 24, 1953, pp.1432-1436.

Kolmogorov A.N., "Interpolation and Extrapolation of Stationary Random Sequences", Bull. Acad. Sci. USSR, Math. Ser., Vol. 5, 1941.

Kushner H.J., "Dynamical Equations for Optimal Nonlinear Filtering", J. Differential Equations, Vol. 3, 1967, pp.179-180.

Kushner H.J., "On the Differential Equations Satisfied by Conditional Probability Densities of Markov Processes with Applications", J. SIAM Control, Vol. 2, 1964, pp.106-119.

Lehan F.W., Parks R.J., "Optimum Demodulation", IRE Nat. Conv. Rec., Pt. 8, 1953, pp.101-103.

McBride A.L., "On Optimum Sampled-data FM Demodulation", IEEE Trans. Commun., Vol. COM-21, Jan. 1973, pp.40-50.

Mehra R.K., "Digital Simulation of Multi-dimensional Gauss-Markov Random Processes", IEEE Trans. Autom. Control (Correspondence), Vol. AC-14, 1969, pp.142-143.

Melsa J.L., Sage A.P., An introduction to Probability and Stochastic Processes, Prentice-Hall, Englewood Cliffs, 1972.

Mendel J.M., Discrete Techniques of Parameter Estimation, Marcel Dekker Inc., New York, 1973.

Miller W.L., Lewis J.B., "Dynamic State Estimation in Power Systems", IEEE Trans. in Auto. Control, Vol. AC-16, 1971, pp.841-846.

Moore J.B., "Discrete Time Fixed-lag Smoothing Algorithms", Automatica, Vol. 9, 1973, pp.163-173.

Moore J.B., Hetrakul P., "Optimum Demodulation of PAM Signals", IEEE Trans. Inform. Theory, Vol. IT-19, 1973, pp.188-196.

Moore J.B., Tam P.K.S., "Fixed Lag Smoothing for Nonlinear Systems and Discrete Measurements", J. Information Sciences, Vol. 6, 1973, pp.151-160.

Nahi N.E., Estimation Theory and Applications, Huntington, New York, 1976.

Ornstein L.S., Uhlenbeck G.E., On the Theory of Brownian Motion, Selected Papers on Noise and Stochastic Processes, Nelson Wax (Ed.), Dover, 1954.

Osborne P.W., Hoffman E., Schilling D.L., "FM Receiver Performance Evaluation Using Computer Techniques", Proc. Symp. Comp. Proc. in Commun., Polytech. Inst. of Brooklyn, N.Y., 1969.

Painter J.H., Gupta S.C., Wilson L.R., "Multipath Modelling for Aeronautical Communications", IEEE Trans. on Communications (Concise Papers), Vol. COM-21, May 1973, pp.658-662.

Painter J.H., Wilson L.R., "Simulation Results for the Decision-Directed MAP Receiver for M-ary Signals in Multiplicative and Additive Gaussian Noise", IEEE Trans. on Communications, Vol. COM-22, May 1974, pp.649-660.

Panter P.F., Modulation, Noise, and Spectral Analysis, McGraw-Hill, New York, 1965.

Papoulis A., Probability, Random Variables, and Stochastic Processes, McGraw-Hill, New York, 1965.

Pasternack G., Whalin R.L., "Analysis and Synthesis of a Digital Phase-locked Loop for FM Demodulation", Bell Syst. Tech. J., Dec. 1968, pp.2207-2237.

Peikari B., Fundamentals of Network Analysis and Synthesis, Prentice-Hall, Englewood Cliffs, N.J., 1974.

Polk D.R., Gupta S.C., "Quasi-optimum Digital Phase-locked Loops", IEEE Trans. Commun. (Concise Papers), Vol. COM-21, 1973, pp.75-82.

Prasad S., Mahalanabis A.K., "Finite-lag Receivers for Analog Communication", IEEE Trans. Commun., Vol. COM-23, Feb. 1975, pp.204-213.

Prasad S., Mahalanabis A.K., "On Finite-lag Receivers for Fading Channels", IEEE Trans. on Aerospace & Electronic Systems, AES-10, Sept. 1974, pp.659-669.

Pyle R.H., "Acquisition Behaviour of a Discrete Nonlinear Frequency Estimator", Fifth Symp. on Nonlinear Estimation, San Diego, 1974, pp.219-223.

Sage A.P., Optimum Systems Control, Prentice-Hall, Englewood Cliffs, N.J., 1968.

Sage A.P., Melsa J.L., Estimation Theory with Applications to Communications and Control, McGraw-Hill, New York, 1971.

Schilling D.L., Nelson E.A., Clarke K.K., "Discriminator Response to an FM Signal in a Fading Channel", IEEE Trans. Commun. Technol., Vol. AC-13, 1968, pp.83-86.

Schwartz L., Stear E.B., "A Computational Comparison of Several Non-linear Filters", IEEE Trans. Autom. Control, Vol. AC-13, 1968, pp.83-86.

Schwartz M., "Maximum Aposteriori Demodulation of Analogue-type Signals through Random Fading Media", Polytech. Inst. of Brooklyn, Res. Rept. PIB:MRI-UIJJ-64, Dec. 1964.

Schwartz M., "Abstract Vector Spaces Applied to Problems in Detection and Estimation Theory", IEEE Trans. Inform. Theory, Vol. IT-12, 1966, pp.327-336.

Schwartz M., Bennet W.R., Stein S., Communication Systems and Techniques, McGraw-Hill, New York, 1966.

Snyder D.L., The State-variable Approach to Continuous Estimation, Res. Mono. 51, M.I.T. Press, Cambridge, Mass., 1969.

Sorenson H.W., "On the Development of Practical Nonlinear Filters", J. Information Sciences, Vol. 7, 1974, pp.253-270.

Sorenson H.W., "Estimation for Dynamic Systems a Perspective", Fifth Symp. on Nonlinear Estimation, San Diego, 1974, pp.291-318.

Takhar G.S., "Discrete Estimation of Continuous Angle-modulated Signal over Multipath Channels for Aeronautical Communications", IEEE Trans. Commun., Vol. COM-24, 1976, pp.365-374.

Tam K.S.Peter, Tam K.S.Dominic, Moore J.B., "Fixed-lag Demodulation of Discrete Noisy Measurements of FM Signals", Automatica, Vol. 9, 1973, pp.725-729.

Tam P.K.S., Moore J.B., "Improved Demodulation of Sampled FM Signals in High Noise", Technical Report EE 7502, University of Newcastle, Australia, Jan. 1975.

Van Trees H.L., "Analog Communication over Randomly Time-varying Channels", IEEE Trans. Inform. Theory, Vol. IT-12, Jan. 1966, pp.51-63.

Van Trees H.L., Detection, Estimation, and Modulation, Part 2: Nonlinear Modulation Theory, Wiley, New York, 1971.

Viterbi A.J., Principles of Coherent Communication, McGraw-Hill, New York, 1966.

Wiener N., The Extrapolation, Interpolation, and Smoothing of Stationary Time Series with Engineering Application, New York, Wiley, 1949.

Youla D.C., "The Use of the Method of Maximum Likelihood in Estimating Continuously-modulated Intelligence which has been Corrupted by Noise", IRE Trans. Inform. Theory, Vol. IT-13, March 1954, pp.90-105.

PUBLICATIONS

"Digital Receivers for Analog FM Signals over Rayleigh Fading Channels", Proc. Tenth New Zealand National Electronics Convention, Auckland, August, 1974.

With Davis B.R., Beare C.T., Coutts R.P., "Computer Simulation of Communication Systems", Proc. International Electronics Convention '75, Sydney, August, 1975.

Also Research Report No. 2-75, Department of Electrical Engineering, University of Adelaide, South Australia, 1975.

With Davis B.R., "Discrete Phase-locked Demodulation of Analog FM Signals over a Rayleigh Fading Channel", Proc. International Electronics Convention '75, Sydney, August, 1975.

With Davis B.R., "A Survey of Analog and Digital Phase-locked-loops for Optimal FM Demodulation", Proc. International Electronics Convention '75, Sydney, August, 1975.